ISSN 2071-4726
2071-0305

Инженерно-строительный журнал

НАУЧНОЕ ИЗДАНИЕ

№2(70) 2017

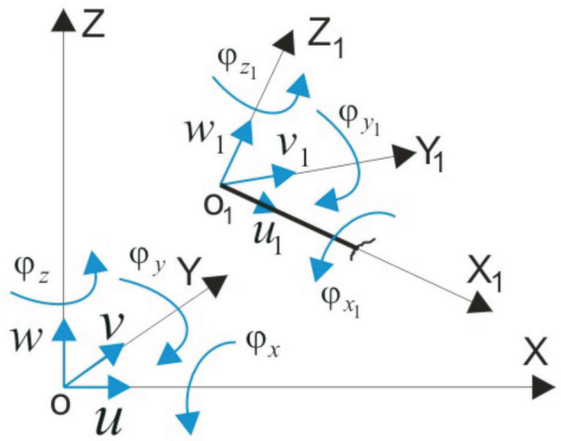

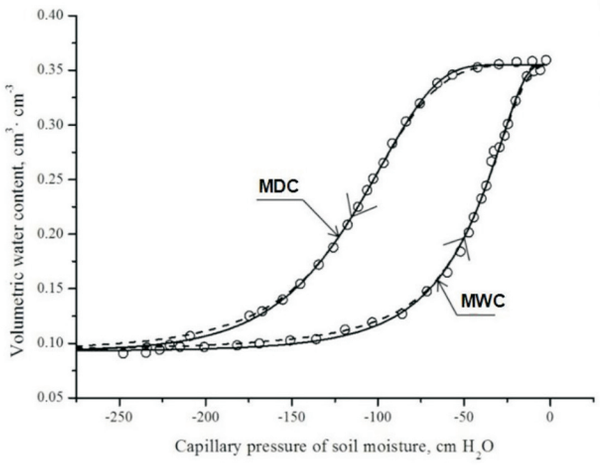

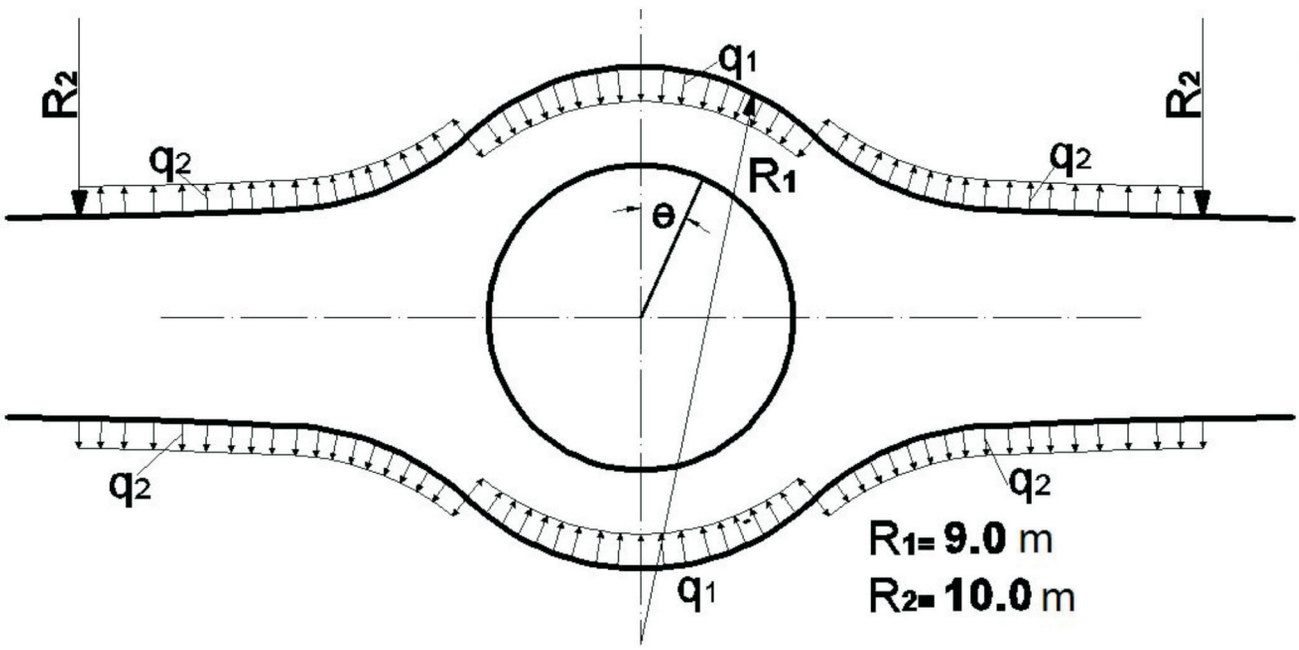

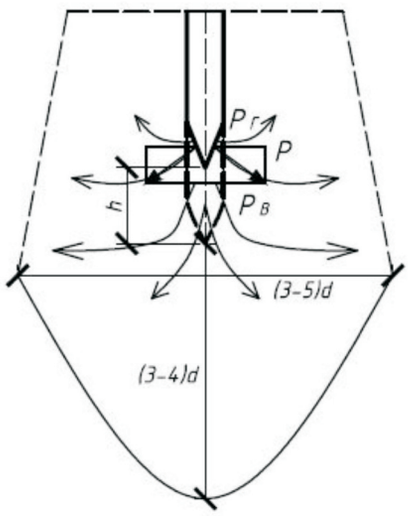

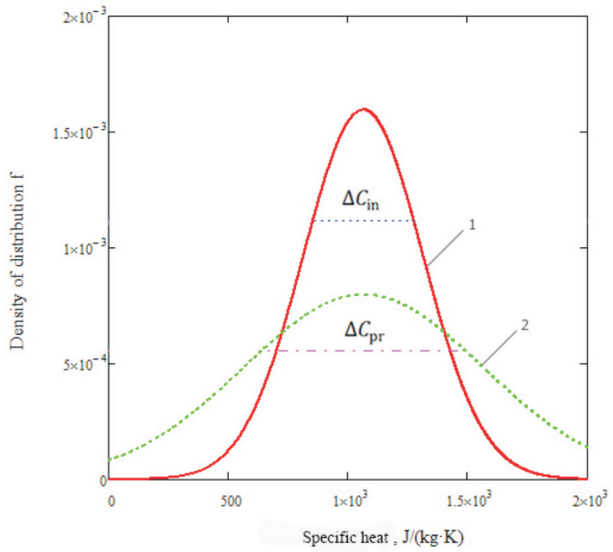

Федеральное государственное автономное образовательное учреждение высшего образования
Санкт-Петербургский политехнический университет Петра Великого

ПОЛИТЕХ
Санкт-Петербургский политехнический университет Петра Великого

Инженерно-строительный институт
Центр дополнительных профессиональных программ

195251, г. Санкт-Петербург, Политехническая ул., 29,
тел/факс: 552-94-60, www.stroikursi.spbstu.ru,
stroikursi@mail.ru

Приглашает специалистов организаций, вступающих в СРО, на курсы повышения квалификации (72 часа)

Код	Наименование программы	Виды работ*
	Курсы по строительству	
БС-01-04	«Безопасность и качество выполнения общестроительных работ»	п.1,2, 3, 5, 6, 7, 9, 10, 11, 12, 13, 14
БС-01	«Безопасность и качество выполнения геодезических, подготовительных и земляных работ, устройства оснований и фундаментов»	1,2,3,5
БС-02	«Безопасность и качество возведения бетонных и железобетонных конструкций»	6,7
БС-03	«Безопасность и качество возведения металлических, каменных и деревянных конструкций»	9,10,11
БС-04	«Безопасность и качество выполнения фасадных работ, устройства кровель, защиты строительных конструкций, трубопроводов и оборудования»	12,13,14
БС-05	«Безопасность и качество устройства инженерных сетей и систем»	15,16,17,18,19
БС-06	«Безопасность и качество устройства электрических сетей и линий связи»	20,21
БС-08	«Безопасность и качество выполнения монтажных и пусконаладочных работ»	23,24
БС-12	«Безопасность и качество устройства мостов, эстакад и путепроводов»	29
БС-13	«Безопасность и качество выполнения гидротехнических, водолазных работ»	30
БС-14	«Безопасность и качество устройства промышленных печей и дымовых труб»	31
БС-15	«Осуществление строительного контроля»	32
БС-16	«Организация строительства, реконструкции и капитального ремонта. Выполнение функций технического заказчика и генерального подрядчика»	33
	Курсы по проектированию	
БП-01	«Разработка схемы планировочной организации земельного участка, архитектурных решений, мероприятий по обеспечению доступа маломобильных групп населения»	1,2,11
БП-02	«Разработка конструктивных и объемно-планировочных решений зданий и сооружений»	3
БП-03	«Проектирование внутренних сетей инженерно-технического обеспечения»	4
БП-04	«Проектирование наружных сетей инженерно-технического обеспечения»	5
БП-05	«Разработка технологических решений при проектировании зданий и сооружений»	6
БП-06	«Разработка специальных разделов проектной документации»	7
БП-07	«Разработка проектов организации строительства»	8
БП-08	«Проектные решения по охране окружающей среды»	9
БП-09	«Проектные решения по обеспечению пожарной безопасности»	10
БП-10	«Обследование строительных конструкций и грунтов основания зданий и сооружений»	12
БП-11	«Организация проектных работ. Выполнение функций генерального проектировщика»	13
Э-01	«Проведение энергетических обследований с целью повышения энергетической эффективности и энергосбережения»	
	Курсы по инженерным изысканиям	
И-01	«Инженерно-геодезические изыскания в строительстве»	1
И-02	«Инженерно-геологические изыскания в строительстве»	2,5
И-03	«Инженерно-гидрометеорологические изыскания в строительстве»	3
И-04	«Инженерно-экологические изыскания в строительстве»	4
И-05	«Организация работ по инженерным изысканиям»	7

***(согласно приказам Минрегионразвития РФ N 624 от 30 декабря 2009 г.)**

По окончании курса слушателю выдается удостоверение о краткосрочном повышении квалификации установленного образца (72 ак. часа)

Для регистрации на курс необходимо выслать заявку на участие, и копию диплома об образовании по телефону/факсу: 8(812) 552-94-60, 535-79-92, , e-mail: stroikursi@mail.ru.

http://www.engstroy.spbstu.ru – полнотекстовая версия журнала в сети Интернет.
Бесплатный доступ, обновление с каждым новым выпуском

Инженерно-строительный журнал
НАУЧНОЕ ИЗДАНИЕ

ISSN 2071-4726

Свидетельство о государственной регистрации: ПИ №ФС77-38070, выдано Роскомнадзором

Специализированный научный журнал. Выходит с 09.2008.

Включен в Перечень ведущих периодических изданий ВАК РФ

Периодичность: 8 раз в год

Учредитель и издатель:

Санкт-Петербургский политехнический университет Петра Великого

Адрес редакции:

195251, СПб, ул. Политехническая, д. 29, Гидрокорпус-2, ауд. 227А

Содержание

На обложке: иллюстрации авторов к статьям номера

Установочный тираж 1000 экз.
Подписано в печать 31.05.2017. Формат 60x84/8, усл. печ. л. 11,5. Заказ № 1419
Отпечатано в типографии СПбПУ. СПб, ул. Политехническая, д. 29

Контакты:
Тел. +7(812)535-52-47 E-mail: mce@ice.spbstu.ru
Web: http://www.engstroy.spbstu.ru

http://www.engstroy.spbstu.ru – full-text open-access version in Internet. It is updated immediately with each new issue.

Magazine of Civil Engineering
SCHOLAR JOURNAL

ISSN 2071-4726
Peer-reviewed scientific journal
Start date: 2008/09
8 issues per year

Publisher:
Peter the Great St. Petersburg Polytechnic University

Indexing:
Scopus, Russian Science Citation Index (WoS), Compendex, DOAJ, EBSCO, Google Academia, Index Copernicus, ProQuest, Ulrich's Serials Analysis System

Corresponding address:
227a Hydro Building, 29 Polytechnicheskaya st., Saint-Petersburg, 195251, Russia

Editor-in-chief:
Ekaterina A. Linnik

Science editor:
Nikolay I. Vatin

Technical editor:
Ksenia D. Borshcheva

Contents

On the cover: authors' illustrations

+7(812) 535-52-47
E-mail: mce@ice.spbstu.ru
Web: http://www.engstroy.spbstu.ru/eng/index.html

doi: 10.18720/MCE.70.1

Temperature in linear elements of enclosing structures

Температура в линейных элементах ограждающих конструкций

O.D. Samarin,
National Research Moscow State University of Civil Engineering, Moscow, Russia

Канд. техн. наук, доцент О.Д. Самарин,
Национальный исследовательский Московский государственный строительный университет, г. Москва, Россия

Key words: window unit; slope; thermal non-uniformity; temperature field; concave corner; energy efficiency; buildings

Ключевые слова: оконный блок; откос; теплотехническая неоднородность; температурное поле; вогнутый угол; энергоэффективность; здания и сооружения

Abstract. Window slopes are one of the most important linear elements of external wall structures with two-dimensional and even three-dimensional temperature field. Thereby, they cause additional risk of non-compliance of sanitary and hygienic requirements. In the proposed work one of the typical designs of window slopes is considered as the object of study, namely the fastening of the window unit with steel fixings to one of the two major layers of the wall – insulation or constructive. Peculiarities of designing two-dimensional stationary temperature field in the structure of the site abutting window units to the aperture of residential and public buildings are considered. Results of calculation of temperature in hazardous adjunction points for the design winter conditions with the help of software that implements the finite element method are presented. The analysis of the obtained data is given and the comparison of the behavior of minimum temperatures in the zone of adjacency of the fill of the lighting aperture with the results of analytical calculation based on the conform transformation for the concave corner is proposed if you move the window block in the cross section of the outer wall. It was discovered that the closer the fill to the outer plane of the facade a minimum of the temperature decreases according to the law which coincides enough closely with the analytical solution. Recommendations on the optimal placement of fill within the structural layer of the wall for the best sanitary-hygienic requirements for outdoor enclosures are confirmed. The presentation is illustrated with examples of temperature fields for the node of adjunction in a residential building on one of the modern projects.

Аннотация. Оконные откосы являются одним из важнейших линейных элементов конструкций наружных стен с двумерным и даже трехмерным температурным полем. Поэтому они вызывают дополнительную опасность невыполнения санитарно-гигиенических требований. В предлагаемой работе исследуется одна из типовых конструкций оконных откосов с креплением оконного блока с помощью стальных закладных деталей к одному из двух основных слоев стены – теплоизоляционному или конструктивному. Рассмотрены особенности расчета стационарного двумерного температурного поля в конструкциях узла примыкания оконных блоков к светопроемам гражданских зданий. Приведены результаты вычисления температуры в опасных точках примыкания для расчетных зимних условий с помощью программы для ЭВМ, реализующей метод конечных элементов. Дан анализ полученных данных и проведено сопоставление характера поведения минимальной температуры в зоне примыкания заполнения светопроема при перемещении оконного блока по сечению наружной стены с результатами аналитического расчета на основе конформного преобразования для вогнутого угла. Обнаружено, что по мере приближения заполнения к наружной плоскости фасада минимальная температура понижается по закону, достаточно близко совпадающему с аналитическим решением. Подтверждены рекомендации по оптимальному размещению заполнения в пределах конструктивного слоя стены для наилучшего обеспечения санитарно-гигиенических требований к наружным ограждениям. Изложение проиллюстрировано примерами температурных полей для узла примыкания в жилом здании по одному из современных проектов.

Самарин О.Д. Температура в линейных элементах ограждающих конструкций // Инженерно-строительный журнал. 2017. № 2(70). С. 3–10.

Introduction

Window slopes are one of the most important linear elements of external wall structures with two-dimensional and even three-dimensional temperature field. Thereby, they make a significant contribution to the overall thermal non-uniformity of walls and cause additional risk of non-compliance of sanitary and hygienic requirements. These requirements relate mainly to the absence of water vapor condensation in the dangerous points of inner surface of enclosures, in order to prevent the development of harmful microorganisms and the destruction of structures themselves; in some cases, mainly for translucent elements – to ensuring of positive temperatures in order to prevent condensate freezing. In the proposed work one of the typical designs of window slopes currently used in residential and public buildings is considered as the object of study, namely the fastening of the window unit with steel fixings to one of the two major layers of the wall – insulation or constructive. As embedded parts are used parts from rolled steel, fixed by anchors to the constructive layer of reinforced concrete, and place of the interface of the window block to the slopes is treated with a sealant and filled with foam. For clarity, the scheme of this solution is shown in figure 1. The more detailed design of this construction is presented in figure 1a. Because of the commonality of the design the obtained results can be applicable for a very wide range of buildings for various purposes.

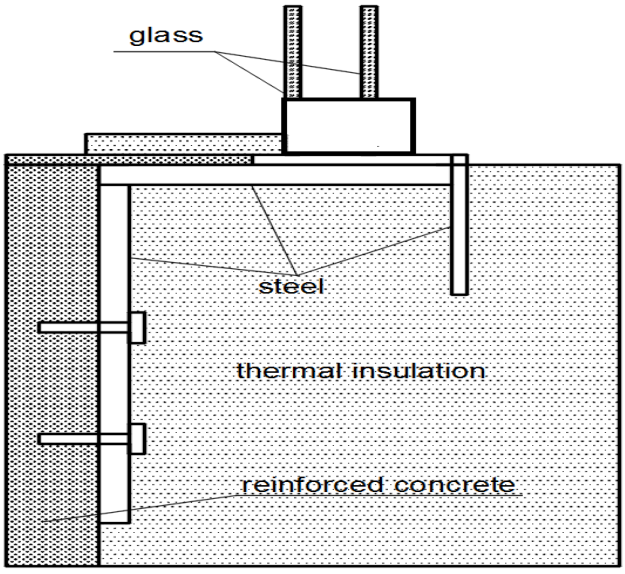

Figure 1. The scheme of the design of the contiguity of the window unit to the building opening (simplified diagram for calculation)

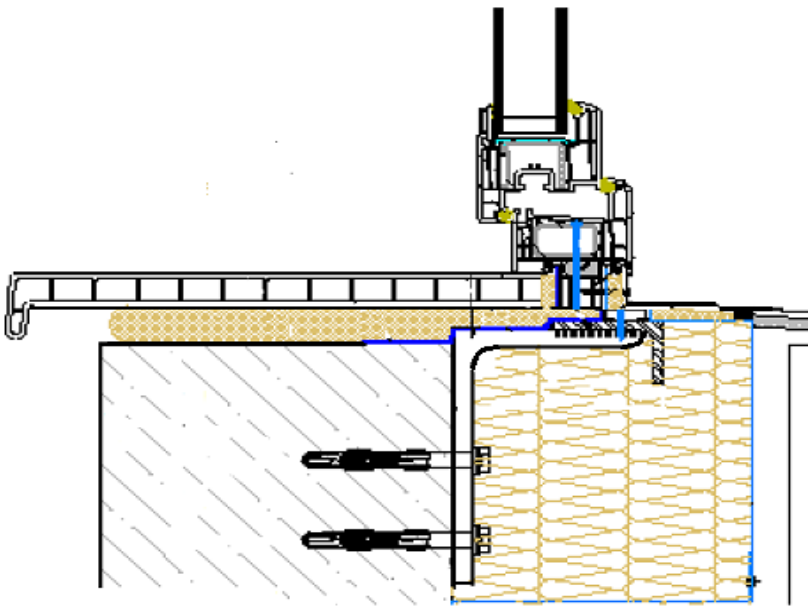

Figure 1a. The detailed scheme for the construction shown in Figure 1

Samarin O.D. Temperature in linear elements of enclosing structures. *Magazine of Civil Engineering.* 2017. No. 2. Pp. 3–10. doi: 10.5862/MCE.70.1

Compliance with sanitary and hygienic requirements to thermal protection of the exterior wall envelopes is currently regarded as a mandatory component of the overall system of measures to reduce energy consumption in residential and public buildings, along with ensuring of comfort and safety of their users [1–3]. Herewith, it is necessary to note that reducing energy costs for heating of buildings seems by itself primarily an economic category, so, first of all, it is necessary to consider low-cost and fast-payback measures [4–8]. However, it is in the buildings with the level of external-walls thermal protection, limited by economic viability, that the risk of non-compliance with the conditions of absence of condensation or freezing in separate points is possible in the first place. To verify this fact, the calculations of temperature fields are carried out [9–10]. And, in view of complexity of the considered areas configuration, it is extremely problematic to use analytical methods here, as was done, for example, in [11–12]. So, the majority of native and foreign authors, who explore similar questions, use the numerical modeling of all others. As a rule, this applies approximation of differential equation of thermal conductivity by the method of finite differences or finite elements. And, on this way, a significant number of computer programs have been developed at the present time, which, among other things, also carry out the visualization of calculated temperature fields, as well as the calculation of their certain integral characteristics [13–19]. However, using such programs is not always an easy task for an average specialist, and for the same reason the need remains for relatively simple engineering techniques in order to estimate temperatures in hazardous areas of exterior enclosures. Thus, the relevance of obtaining analytical dependences to check for condensation or freezing continues to the present time.

Therefore, the goal of our research is the development of relatively simple engineering techniques in order to estimate temperatures in one of the most hazardous areas of exterior enclosures, namely, in the area between the window unit to a building aperture, which could be used for a preliminary assessment, especially under the conditions of the limited terms of designing. To achieve this goal it is necessary to obtain the solution of a problem of calculation of temperature fields in the specified area and creating the mathematical descriptions which is available for use in engineering practice.

Methods

If you pay attention to the geometry of the area of the window block abutting to the opening shown in the scheme at the figure 1, you may notice that a part of the window slope and the adjacent wall part, facing into the room, are sufficiently similar in form to the element, which is called “concave angle”. As it is known, such distribution of temperature is described by the differential equation of stationary heat conduction (Laplace equation):

$$\frac{\partial^2 t}{\partial x^2} + \frac{\partial^2 t}{\partial y^2} = 0 \quad , \tag{1}$$

where t – temperature, ^{O}C, in the cross section of the structure at the point with coordinates x and y, m.

The solution of (1) for such area can be quite easily obtained by conformal transformations method. Herewith, the angle π/2 remains, which can be obtained from the upper half-plane, i.e., the straight angle equal to π, by the transformation $z' = z^2$, where 2 = π/(π/2). In this case, the projecting angle vertex, i.e. the joint of the wall and the slope from the room side, is accepted as the origin of coordinates.

Now, if we assume, as is usually done, that the temperature is the imaginary part of the obtained solution, we find:

$$\theta = \mathrm{Im}\left(Cz^2\right) = \mathrm{Im}\left(C\left[x+iy\right]^2\right) = 2Cxy, \tag{2}$$

where C is a certain constant. In other words, the isotherms are a set of hyperbolas with asymptotes coinciding with the coordinate axes. For generality, the solution is written down with respect to the dimensionless temperature $\theta = (t - t_{ext})/(t_{in} - t_{ex})$, where t_{in} and t_{ex} are correspondingly the calculated temperatures of inner and outer air, °C. Strictly speaking, the expression (2) holds for the boundary conditions of the 1st kind, when the temperature on the surface is set, but, without much error, this can be taken into account by introducing an additional conditional layer with thickness $\delta_o = \lambda_{in}/\alpha_{in}$, m, where α_{in} is the coefficient of total heat exchange on the surface facing into the room, W/(m^2•K); λ_{in} is the thermal conductivity of material of this surface, W/(m•K).

Figures 2 and 2a shows the temperature field in the area of abutting of the light-opening filling to the window slope, which is obtained by numerical calculation according to one of the standard computer

programs (FEMLAB – multipurposal and multifunctional product of Comsol), using an approximation of the Laplace equation by the finite element method which was accepted also in the international engineering guidelines [20], [21]. These figures present the distribution of the temperature like one of the most used sources of such solutions [22]. In the simplest case of identical elements the corresponding differential ratio, allowing to calculate the temperature $t_{i,j}$ in a regular grid, as it is known, can be written as follows:

$$t_{i,j} = \left(t_{i-1,j} + t_{i+1,j} + t_{i,j-1} + t_{i,j+1}\right)/4; \quad (3)$$

i.e. the temperature at the node is obtained as the arithmetic average between its value in the neighboring nodes. In this case on the surfaces of glazing and of the wall the boundary conditions of the 3rd type are used. They can be written as follows:

$$-\lambda_{in}\left(\frac{\partial t}{\partial n}\right)_{in} = \alpha_{in}\left(t_{in} - \tau_{in}\right). \quad (4)$$

Here, n is the distance along the internal normal to the surface angle, m; τ_{in} is the temperature of the surface in the considered point, °C; the rest of the notation is given above. The value of α_{in} is equal to 8.7 W/(m²•K) for the wall surface and to 8 W/(m²•K) for the glazing.

It is easy to see that the distribution of temperatures from the room side indeed sufficiently closely resembles the one obtained by the equation (2).

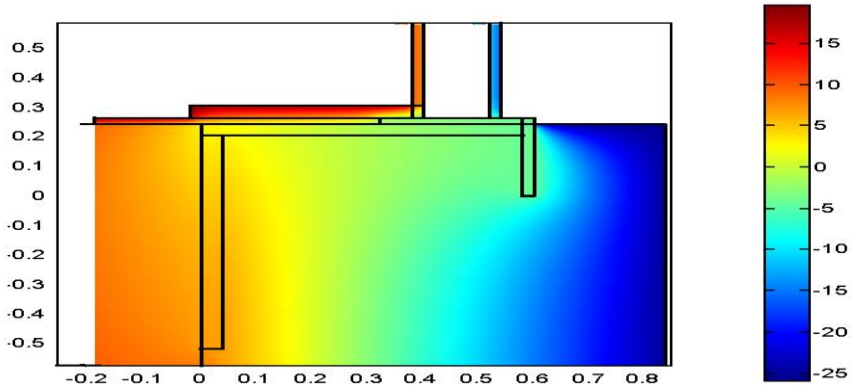

Figure 2. Temperature field of the side section of the window slope

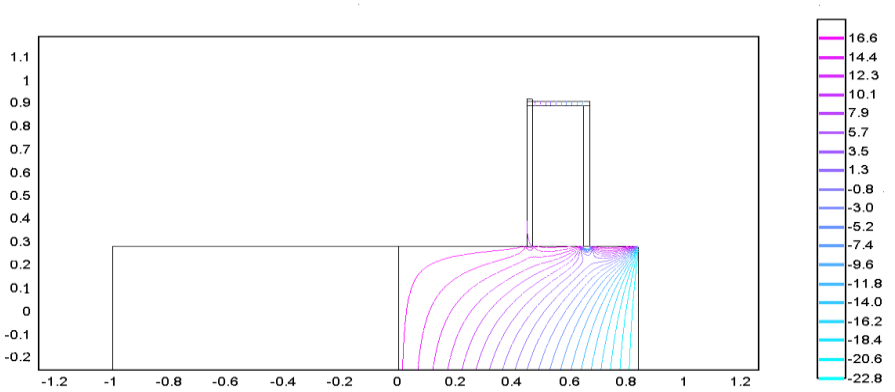

Figure 2a. Isotherms of the side section of the window slope (simplified view)

Here, the constructional layer of reinforced concrete with thermal conductivity λ_{cl} = 2.04 W/(m•K) and thickness δ_{cl} = 0.2 m is located on the left, from the room side; and the thermal insulation one, with λ_{ti} = 0.035 W/(m•K) and δ_{ti} = 0.16 m, on the right. Herewith, 0.2 m of width or thickness of the structure corresponds to one unit of the coordinate grid. Let's note that the constructional layer presence has almost no effect on the distribution of isotherms. As a matter of fact, its thermal resistance away from the thermal non-uniformities equals to δ_{cl}/λ_{cl} = 0.2/2.04 = 0.1 m²•K/W, which is only two percent of the total conditional heat transmission resistance of the wall, which can be estimated by the value

$R_{o.cond}$ = 4.85 m²•K/W. Therefore, this layer can be added to the conventional layer associated with heat exchange on the inner surface. Then $\delta_o = \lambda_{ti} = (1/\alpha_{in} + \delta_{cl}/\lambda_{cl})$.

Results and Discussion

In paper [23] and some other sources, it is indicated that the zone of thermal non-uniformity influence extends to a distance from it, roughly equal to two calibers, with the caliber value which can be taken as the thermal insulation layer thickness. Then we can assume that, with $x = \delta_o$ and $y = 2\delta_{ti}$, or, conversely, with $y = \delta_o$ and $x = 2\delta_{ti}$, the dimensionless temperature θ_{slope} in the expression (1) coincides with the temperature on the inner wall surface away from the slope θ_{in}, which, obviously, is equal to $1 - R_{in}/R_{o.cond}$. Here, $R_{in} = 1/\alpha_{in}$ is heat exchange resistance on the inner surface, m²•K/W (Figure 3).

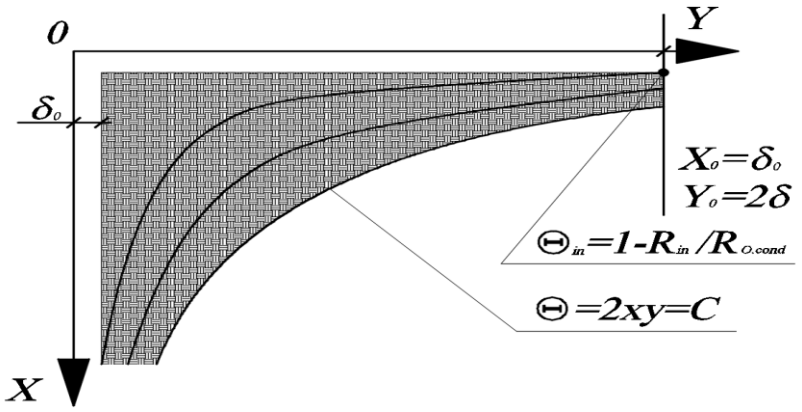

Figure 3. Theoretical distribution of the temperature field at the outer surface of the angle

Consequently, on one side there is $2xy = 4\delta_o\delta_{ti}$, from which $y = 2\delta_o\delta_{ti}/x$, and, simultaneously, for arbitrary y in case of single-layer structure, the current thermal resistance from the inner surface, taking into account the additional layer, is equal $R_y = y/\lambda_{ti}$. Then we get:

$$\theta = 1 - \frac{y/\lambda_{ti}}{\delta_{ti}/\lambda_{ti}} = 1 - \frac{y}{\delta_{ti}} = 1 - \frac{2\delta_o\delta_{ti}/x}{\delta_{ti}} = 1 - \frac{2\delta_o}{x} \quad (5)$$

Thus, it appears that as the window block abutting moves away from the origin of coordinates, for which the vertex of the angle of the thermal insulation layer is taken, i.e., with the approach of the filling to the outer plane of the facade, the relative temperature value should increase gradually.

Figure 4 shows a comparison of τ_{slope} values obtained by direct calculation using a computer program (solid line), and by calculation according to the expression (5) – dotted line.

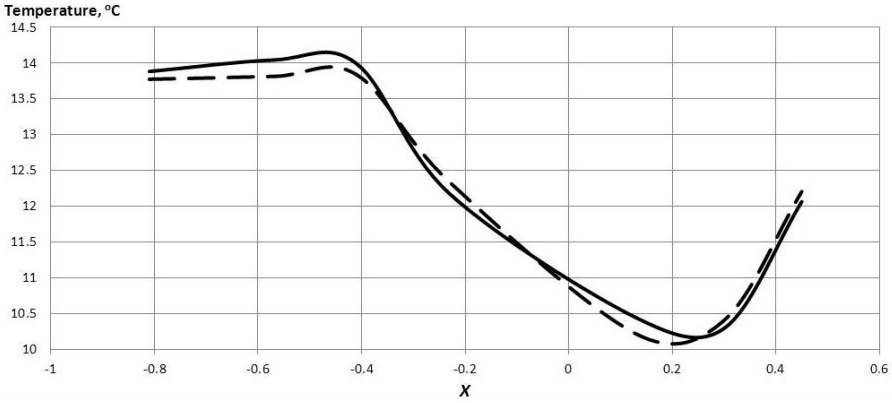

Figure 4. Values of the minimum temperature τ_{slope} by changing the window block position

In the transition to the dimensional values, it was thought that t_{in} = +20°C, t_{ex} = -25°, as is the case with Figure 2 plotting. It can be noted that both curves have quite good qualitative and quantitative matching, which was further improved by a certain modification (5). Basically it resolved itself to the fact

that, while calculating δ_o, the conditional equivalent thermal conductivity of the wall was used, reduced to a single-layer embodiment: $$\lambda_{\text{cond}} = \frac{\delta_{\text{ti}} + \delta_{\text{cl}}}{\delta_{\text{ti}}/\lambda_{\text{ti}} + \delta_{\text{cl}}/\lambda_{\text{cl}}}$$ and, moreover, the value *x* was substituted with some shift: 0.13 m within the constructional layer, and 0.05 m – in the thermal insulation one. It is easy to see that the theoretical expression (5) subject to the adopted amendments is confirmed very well. Moreover, the minimum temperature in figure 4 coincides well with the theoretical temperature at the edge of the corner [11], if the value of R_{in} to be set taking into account the thermal resistance of the structural layer $1/\alpha_{in} + \delta_{cl}/\lambda_{cl}$:

$$\theta_{\text{cor}} = 1 - \frac{R_{\text{in}}}{R_{\text{o.cond}}} + \frac{1}{2}\left(\frac{R_{\text{in}}}{R_{\text{o.cond}}}\right)^2 - \sqrt{\frac{R_{\text{in}}}{2R_{\text{o.cond}}}} + \left(\frac{1}{\sqrt{2}} - \frac{1}{2}\right)\left(\frac{R_{\text{in}}}{R_{\text{o.cond}}}\right)^{3/2}, \quad (6)$$

where for higher adopted $R_{o.cond}$ we get $\theta_{cor} = 0.19$, and therefore $\tau_{cor} = 20 - 0.19 \cdot (20 + 25) = 11.45$ °C. We should also pay attention to the fact that the resistance to heat transfer on the inner surface of the glazing, of course, is different from the resistance on the inner surface of the wall R_{in}, but in this case it is not critical, since in the theoretical formula (5), which compares the data of numerical calculation, this resistance does not appear anywhere.

The result is also consistent with the concept of the distribution of the temperature field in the area of contiguity of translucent structures to building openings, considered in [13–15], although their authors don't present the specific analytical dependences similar to (5), and with recommendations for the implementation of energy saving measures presented in [3], [6], [8], [19]. Thus, the proposed solution is qualitatively confirmed by other sources and is therefore sufficiently reliable.

Conclusions

1. It is shown that the presentation (5) basically corresponds to the actual distribution of the temperature field in the zone of the window slope abutting to the light-opening filling, and therefore, the results obtained by numerical calculation, are also valid.

2. It is discovered that the minimum value τslope is obtained by placing the window unit within the insulating layer near its boundary with the constructional one.

3. It is noted that the preferred installation of the window block is from the room side within the constructional layer, as the one which mostly meets sanitary and hygienic safety requirements. Otherwise there might be condensation of water vapor in the zone of contiguity since the calculated value τslope may be below the dew point of the interior air.

4. It is noted that the expression (5) is the main form of the theoretical description of the temperature distribution in the area of the window reveal and can be considered as the most significant result of the study.

5. It is proposed to apply the relations of the type (5) in some cases and for analytical assessment of minimum temperature, which will allow using not only program-based, but also engineering methods of verification of compliance with sanitary and hygiene norms.

6. It is found that the greatest accuracy of the engineering method is achieved by calculating the thickness of the additional conditional layer δo using conditional equivalent thermal conductivity of the wall λcond. In this case, the maximum error does not exceed 0.5 °C.

References

1. Gorshkov A.S., Vatin N.I., Ryimkevich P.P. Realizatsiya gosudarstvennoy programmyi povyisheniya energeticheskoy effektivnosti zhilyih i obschestvennyih zdaniy [Realization of a State Program of Increase of Power Efficiency of Residential and Public Buildings]. *Construction materials, equipment, XXI centuries technologies.* 2014. No. 1. Pp. 39–46. (rus)
2. Jedinák R. Energy efficiency of building envelopes. *Advanced Materials Research.* 2013. No. 855. Pp. 39-42.
3. Friess W.A, Rakhshan K., Hendawi T.A., Tajerzadeh S. Wall insulation measures for residential villas in Dubai: A case study in energy efficiency. *Energy and Buildings.* 2012. No. 44. Pp. 26–32.

Литература

1. Горшков А.С., Ватин Н.И., Рымкевич П.П. Реализация государственной программы повышения энергетической эффективности жилых и общественных зданий // Строительные материалы, оборудование, технологии XXI века. 2014. № 1. С. 39–46.
2. Jedinák R. Energy efficiency of building envelopes // Advanced Materials Research. 2013. No. 855. Pp. 39–42.
3. Friess W.A, Rakhshan K., Hendawi T.A., Tajerzadeh S. Wall insulation measures for residential villas in Dubai: A case study in energy efficiency // Energy and Buildings. 2012. № 44. Pp. 26–32.
4. Гагарин В.Г., Пастушков П.П. Об оценке энергетической эффективности энергосберегающих мероприятий //

Samarin O.D. Temperature in linear elements of enclosing structures. *Magazine of Civil Engineering.* 2017. No. 2. Pp. 3–10. doi: 10.5862/MCE.70.1

4. Gagarin V.G., Pastushkov P.P. Ob otsenke energeticheskoy effektivnosti energosberegayuschih meropriyatiy [About an Assessment of Power Efficiency of Energy Saving Actions]. *Engineering systems. AVOK NORTH-WEST.* 2014. No. 2. Pp. 26–29. (rus)
5. Hani A., Koiv T.-A. Energy consumption monitoring analysis for residential, educational and public buildings. *Smart Grid and Renewable Energy.* 2012. Vol. 3. No. 3. Pp. 231–238.
6. Paiho S., Abdurafikov R., Hoang H. Cost analyses of energy-efficient renovations of a Moscow residential district. *Sustainable Cities and Society.* 2015. Vol. 14. No. 1. Pp. 5–15.
7. Dylewski R., Adamczyk J. Economic and ecological indicators for thermal insulating building investments. *Energy and Buildings.* 2012. No. 54. Pp. 88–95.
8. Lapinskiene V., Paulauskaite S., Motuziene V. The analysis of the efficiency of passive energy saving measures in office buildings. *Papers of the 8th International Conference "Environmental Engineering".* Vilnius, 2011. Pp. 769–775.
9. Gagarin V.G., Dmitriev K.A. Uchet teplotekhnicheskikh neodnorodnostey pri ocenke teplozashchity ograzhdayushchikh konstrukciy v Rossii i evropeyskikh stranakh [Account of thermal non-uniformities during estimation of thermal performance of building enclosures in Russia and European countries]. *Construction materials.* 2013. No. 6. Pp. 14–16. (rus)
10. Gagarin V.G., Kozlov V.V. Teoreticheskiye predposylki rascheta privedennogo soprotivleniya teploperedache ograzhdayushchikh konstrukciy [Theoretical reasons for calculation of reduced thermal resistance of building enclosures]. *Construction materials.* 2010. No. 12. Pp. 4–12. (rus)
11. Samarin O.D. Raschet temperatury na vnutrenney poverkhnosti naruzhnogo ugla zdaniya s sovremennym urovnem teplozashchity [Calculation of temperature in the internal surface of the external corner of a building with modern level of thermal protection]. *News of Higher Educational Institutions. Construction.* 2005. No. 8. Pp. 52–56. (rus)
12. Parfentyeva N., Samarin O., Lushin K., Paulauskaitė S. The numerical and analytical methods of calcula-tions of two-dimensional temperature fields in dangerous members of building enclosures. *Proceedings of 7th conference Environmental Engineering.* Vilnius: VGTU Publishers, 2008. Pp. 854–858.
13. Krivoshein A.D. K voprosu o proektirovanii teplovoy zashityi svetoprozrachnyikh I neprozrachnyikh konstruktsiy [On the question of design of thermal protection of translucent and opaque constructions]. [Electronic resource]. URL: http://odf.ru/k-voprosu-o-proektirovanii-tep-article_579.html (date of application: 28.02.2016) (rus)
14. Verkhovsky A.A., Nanasov I.I., Yelizarova E.V., Galtsev D.I., Shcheredin V.V. Novyi podkhod k otsenke energoeffektivnosti svetoprozrachnykh konstruktsiy [A new approach to the estimation of energy efficiency of transparent constructions]. *Transparent constructions.* 2012. No. 1(81). Pp. 10–15. (rus)
15. Kornienko S.V. Metod resheniya trekhmernoy zadachi sovmestnogo nestacionarnogo teplo- i vlagoperenosa dlya ograzhdayushchikh konstrukciy zdaniy [The procedure of solving the three-dimensional problem of joint heat and moisture transfer for the building enclosures]. *News of Higher Educational Institu-tions. Construction.* 2006. No. 2. Pp. 108–110. (rus)
16. Brunner G. Heat transfer. *Supercritical fluid science and technology.* 2014. Vol. 5. Pp. 228–263.
17. Horikiri K., Yao Y., Yao J. Modelling conjugate flow and heat transfer in a ventilated room for indor thermal comfort assessment. *Building and Environment.* 2014. Vol. 77. Pp. 135–147.
18. Yun T.S., Jeong Y.J., Han T.-S., Youm K.-S. Evaluation of

Инженерные системы. АВОК-Северо-Запад. 2014. № 2. С. 26–29.

5. Hani A., Koiv T.-A. Energy consumption monitoring analysis for residential, educational and public buildings // Smart Grid and Renewable Energy. 2012. Vol. 3. № 3. Pp. 231–238.
6. Paiho S., Abdurafikov R., Hoang H. Cost analyses of energy-efficient renovations of a Moscow residential district. Sustainable Cities and Society. 2015. № 14. Pp. 5–15.
7. Dylewski R., Adamczyk J. Economic and ecological indicators for thermal insulating building investments // Energy and Buildings. 2012. № 54. Pp. 88–95.
8. Lapinskiene V., Paulauskaite S., Motuziene V. The analysis of the efficiency of passive energy saving measures in office buildings // Papers of the 8th International Conference "Environmental Engineering". Vilnius. 2011. Pp. 769–775.
9. Гагарин В.Г., Дмитриев К.А. Учет теплотехнических неоднородностей при оценке теплозащиты ограждающих конструкций в России и европейских странах // Строительные материалы. 2013. № 6. С. 14-16.
10. Гагарин В.Г., Козлов В.В. Теоретические предпосылки расчета приведенного сопротивления теплопередаче ограждающих конструкций // Строительные материалы. 2010. № 12. С. 4–12.
11. Самарин О.Д. Расчет температуры на внутренней поверхности наружного угла здания с современным уровнем теплозащиты // Известия вузов. Строительство. 2005. № 8. С. 52–56.
12. Parfentyeva N., Samarin O., Lushin K., Paulauskaitė S. The numerical and analytical methods of calculations of two-dimensional temperature fields in dangerous members of building enclosures // Proceedings of 7th conference «Environmental Engineering». Vilnius: VGTU Publishers, 2008. Pp. 854–858.
13. Кривошеин А.Д. К вопросу о проектировании тепловой защиты светопрозрачных и непрозрачных конструкций [Электронный ресурс]. URL: http://odf.ru/k-voprosu-o-proektirovanii-tep-article_579.html (дата обращения: 28.02.2016).
14. Верховский А.А., Нанасов И.И., Елизарова Е.В., Гальцев Д.И., Щередин В.В. Новый подход к оценке энергоэффективности светопрозрачных конструкций // Светопрозрачные конструкции. 2012. № 1(81). С. 10–15.
15. Корниенко С.В. Метод решения трехмерной задачи совместного нестационарного тепло- и влагопереноса для ограждающих конструкций зданий // Известия высших учебных заведений. Строительство. 2006. № 2. С. 108–110.
16. Brunner G. Heat transfer // Supercritical fluid science and technology. 2014. № 5. Pp. 228–263.
17. Horikiri K., Yao Y., Yao J. Modelling conjugate flow and heat transfer in a ventilated room for indor thermal comfort assessment // Building and Environment. 2014. № 77. Pp. 135–147.
18. Yun T.S., Jeong Y.J., Han T.-S., Youm K.-S. Evaluation of thermal conductivity for thermally insulated concretes // Energy and Buildings. 2013. № 61. Pp. 125–132.
19. Kracka M., Zavadskas E. K., Brauers W. K. M. Ranking heating losses in a building by applying the multimoora // Engineering Economics. 2010. Vol. 21. № 4. Pp. 352–359.
20. ASHRAE. Standard method for determining and expressing the heat transfer and total optical properties of fenestration products, public review draft of standard 142P // American Society of Heating, Refrigerating and Air Conditioning Engineers. Atlanta, 1998.
21. ISO 15099:2003. Thermal performance of windows, doors and shading devices – Detailed calculations. ISO/TC 163/SC 2 Calculation methods. Geneva, 2003. 71 p.

Самарин О.Д. Температура в линейных элементах ограждающих конструкций // Инженерно-строительный журнал. 2017. № 2(70). С. 3–10.

thermal conductivity for thermally insulated concretes. *Energy and Buildings.* 2013. Vol. 61. Pp. 125–132.

19. Kracka M., Zavadskas E.K., Brauers W.K.M. Ranking heating losses in a building by applying the multimoora. *Engineering Economics.* 2010. Vol. 21. No. 4. Pp. 352–359.
20. ASHRAE. Standard method for determining and expressing the heat transfer and total optical properties of fenestration products, public review draft of standard 142P. *American society of heating, refrigerating and air conditioning engineers.* Atlanta, 1998.
21. *ISO 15099:2003.* Thermal performance of windows, doors and shading devices – Detailed calculations. ISO/TC 163/SC 2 Calculation methods. Geneva, 2003. 71 p.
22. *THERM. Two-Dimensional Building Heat-Transfer Modeling* [Electronic resource]. URL: https://windows.lbl.gov/software/therm/therm.html (date of application: 04.03.2017).
23. Bogoslovsky V.N. Stroitel'naya teplofizika [Building thermal physics]. St.Petersbourg: AVOK SEVERO-ZAPAD Publishers, 2006. 400 p. (rus)

22. THERM. Two-Dimensional Building Heat-Transfer Modeling [Электронный ресурс]. URL: https://windows.lbl.gov/software/therm/therm.html (дата обращения: 04.03.2017).
23. Богословский В.Н. Строительная теплофизика. СПб.: АВОК Северо-Запад, 2006. 400 с.

Oleg Samarin,
+7(916)1077701; samarin-oleg@mail.ru

Олег Дмитриевич Самарин,
+7(916)1077701;
эл. почта: samarin-oleg@mail.ru

Samarin O.D. Temperature in linear elements of enclosing structures. *Magazine of Civil Engineering.* 2017. No. 2. Pp. 3–10. doi: 10.5862/MCE.70.1

doi: 10.18720/MCE.70.2

Moisture transport in the ventilated channel with heating by coil

Влагоперенос в вентилируемом канале с нагревательным элементом

E.A. Statsenko,
T.A. Musorina,
A.F. Ostrovaia,
V.Ya. Olshevskiy,
A.L. Antuskov,
Peter the Great St. Petersburg Polytechnic University, St. Petersburg, Russia

Студент Е.А. Стаценко,
студент Т.А. Мусорина,
студент А.Ф. Островая,
аспирант В.Я. Ольшевский,
студент А.Л. Антуськов,
Санкт-Петербургский политехнический университет Петра Великого, г. Санкт-Петербург, Россия

Key words: buildings; ventilated facades; moisture transport; facing layer; thermal insulation; air gap; heating coil

Ключевые слова: здания; вентилируемый фасад; влагоперенос; облицовочный слой; теплоизоляция; воздушный зазор; нагревательный элемент

Abstract. This article considers the moisture transport phenomenon in the vertical ventilated channel. HVF construction parameters are determined influencing the rate of moisture transport. It is necessary to have h ≤ L/25 ≈ 8 cm. The greatest air movement is created in the construction with the open rustications. The optimal location of the heat sources on the channel height, as well as their favorable combination from the point of view for the process of drying the outer surface of the thermal insulation material, was identified. The air velocity dependences on height of an air gap are determined and it was found that the greatest values taken at the maximum height velocity. Ratio between the moisture transport and the distance to the heat source is installed. Drying processes are compared with the various combinations of heat sources. The direct dependence of the vaporation weight rate of the time is installed.

Аннотация. В данной статье изучается явление влагопереноса в вертикальном вентилируемом канале. Определяются параметры конструкции НВФ, оказывающие влияние на скорость влагопереноса. Необходимо иметь h ≤ L/25 ≈ 8 см. Наибольшее движение воздуха создается в конструкции с открытыми рустами. Выявлено оптимальное расположение источников тепла по высоте канала, а также их выгодные сочетания с точки зрения процесса высушивания наружной поверхности теплоизоляционного материала. В результате исследования скорости движения воздуха по высоте вентилируемого зазора, было установлено, что на максимальной высоте скорости принимают наибольшие значения. А также выведено соотношение между массовой скоростью переноса влаги и расстоянием до источника тепла. Сравниваются процессы высушивания при различных сочетаниях нагревательных элементов. Установлена прямая зависимость массовой скорости испарения от времени.

Introduction

In the design of these systems radically affected increasing requirements for heat transmission resistance of enclosure structures. It is a practical impossibility to create a high-quality enclosing parts without using effective thermal insulation materials.

Clearly, the most favorable location of the thermal insulation in the design is its location at the outer surface. This ensures the offset of dewpoint temperature in the stream.

This is the principle used in the HVF constructions.

Fiber thermal insulation material having a high air permeance is most popular for the HVF constructions.

Стаценко Е.А., Мусорина Т.А., Островая А.Ф., Ольшевский В.Я., Антуськов А.Л. Влагоперенос в вентилируемом канале с нагревательным элементом // Инженерно-строительный журнал. 2017. № 2(70). С. 11–17.

Modern fibrous mineral-cotton materials have low density, their use is economic. The lower the density of the mineral wool, the higher its air permeance. This parameter has an effect on moisture removal rate from the ventilated gap.

The moisture transport is the process of the movement of moisture which represents transfer of vacant and physically-bounded water under the influence of gravitational and sorption (molecular and capillary) forces.

The control of moisture level is necessary is necessary to create an optimum operating conditions of the ventilated facade. The timely identification of excessive moisture appearance sources avoids the adverse effects of excessive moistening such as corrosion of metal products and parts, destruction of concrete, stone and brickwork during freezing and thawing, the color change of the building architectural detail, biological damage and deterioration of thermal properties.

Thus, quantitative calculation of moisture transfer is one of the most important in the multilayered enclosure structure designing.

This article conditions conducive to the most optimal process of removing moisture from the hinged ventilated facade gap by simulating moisture transport processes in different parameters HVF model are formulated.

A special contribution to the study of moisture transport process in the vertical ventilated channel was made by [1-24].

In this work [1] is investigated the impact of the presence of the technological gaps (rustication) the rate of air flow in the gap. The speed dependence on the width of the ventilated gap is established empirically for the construction with open and closed rustications.

The authors identify in the article [2] the conditions under which there is a cold air filtration in the ventilated gap. The publication [3] considers features of work of facades with and without rustications. The article [11] is assessed the effect of moisture transport on the dispersed and cellular materials. The authors of the publication [14] define adequate existence conditions of the free convection stream in the vertical conduit. In the work [22] consider issues of a natural ventilation of the vertical channel. In the work [27] the wall building with the ventilated facade thermal protection taking into account a longitudinal air filtration are investigated.

Purpose and goals of article are:

- to determine the most effective combination of heat sources depending on the air velocity in the gap.
- to consider the influence of the sources location of mechanical heat on the moisture transfer in the HVF gap.
- to determine the mass rate of moisture vaporization.
- to identify the mass velocity dependence on the distance from the heat source.

Methods and Results

The imperfection of building structures leads to their excessive moistening. Therefore, more and more attention is given to the moisture accumulation ability of materials and the possibility of their drying out. The majority of the moisture control methods are focused on reducing the heat- and moisture input into the air gap.

The main reason for the movement of moisture in the HVF construction is a difference of humidity, temperature and differential pressure of the air-steam mixture in the material. A zone of the greatest moistening is the layer of a mineral wool heat insulation adjoining the gap. Let us consider its rate of drying for different parameters HVF design.

To identify the optimal design parameters for the study of moisture vented we will consider the stylized scheme of the ventilated gap between the "hot" plane y = 0 (with T_h = 67 °C) and the cold plane y = h (with T_c = 22 °C).

Heating is provided with three heating elements located throughout the height of the installation. For equal distribution of heat elements attach to a tin sheet, therefore T_h = const. The model height is equal to L = 204 cm, and $L \gg h$. While producing a facade sample we consider the temperature

Statsenko E.A., Musorina T.A., Ostrovaia A.F., Olshevskiy V.Ya., Antuskov A.L. Moisture transport in the ventilated channel with heating by coil. *Magazine of Civil Engineering*. 2017. No. 2. Pp. 11–17. doi: 10.18720/MCE.70.2

difference of external and internal layers proved by performance of heating systems. The model considers wall heating and heat input from it in the air layer. The external air is supposed to come into the air layer through the lower air hole. It rises through the ventilated channel and leaves through the top air holes. Air temperature increases and its relative moisture changes during the rise. At the same time moisture increases throughout the height of the layer [1]. To conduct this experiment a different combination of heat sources: “lower-middle”, “lower-upper”, “middle-upper” are used.

To identify an optimum variant for the study of moisture transport construction it is necessary to know the air velocity in the gap. It depends on the supply air method into the installation - with open or pressurized rustications.

Let us carry out an experiment. We measure the air velocity inside the HVF model depending on the gap width with and without rustications with various combinations of heat sources. We use thermal anemometer for measurement.

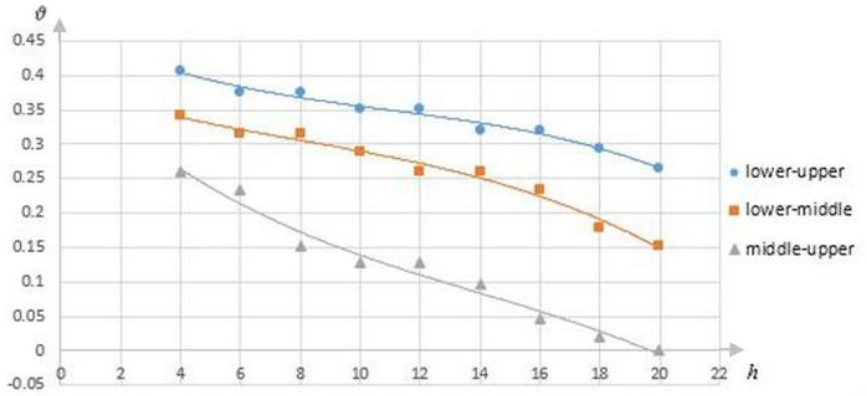

Figure 1. Sealed rustications

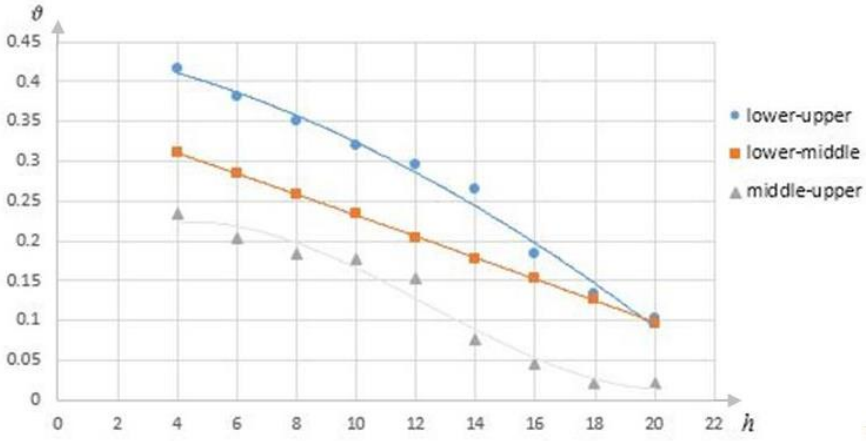

Figure 2. Open rustications

From the resulting graphs it follows that:

- the most air movement is created in the open rustications, because of the greater volume of heated air, as well as of various combinations of heat sources.
- in the design with a sealed rustications – "perfect channel" – is the air volume is less because the current is only from the bottom, reducing the drying speed.
- the most disadvantageous of the considered combination is the combination of heating elements – “middle-upper”. This is due to the fact that the air is not heated when entering to the canal at the bottom of the battery, and there is no difference in temperature, therefore, there is no active air movement. Basically, the current is through the rustications, involving the construction of cold air. At the same time the height velocity decreases and tends to zero when large gaps.

We will use mineral-cotton samples 95 x 210 x 50 mm for further experience. The dry sample weight is 140 g. The wetted sample weight is 160 g.

We will put the first sample in the HVF air gap with a combination of batteries “lower-middle”, the second sample with a combination of “lower-upper” and will consistently record the mass at regular intervals under the above combinations of heating elements.

To simulate channel is necessary to have L/h ≥ 25, $h \leq \frac{L}{25} \approx 8\ cm$ [1].

We will find a mass rate of vaporization for each measurement:

$$m^* = \frac{\Delta m}{\Delta t} \tag{1}$$

where Δm – the mass difference of two consecutive measurements, Δt – the interval between measurements, Δt = 600 s.

We will construct a dependency graph of the mass velocity m^* on the distance from a moisture source for height z to of the heating element.

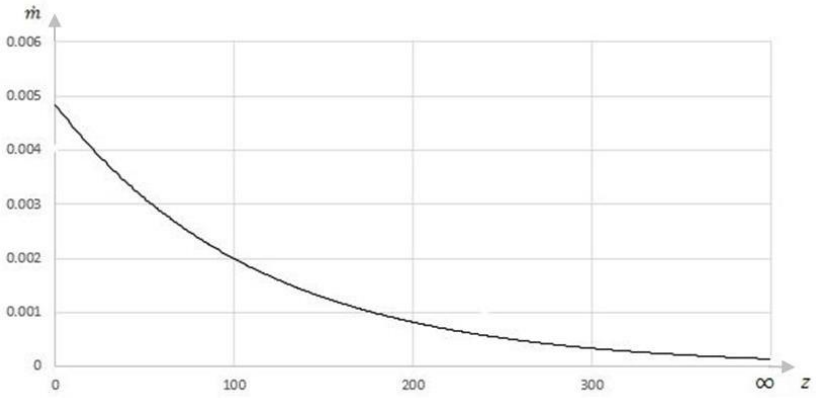

Figure 3. The dependency graph of the mass velocity on the distance from a moisture source for height.

It can be observed that in the case when the lower battery is disconnected, the current is not carried out, the mass transfer rate in the model equivalent to the mass transfer rate in natural conditions, therefore, the chosen combination is enabled the lower heat source are optimal.

Thus, it was established that the combination of “lower-middle”, “lower-upper” with open rustications are the best for mass transfer mechanisms studying in the HVF construction.

The average mass rate of vaporization are:

$m_1^* = \frac{\Delta m}{\Delta t} = \frac{13}{5400} = 0.0024$, combination of “lower-middle”,

$m_2^* = \frac{\Delta m}{\Delta t} = \frac{14}{5400} = 0.0026$ combination of “lower-upper”.

Thus, it was established that the maximum mass transfer rate is observed at the open rustications.

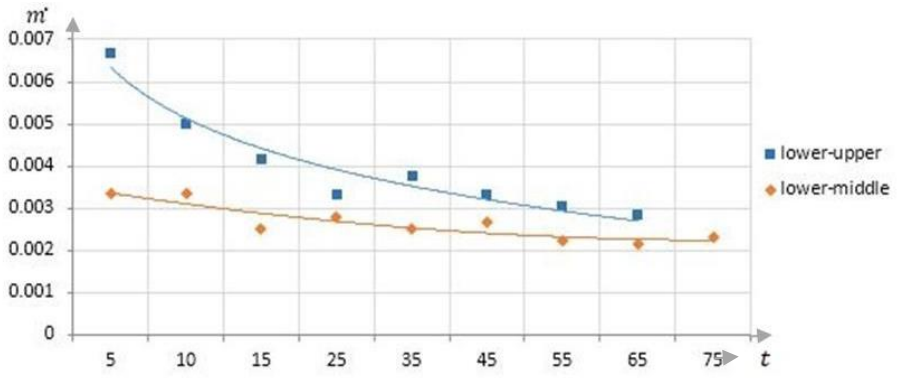

Figure 4. Dependence of m^* on t

Statsenko E.A., Musorina T.A., Ostrovaia A.F., Olshevskiy V.Ya., Antuskov A.L. Moisture transport in the ventilated channel with heating by coil. *Magazine of Civil Engineering*. 2017. No. 2. Pp. 11–17. doi: 10.18720/MCE.70.2

Thus, it was established that the maximum mass transfer rate is observed at the open rustications.

Obviously, the rate of vaporization repeated the air velocity. The greater the air velocity, the greater the rate of vaporization.

The highest velocity values were observed when combinations of heat sources “lower-upper”.

We give a graph of air velocity in the HVF gap on the installation height.

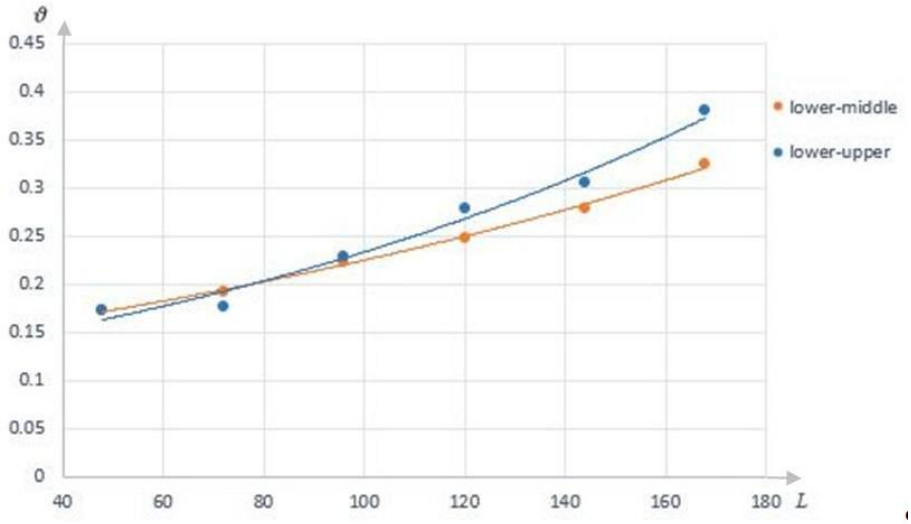

Figure 5. Dependence air velocity in the HVF gap on the installation height

Based on the obtained results, it may be concluded that that the greatest values taken at the maximum height of the velocity. Therefore, the installation upper part is the most favorable location for the study of mass transfer.

Discussion

The great bulk of work on this topic is aimed at the moisture transport mechanisms study from the point of view of physics, practical tests was conducted [10, 25–26]. In this article the emphasis is placed on the experimental determination of the air flow dependences in the ventilated facade channel.

In the articles of other authors on the same topic is assumed constant the temperature of the warm surface wall ($T_h = const$), whereas in this study the effect of the variable position of the heat sources.

Conclusions

Building humidity control is a key condition of increase of their durability, effective use and a healthy microclimate.

On the ground of the experiments we draw the following conclusions:

- the greatest air movement is created in the construction with the open rustications because of larger volume of heated air, as well as the use of different heat combinations, which contributes to the process of moisture transfer.
- the heating the air at the entrance of channel is not when the heat source is off , and there is no difference in temperature, consequently, there is no active air movement.
- the greatest values taken at the maximum height velocity.]

References

1. Musorina T., Olshevskyi V., Ostrovaia A., Statsenko E. Experimental assessment of moisture transfer in the vertical ventilated channel. *MATEC Web of Conferences, TPACEE*. 2016. Vol. 73. Pp. 02002.
2. Nemova D.V., Olshevskyi V.Ja., Cejtin D.N. Gidrostatika termogravitacionnoj konvekcii v vertikal'nom kanale [Hydrostatics of thermogravitational convection in the vertical channel]. *Nauchno-tehnicheskie vedomosti*

Литература

1. Musorina T., Olshevskyi V., Ostrovaia A., Statsenko E. Experimental assessment of moisture transfer in the vertical ventilated channel // MATEC Web of Conferences, TPACEE 2016. Vol. 73. Pp. 02002.
2. Немова Д.В., Ольшевский В.Я., Цейтин Д.Н. Гидростатика термогравитационной конвекции в вертикальном канале // Научно-технические ведомости Санкт-Петербургского государственного

Стаценко Е.А., Мусорина Т.А., Островая А.Ф., Ольшевский В.Я., Антуськов А.Л. Влагоперенос в вентилируемом канале с нагревательным элементом // Инженерно-строительный журнал. 2017. № 2(70). С. 11–17.

SPBGPU. 2013. No. 4-1 (183). Pp. 295–301. (rus)

3. Vatin N., Petrichenko M., Nemova D., Staritcyna A., Tarasova D. Renovation of educational buildings to increase energy efficiency. *Applied Mechanics and Materials.* 2014. Vol. 633–634. Pp. 1023–1028.
4. Nemova D.V., Emel'janova V.A., Miftahova D.R. Jeksperimental'nye zadachi rascheta svobodnokonvektivnyh dvizhenij v navesnyh ventiliruemyh fasadah [Experimental problems of calculation the free-convection movements in the hinged ventilated facades]. *Magazine of Civil Engineering.* 2010. No. 8. Pp. 46–53. (rus)
5. Emel'janova V.A., Nemova D.V., Miftahova D.R. Optimizirovannaja konstrukcija navesnogo ventiliruemogo fasada [The optimized design of the hinged ventilated facade]. *Magazine of Civil Engineering.* 2014. No. 6. Pp. 67–74. (rus)
6. Petrichenko M.R. Convective heat and mass transfer in combustion chambers of piston engines. Basic results. Heat transfer. *Soviet research*. 1991. Vol. 5. No. 23. Pp. 703–715.
7. Ostrovaja A.F., Petrichenko M.R., Stacenko E.A. The glass ventilated facades. Research of an air gap. *Applied Mechanics and Materials.* 2015. Pp. 725–726.
8. Petrichenko M.R. Rasshcheplyayushchie razlozheniya v predel'nyh zadachah dlya obyknovennyh kvazilinejnyh differencial'nyh [The splitting decomposition in limit tasks for the ordinary quasilinear differential equations]. *Second Edition St. Petersburg State Polytechnical University Journal. Physics and Mathematics.* 2012. Pp. 143–149. (rus)
9. Petrichenko M.R., Petrochenko M., Yevtushenko E.B., Gidravlicheski optimal'naya ventiliruemaya shchel' [Hydraulically optimum ventilated gap]. *Magazine of Civil Engineering.* 2013. No. 2 (37). Pp. 35–40. (rus)
10. Vatin N., Petrichenko M., Nemova D. Hydraulic methods for calculation of system of rear ventilated facades. *Applied Mechanics and Materials.* 2014. Vol. 633–634. Pp. 1007–1012.
11. Gamajunov N.I., Gamajunov S.N. Massoperenos v poristyh i dispersnyh materialah [Mass transfer in porous and disperse materials]. *Vestnik TvGTU.* 2012. Vol. 22. No. 128. Pp. 46–54. (rus)
12. Kornienko S.V. Testirovanie metoda rascheta temperaturno-vlazhnostnogo rezhima ograzhdajushhih konstrukcij na rezul'tatah naturnyh izmerenij parametrov mikroklimata pomeshhenij [Testing of a method of calculation of temperature moisture conditions of the protecting designs on results of natural measurements of parameters of a microclimate of rooms]. *Magazine of Civil Engineering.* 2012. No. 2(28). Pp. 18-23. (rus)
13. Kornienko S.V. Kompleksnaja ocenka teplozashhity ograzhdajushhih konstrukcij obolochki zdanija [Complex assessment of a heat-shielding of the protecting building cover designs]. *Magazine of Civil Engineering.* 2012. No. 7. Pp. 43–49. (rus)
14. Petrichenko M.R., Petrochenko M.V. Dostatochnye uslovija sushhestvovanie svobodno-konvektivnogo techenija v vertikal'nom shhelevom kanale [Sufficient conditions existence of a free and convective current in the vertical slot-hole channel]. *Nauchno-tehnicheskie vedomosti SPBGPU.* 2012. No. 2. (rus)
15. Petrosova D.V. *Neizotermicheskaja fil'tracija vozduha cherez ograzhdajushhie konstrukcii zamknutyh pomeshhenij* [Not isothermal filtration of air through the protecting designs of the closed rooms]. Sankt-Peterburg, 2012. 118 p. (rus)
16. Yevtushenko E.B., Petrochenko M.V. Diffuzornaya konstrukciya navesnogo ventiliruemogo fasada [The diffuser design of ventilated facades]. *Magazine of Civil*

политехнического университета. 2013. № 4-1(183). С. 295–301.

3. Vatin N., Petrichenko M., Nemova D., Staritcyna A., Tarasova D. Renovation of educational buildings to increase energy efficiency // Applied Mechanics and Materials. 2014. Vols. 633–634. Pp. 1023–1028.
4. Немова Д.В., Емельянова В.А., Мифтахова Д.Р. Экстремальные задачи расчета свободноконвективных движений в навесных вентилируемых фасадах // Инженерно-строительный журнал. 2010. № 8. С. 46–53.
5. Емельянова В.А., Немова Д.В., Мифтахова Д.Р. Оптимизированная конструкция навесного вентилируемого фасада // Инженерно-строительный журнал. 2014. № 6. С. 67–74.
6. Petrichenko M.R. Convective heat and mass transfer in combustion chambers of piston engines. Basic results. Heat transfer // Soviet research. 1991. Vol. 5. № 23. Pp. 703–715.
7. Ostrovaja A.F., Petrichenko M.R., Stacenko E.A. The glass ventilated facades. Research of an air gap // Applied Mechanics and Materials. 2015. Vols. 725–726. Pp. 725–726.
8. Петриченко М.Р. Расщепляющие разложения в предельных задачах для обыкновенных квазилинейных дифференциальных уравнений // Научно-технические ведомости Санкт-Петербургского государственного политехнического университета. 2012. С. 143–149.
9. Петриченко М.Р., Петроченко М.В., Явтушенко Е.Б. Гидравлически оптимальная вентилируемая щель // Инженерно-строительный журнал. 2013. № 2(37). С. 35–40.
10. Vatin N., Petrichenko M., Nemova D. Hydraulic methods for calculation of system of rear ventilated facades // Applied Mechanics and Materials. 2014. Vols. 633–634. Pp. 1007–1012.
11. Гамаюнов Н.И., Гамаюнов С.Н. Массоперенос в пористых и дисперсных материалах //Вестник ТвГТУ. 2012. № 128(22). С. 46–54.
12. Корниенко С.В. Тестирование метода расчета температурно-влажностного режима ограждающих конструкций на резкльтаттах натурных измерений параметров микроклимата помещений // Инженерно-строительный журнал. 2012. №. 2. С. 18–23.
13. Корниенко С.В. Комплексная оценка теплозащиты ограждающих конструкций оболочки здания // Инженерно-строительный журнал. 2012. №. 7. С. 43–49.
14. Петриченко М.Р., Петроченко М.В. Достаточные условия существование свободно-конвективного течения в вертикальном щелевом канале // Научно-технические ведомости Санкт-Петербургского государственного политехнического университета. 2012. №. 2(147). С. 276-282.
15. Петросова Д.В. Неизотермическая фильтрация воздуха через ограждающие конструкции замкнутых помещений. Автореферат дисс на соиск. учен. степ. к.т.н.: Спец. 05.23.16. СПб: Сакнт-Петерубргский государственный политехнический университет, 2012. 118 с.
16. Явтушенко Е.Б., Петроченко М.В. Диффузорная конструкция навесного вентилируемого фасада // Инженерно-строительный журнал. 2013. № 8. С. 38–45.
17. Немова Д.В. Системы вентиляции в жилых зданиях как средство повышения энергоэффективности // Строительство уникальных зданий и сооружений. 2012. № 3. С. 84–86.
18. Петриченко М.Р., Петросова Д.В., Петроченко М.В. Фильтрационный перенос воздухом консервативной

Statsenko E.A., Musorina T.A., Ostrovaia A.F., Olshevskiy V.Ya., Antuskov A.L. Moisture transport in the ventilated channel with heating by coil. *Magazine of Civil Engineering*. 2017. No. 2. Pp. 11–17. doi: 10.18720/MCE.70.2

Engineering. 2013. No. 8. Pp. 38–45. (rus)

17. Nemova D.V. Sistemy ventilyacii v zhilyh zdaniyah kak sredstvo povysheniya ehnergoehffektivnosti [Systems of ventilation in residential buildings as means of increase of energy efficiency]. *Construction of Unique Buildings and Structures.* 2012. Pp. 84–86. (rus)
18. Petrichenko M.R., Petrosova D.V., Petrochenko M.V. Fil'tracionnyj perenos vozduhom konservativnoj primesi (temperatury i teploty) skvoz' stenu [Filtrational transfer by air of conservative impurity (temperature and warmth) through a wall]. *NTV SPbGPU. Fiziko-matematicheskie nauki.* 2012. Pp. 68–72. (rus)
19. Darkwa J., Li J., Chow D.H.C. Heat transfer and air movement behaviour in a double-skin façade. *Centre for Sustainable Energy Technologies (CSET).* 2014. Pp. 198–203.
20. Hana J., Lua L., Penga J. Hongxing Yanga Performance of ventilated double-sided PV facade compared with conventional clear glass façade. *Energy and Buildings.* 2013. Vol. 56. Pp. 204–209.
21. Bukhartsev V.N., Petrichenko M.R. Approximation of the depression curve of the inflow to an ideal trench. *Power Technology and Engineering.* 2011. No. 5. Pp. 374–377.
22. Rosca A.V., Pop I. Flow and heat transfer over a vertical permeable stretching/shrinking sheet with a second order slip. *International Journal of Heat and Mass Transfer.* 2013. Vol. 60. Pp. 355–364.
23. Barrios G., Huelsz G., Rechtman R., Rojas J. Wall/roof thermal performance differences between air- conditioned and non air-conditioned rooms. *Energy and Buildings.* 2011. Vol. 43. Pp. 219–223.
24. Gaillard L., Giroux-Julien S., Menezo C., Pabiou H. Experimental evaluation of a naturally ventilated PV double-skin building envelope in real operating conditions. *Chair Habitats and Energy Innovations.* 2012. Pp. 54–67.
25. Petrichenko M., Vatin N., Nemova D., Kharkov N., Korsun A. Numerical modeling of thermogravitational convection in air gap of system of rear ventilated facades. *Applied Mechanics and Materials.* 2014. Vols. 672–674. Pp. 1903–1908.
26. Olshevskyi V., Statsenko E., Musorina T., Nemova D., Ostrovaia A. Moisture transfer in ventilated facade structures. *MATEC Web of Conferences.* 2016. Vol. 53. Pp. 1–5.

примеси (температуры и теплоты) сквозь стену // Научно-технические ведомости Санкт-Петербургского государственного политехнического университета. 2012. № 4(159). С. 68–72.

19. Darkwa J., Li J., Chow D.H.C. Heat transfer and air movement behaviour in a double-skin façade // Centre for Sustainable Energy Technologies (CSET). 2014. Pp.198–203.
20. Hana J., Lua L., Penga J. Hongxing Yanga Performance of ventilated double-sided PV facade compared with conventional clear glass façade // Energy and Buildings. 2013. Vol. 56. Pp. 204–209.
21. Bukhartsev V.N., Petrichenko M.R. Approximation of the depression curve of the inflow to an ideal trench // Power Technology and Engineering. 2011. No. 5. Pp. 374–377.
22. Rosca A.V., Pop I. Flow and heat transfer over a vertical permeable stretching/shrinking sheet with a second order slip // International Journal of Heat and Mass Transfer. 2013. Vol. 60. Pp. 355–364.
23. Barrios G., Huelsz G., Rechtman R., Rojas J. Wall/roof thermal performance differences between air- conditioned and non air-conditioned rooms // Energy and Buildings. 2011. Vol. 43. Pp. 219–223.
24. Gaillard L., Giroux-Julien S., Menezo C., Pabiou H. Experimental evaluation of a naturally ventilated PV double-skin building envelope in real operating conditions // Chair Habitats and Energy Innovations. 2012. Pp. 54–67.
25. Petrichenko M., Vatin N., Nemova D., Kharkov N., Korsun A. Numerical modeling of thermogravitational convection in air gap of system of rear ventilated facades // Applied Mechanics and Materials. 2014. Vols. 672–674. Pp. 1903–1908.
26. Olshevskyi V., Statsenko E., Musorina T., Nemova D., Ostrovaia A. Moisture transfer in ventilated facade structures // MATEC Web of Conferences. 2016. Vol. 53. Pp. 1–5.

Elena Statsenko,
+7(981)8398538; staclena@mail.ru

Tatiana Musorina,
+7(952)2860376; flamingo-93@mail.ru

Anastasia Ostrovaia,
+7(953)3449063; stasya2609@yandex.ru

Vyacheslav Olshevskiy,
+7(911)9199526; 79119199526@yandex.ru

Anton Antuskov,
+7(921)4257517; antuskov.anton@gmail.com

Елена Александровна Стаценко,
+7(981)8398538; эл. почта: staclena@mail.ru

Татьяна Александровна Мусорина,
+7(952)2860376;
эл. почта: flamingo-93@mail.ru

Анастасия Федоровна Островая,
+7(953)3449063;
эл. почта: stasya2609@yandex.ru

Вячеслав Янушевич Ольшевский,
+79119199526;
эл. почта: 79119199526@yandex.ru

Антон Леонидович Антуськов,
+7(921)4257517;
эл. почта: antuskov.anton@gmail.com

Стаценко Е.А., Мусорина Т.А., Островая А.Ф., Ольшевский В.Я., Антуськов А.Л. Влагоперенос в вентилируемом канале с нагревательным элементом // Инженерно-строительный журнал. 2017. № 2(70). С. 11–17.

doi: 10.18720/MCE.70.3

The functional of additional energy for stability analysis of spatial rod systems

Функционал дополнительной энергии для анализа устойчивости пространственных стержневых систем

Yu.Ya. Tyukalov,
Vyatka State University, Kirov, Russia

Д-р техн. наук, профессор Ю.Я. Тюкалов,
Вятский государственный университет, г. Киров, Россия

Key words: stability; finite element method in stresses; piecewise constant stress; an additional energy functional; the lower limit of solutions; critical force; reserve of stability

Ключевые слова: устойчивость; метод конечных элементов в напряжениях; кусочно-постоянные напряжения; функционал дополнительной энергии; нижняя граница решения; критические силы; запас устойчивости

Abstract. The problem solutions of stability of spatial rod systems by finite elements method in stresses were considered. The proposed method is based on a combination of functional additional energy and the principle of virtual displacements, used for the construction of the equilibrium equations. After discrediting of the subject field, solution of the problem is reduced to the search of the minimum of additional strain energy functional with constraints in the form of the system of linear algebraic equilibrium equations of the nodes. The equilibrium equations are included in the functional with the help of Lagrange multipliers, which are displacements of the nodes. Equations are derived for the static analysis based on approximations of internal forces (stresses) for the spatial rod systems. To solve the stability problems, in the functional of additional energy there are added additional energy the longitudinal deformations, arising due to the bending of rods. Form of the rod buckling is approximated by a linear function on finite element field. Two variants of the internal forces approximations on the finite element field: linear and piecewise constant were considered. Calculations of critical forces (loads) have been performed by the proposed method for the straight rods with different variants of the ends support and the spatial frameworks. The calculation results were compared with the analytical solutions and the solutions obtained by the method of finite elements in displacements. Analysis of the results shows that the use of piecewise constant approximations of internal forces leads to convergence to the exact values of the critical forces (loads) is strictly from below and provides solution with the reserve of stability.

Аннотация. Рассматривается решение задач устойчивости пространственных стержневых систем методом конечных элементов в напряжениях. Предлагаемая методика основывается на сочетании функционала дополнительной энергии и принципа возможных перемещений, используемого для построения уравнений равновесия узлов конечно-элементной сетки. После дискретизации предметной области, решение задачи сводится к поиску минимума функционала дополнительной энергии деформации при наличии ограничений в виде системы линейных алгебраических уравнений равновесия узлов. Уравнения равновесия включаются в функционал при помощи множителей Лагранжа, которыми являются перемещения узлов. Получены разрешающие уравнения для статического расчета пространственных стержневых систем на основе аппроксимации усилий (напряжений). Для решения задач устойчивости в функционале учитывается дополнительная энергия от продольных деформаций, возникающих за счет изгиба стержней. Форма потери устойчивости по области конечного элемента аппроксимируется линейной функцией. Рассматриваются два варианта аппроксимации внутренних усилий по области конечного элемента: линейная и кусочно-постоянная. По предложенной методике были выполнены расчеты критических сил (нагрузок) для прямых стержней при различных вариантах закрепления концов и пространственных рам. Выполнено сравнение результатов с аналитическим решениями и решениями, полученными по методу конечных элементов в перемещениях. Анализ полученных результатов показывает, что использование кусочно-постоянных аппроксимаций внутренних усилий приводит к сходимости к точному значению критических сил (нагрузок) строго снизу и позволяет получить решение в запас устойчивости.

Tyukalov Yu.Ya. The functional of additional energy for stability analysis of spatial rod systems. *Magazine of Civil Engineering*. 2017. No. 2. Pp. 18–32. doi: 10.18720/MCE.70.3

Introduction

The finite element method in displacements is successfully used to solve the widest range of structural mechanic problems, including stability problems [1–27]. In recent years, for rod systems the greatest attention was given to the build functional for solving the problems of stability of thin-walled rods [4, 6, 9, 13, 17, 20, 26] and given the effect of shear and longitudinal deformations [3, 4, 9, 13]. Also, in some articles the methods of solving rods stability problems [15] with considering the physical non-linearity [12, 16] and the torsion of the cross sections were introduce. A series of articles are devoted to the calculations the stability of rods based on direct solution of differential equations for compressed-bent rods [18–25], including rods with variable cross-section [20, 21, 23–25].

In [3, 4, 28–36] the solutions of problems by mixed finite elements methods and in stresses are considered. In [4], in order to solve the problems of constructions stability the mixed Reissner's functional is used. For this purpose, the functional is complemented by summand that considers the additional energy of longitudinal deformation occurring by the bending. Also, it is considered functional for solving stability problems of the open profiles rods and flexural-torsional forms of buckling spatial rods systems.

In [38] two variants of extreme energy principles to solve static problems of structural mechanics are considered. It includes the Castilian principle which involves the static equations (equilibrium) as constraints. The equations of statics were based on differential dependencies which bind forces and external loads. The equilibrium equations of the longitudinal and transverse forces are prepared for separate nodes. There were introduced different types of rod elements, the equilibrium equations are constructed using a special algorithm. Stability problems are not considered.

In [32–36] solutions of static and dynamic problems of structural mechanics by finite elements method in stresses were constructed. The equilibrium equations, formed on virtual displacement's principle, are included in the functional by the Lagrange's multipliers or using penalty functions method. It is shown that, if for approximation of the stress (forces) in the field of finite element constant or piecewise constant functions were used, then displacements of nodes seek to exact values from above by crushing the finite elements mesh. Thus, it is possible to receive the opposite, compared to the traditional finite element method in displacements, border exact solutions.

It is known [1–3] that the solution, obtained by the method of finite elements in displacements, under certain conditions, converges to the lower border of the exact values of displacements. Solutions, obtained by the minimum principle of additional energy, also under certain conditions, allow getting opposite bound of the exact values of displacements.

The purpose of this work is the construction of solution algorithm of stability problems of spatial rod systems on the basis the functional of additional energy and the principle of virtual displacements, which allow determine the lower limit of the critical loads.

Methods

In [32–36], founding by the functional of additional energy and principle of virtual displacements, solving the building structures problems by finite element analysis in stresses were built. Using constant or piecewise constant functions for the approximations of stresses (forces) in the field of finite element we will get the upper border of displacements. In general, the solution of the problem reduces to finding the minimum of the additional energy functional (1) in the presence of limitations in the form of equilibrium equations of nodes (2).

$$\Pi^c = U^* + V^* = \frac{1}{2}\int \{\sigma\}^T [E]^{-1}\{\sigma\} d\,\Omega - \int \{T\}^T \{\overline{\Delta}\} dS \to min, \tag{1}$$

$$\begin{aligned} \{C_{i,x}\}^{\mathrm{T}}\{\overline{\sigma}_i\} + \overline{P}_{i,x} = 0, \quad i \in \Xi_x, \\ \{C_{i,y}\}^{\mathrm{T}}\{\overline{\sigma}_i\} + \overline{P}_{i,y} = 0, \quad i \in \Xi_y, \\ \{C_{i,z}\}^{\mathrm{T}}\{\overline{\sigma}_i\} + \overline{P}_{i,z} = 0, \quad i \in \Xi_z. \end{aligned} \tag{2}$$

U^* – additional energy of the strains, V^*– potential boundary forces corresponding to the specified displacements [1]; $\{\overline{\sigma}_i\}$ – vector of unknown node stresses (forces) of finite elements adjacent to the node i; Ξ_x, Ξ_y, Ξ_z – sets of nodes that have free displacements along the axes X, У и Z respectively; $\{\overline{\Delta}\}$ – vector given displacements of nodes; $\{T\}$ – vector boundary forces; S – boundary surface, on which the displacement nodes are given; $\{C_{i,x}\}, \{C_{i,x}\}, \{C_{i,z}\}$ – vectors, which elements are the

Тюкалов Ю.Я. Функционал дополнительной энергии для анализа устойчивости пространственных стержневых систем // Инженерно-строительный журнал. 2017. № 2(70). С. 18–32.

coefficients (multipliers) of the unknown node stresses (forces) of finite elements adjacent to the node i; $\overline{P}_{i,x}, \overline{P}_{i,y}, \overline{P}_{i,z}$ – external loads potential corresponding to the virtual unit displacements of the node i along axes x, y, z respectively. The equations of equilibrium (2) are formed using the principle of virtual displacements for all admissible displacements of nodes along the coordinate axes.

In order to go on to unconstrained minimization problem, we use the method of Lagrange's multipliers. Then advanced functional of additional energy takes the following form:

$$\Pi_c^u = U^* + V^* + \sum_{j=x,y,z} \sum_{i \in \Xi_j} u_{i,j} \left(\{C_{i,j}\}^{\mathrm{T}} \{\overline{\sigma}_i\} + \overline{P}_{i,j} \right) \to min. \quad (3)$$

$u_{i,j}$ – the actual displacement of the node *i* towards *j*, which is the Lagrange's multiplier for the corresponding equilibrium equation. When using the functional (3) there is not necessary to use a stress field that satisfies the differential equations of equilibrium, as required by the principle of minimum additional energy. The equilibrium equations will be carried out in discrete sense – in the form of the equilibrium equations of the finite element mesh nodes.

Let us consider the application of the proposed approach to solve static problems of the spatial rod systems. Using the notations for rods systems, the functional (1) without the given displacements of nodes will be as follows:

$$\Pi^c = \sum_{i=1}^{n} \left(\frac{1}{2} \int_0^l \frac{M_y(x)^2}{EI_y} dx + \frac{1}{2} \int_0^l \frac{M_z(x)^2}{EI_z} dx + \frac{1}{2} \int_0^l \frac{M_k(x)^2}{GI_k} dx + \frac{1}{2} \int_0^l \frac{N(x)^2}{EA} dx \right) \to min. \quad (4)$$

EI_y, EI_z – bending stiffness, GI_k – torsional stiffness; $M_y(x)$, $M_z(x)$ – the bending moments directed around axes Y_1 and Z_1 respectively (fig. 1b), $M_k(x)$ – torque (directed around the axis X_1); EA – longitudinal stiffness; $N(x)$ – longitudinal force; l – length of the finite element; n – number of finite elements.

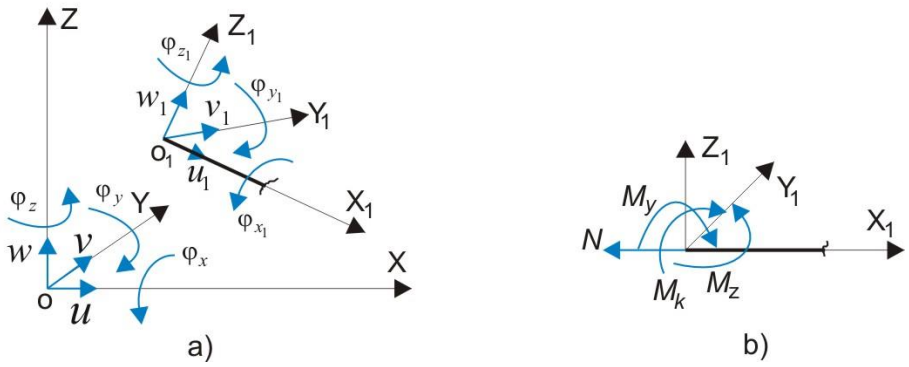

Figure 1. Positive directions of nodal displacements: a) global XYZ coordinate system and local coordinate system $X_1Y_1Z_1$ at the beginning of finite element; b) positive directions of the nodal internal forces at the beginning of finite element

The approximations of internal forces (longitudinal forces and moments) will take linear (5) or piecewise constant (6).

$$S(x) = S_1 \left(1 - \frac{x}{l}\right) + S_2 \frac{x}{l}, \quad (5)$$

$$S(x) = \begin{Bmatrix} S_1, & x \in [0, l/2] \\ S_2, & x \in [l/2, l] \end{Bmatrix}. \quad (6)$$

In (5) and (6) under the symbol S any of the internal forces – N, M_y, M_z, M_k, is meant. The positive directions for the beginning finite element are shown in Figure 1b.

Substituting (5) or (6) into (4) we obtain the expression of the finite element additional energy in matrix form:

$$\Pi^c = \frac{1}{2} \{S_e\}^T [D_e] \{S_e\}, \quad \{S_e\}^T = (M_{y,1} \quad M_{y,2} \quad M_{z,1} \quad M_{z,2} \quad M_{k,1} \quad M_{k,2} \quad N_1 \quad N_2). \quad (7)$$

$\{S_e\}$ – vector of unknown nodal forces for finite element. Flexibility matrix $[D_e]$ of finite element for the case of linear – $[D_e]_L$ (8), and piecewise constant approximations – $[D_e]_C$ (9), will be as follows:

$$[D_e]_L = \begin{bmatrix} \frac{l}{3EI_y} & \frac{l}{6EI_y} & 0 & 0 & 0 & 0 & 0 & 0 \\ \frac{l}{6EI_y} & \frac{l}{3EI_y} & 0 & 0 & 0 & 0 & 0 & 0 \\ 0 & 0 & \frac{l}{3EI_z} & \frac{l}{6EI_z} & 0 & 0 & 0 & 0 \\ 0 & 0 & \frac{l}{6EI_z} & \frac{l}{3EI_z} & 0 & 0 & 0 & 0 \\ 0 & 0 & 0 & 0 & \frac{l}{3GI_k} & \frac{l}{6GI_k} & 0 & 0 \\ 0 & 0 & 0 & 0 & \frac{l}{6GI_k} & \frac{l}{3GI_k} & 0 & 0 \\ 0 & 0 & 0 & 0 & 0 & 0 & \frac{l}{3EA} & \frac{l}{6EA} \\ 0 & 0 & 0 & 0 & 0 & 0 & \frac{l}{6EA} & \frac{l}{3EA} \end{bmatrix}, \quad (8)$$

$$[D_e]_C = \begin{bmatrix} \frac{l}{2EI_y} & 0 & 0 & 0 & 0 & 0 & 0 & 0 \\ 0 & \frac{l}{2EI_y} & 0 & 0 & 0 & 0 & 0 & 0 \\ 0 & 0 & \frac{l}{2EI_z} & 0 & 0 & 0 & 0 & 0 \\ 0 & 0 & 0 & \frac{l}{2EI_z} & 0 & 0 & 0 & 0 \\ 0 & 0 & 0 & 0 & \frac{l}{2GI_k} & 0 & 0 & 0 \\ 0 & 0 & 0 & 0 & 0 & \frac{l}{2GI_k} & 0 & 0 \\ 0 & 0 & 0 & 0 & 0 & 0 & \frac{l}{2EA} & 0 \\ 0 & 0 & 0 & 0 & 0 & 0 & 0 & \frac{l}{2EA} \end{bmatrix}. \quad (9)$$

Note, that the unknown nodal forces are accepted independently for each finite element. Therefore, the size of the global vector of unknown nodal forces $\{S\}$ will be equal to 8n. Global flexibility matrix $[D]$ to the whole system, and its inverse$[D]^{-1}$, will have a block-diagonal (or diagonal) form:

$$[D] = \begin{bmatrix} [D_1] & \cdots & 0 \\ \vdots & \ddots & \vdots \\ 0 & \cdots & [D_n] \end{bmatrix}, [D]^{-1} = \begin{bmatrix} [D_1]^{-1} & \cdots & 0 \\ \vdots & \ddots & \vdots \\ 0 & \cdots & [D_n]^{-1} \end{bmatrix} \quad (10)$$

Using (10), the functional (4) can be written as follows:

$$\Pi^c = \frac{1}{2}\{S\}^T[D]\{S\} \to min. \quad (11)$$

To form the equilibrium equations nodes of finite element we consider displacements of nodes in the local coordinate system (Figs. 2–3) and obtain corresponding expressions the strain energy of finite element.

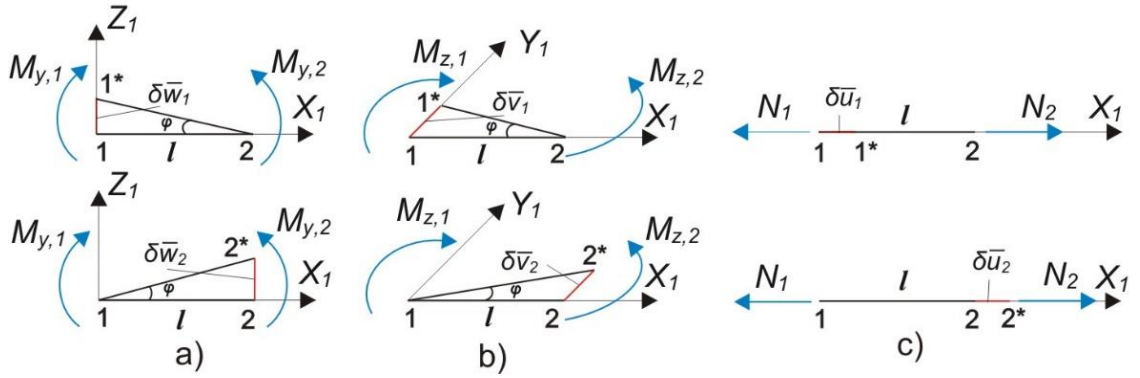

Figure 2. Possible displacements finite element nodes along the local axes: a) along the $Z_1 - \delta\overline{w}$; b) along the $Y_1 - \delta\overline{v}$; c) along the $X_1 - \delta\overline{u}$

We assume that the possible displacements are changed along length of finite element according to linear law. The displacements $\delta\overline{w}$ and $\delta\overline{v}$ will give the rotations of finite element, as rigid body rotations. The displacement of node $\delta\overline{w}_1$ causes the angle of finite element rotation:

$$\varphi = \frac{\delta\overline{w}_1}{l}. \tag{12}$$

When the element is rotated at an angle φ, the nodal moments will perform the work $\delta\overline{A}_{\overline{w},1}$ as the external forces:

$$\delta\overline{A}_{\overline{w},1} = -M_{y,1}\varphi + M_{y,2}\varphi = \delta\overline{w}_1\left(\frac{-M_{y,1}+M_{y,2}}{l}\right). \tag{13}$$

The internal moments are opposite in sign, so the energy of deformations:

$$\delta\overline{U}_{\overline{w},1} = -\delta\overline{A}_{\overline{w},1} = \delta\overline{w}_1\left(\frac{M_{y,1}-M_{y,2}}{l}\right). \tag{14}$$

Similarly, we obtain

$$\delta\overline{U}_{\overline{w},2} = \delta\overline{w}_2\left(\frac{-M_{y,1}+M_{y,2}}{l}\right),\ \delta\overline{U}_{\overline{v},1} = \delta\overline{v}_1\left(\frac{M_{z,1}-M_{z,2}}{l}\right),\ \delta\overline{U}_{\overline{v},2} = \delta\overline{v}_2\left(\frac{-M_{z,1}+M_{z,2}}{l}\right). \tag{15}$$

At possible displacement $\delta\overline{u}_1$ along the axis X_1:

$$u(x) = \delta\overline{u}_1\left(1 - \frac{x}{l}\right),\ \ \varepsilon(x) = \frac{du(x)}{dx} = \frac{-\delta\overline{u}_1}{l}. \tag{16}$$

Then, the energy of deformations

$$\delta\overline{U}_{\overline{u},1} = \frac{-\delta\overline{u}_1}{l}\int_0^l N(x)dx. \tag{17}$$

If we substitute in (16) the expression for N (x) from (5) or (6) the result is the same:

$$\delta\overline{U}_{\overline{u},1} = \delta\overline{u}_1\frac{-(N_1+N_2)}{2}. \tag{18}$$

The similar expression can be obtained for a possible displacement of node 2

$$\delta\overline{U}_{\overline{u},2} = \delta\overline{u}_2\frac{(N_1+N_2)}{2}. \tag{19}$$

Next, let us consider possible displacements, as nodes rotation (Fig. 3a) and as element rotation (Fig. 3b), around axes of the local coordinate system

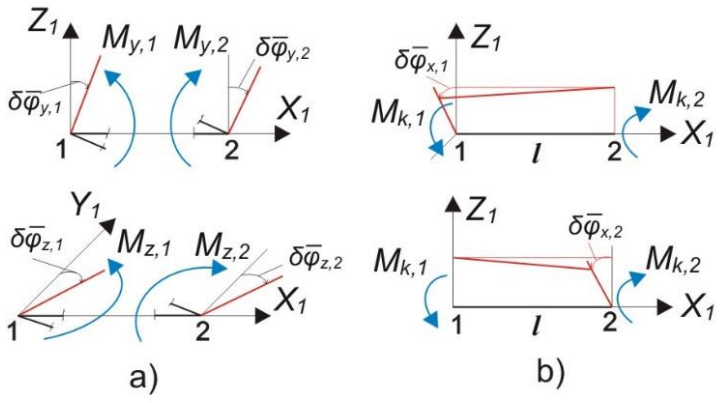

Figure 3. The possible turns: a) $\delta\overline{\varphi}_y$, $\delta\overline{\varphi}_z$ – around Y1 and Z1 axes; b) $\delta\overline{\varphi}_x$ – around the axis X1

For rotations around the axes Y1 and Z1, expressions of strain energy will be written simply:

$$\begin{aligned} \delta\overline{U}_{\overline{\varphi}_{y,1}} &= -M_{y,1}\delta\overline{\varphi}_{y,1}, \qquad \delta\overline{U}_{\overline{\varphi}_{y,2}} = M_{y,2}\delta\overline{\varphi}_{y,2}, \\ \delta\overline{U}_{\overline{\varphi}_{z,1}} &= -M_{z,1}\delta\overline{\varphi}_{z,1}, \qquad \overline{\delta U}_{\overline{\varphi}_{z,2}} = M_{z,2}\delta\overline{\varphi}_{z,2}. \end{aligned} \tag{20}$$

For rotations around the axis X1 (Fig. 3b) strain energy expressions are like equations (17) and (18) with substitution longitudinal forces by torques:

$$\delta\overline{U}_{\overline{\varphi}_{x,1}} = \delta\overline{\varphi}_{x,1}\frac{-(M_{k,1}+M_{k,2})}{2}, \quad \delta\overline{U}_{\overline{\varphi}_{x,2}} = \delta\overline{\varphi}_{x,2}\frac{(M_{k,1}+M_{k,2})}{2}. \tag{21}$$

The possible nodal displacements in the global and the local coordinate systems are connected by a matrix of the direction cosines $[t]$:

$$\begin{Bmatrix}\delta u_1\\ \delta v_1\\ \delta w_1\end{Bmatrix} = [t]\begin{Bmatrix}\delta\overline{u}_1\\ \delta\overline{v}_1\\ \delta\overline{w}_1\end{Bmatrix}, \begin{Bmatrix}\delta\varphi_{x,1}\\ \delta\varphi_{y,1}\\ \delta\varphi_{z,1}\end{Bmatrix} = [t]\begin{Bmatrix}\delta\overline{\varphi}_{x,1}\\ \delta\overline{\varphi}_{y,1}\\ \delta\overline{\varphi}_{z,1}\end{Bmatrix}, \begin{Bmatrix}\delta u_2\\ \delta v_2\\ \delta w_2\end{Bmatrix} = [t]\begin{Bmatrix}\delta\overline{u}_2\\ \delta\overline{v}_2\\ \delta\overline{w}_2\end{Bmatrix}, \begin{Bmatrix}\delta\varphi_{x,2}\\ \delta\varphi_{y,2}\\ \delta\varphi_{z,2}\end{Bmatrix} = [t]\begin{Bmatrix}\delta\overline{\varphi}_{x,2}\\ \delta\overline{\varphi}_{y,2}\\ \delta\overline{\varphi}_{z,2}\end{Bmatrix}. \tag{22}$$

$$[t] = \begin{bmatrix} t_{11} & t_{12} & t_{13} \\ t_{21} & t_{22} & t_{23} \\ t_{31} & t_{32} & t_{33} \end{bmatrix}. \tag{23}$$

The energies of strains in the global and the local coordinate systems are connected also. Formation of the matrix of direction cosines $[t]$ is executed as in the calculation of spatial rod systems by finite elements method in displacements [1–5]. The deformation energy values for possible displacements of finite element nodes in the global coordinate system are placed into the vector $\{\delta U_e\}$ as follows:

$$\{\delta U_e\}^T = \{\delta U_{u,1}\ \delta U_{v,1}\ \delta U_{w,1}\ \delta U_{\varphi_{x,1}}\ \delta U_{\varphi_{y,1}}\ \delta U_{\varphi_{z,1}}\ \delta U_{u,2}\ \delta U_{v,2}\ \delta U_{w,2}\ \delta U_{\varphi_{x,2}}\ \delta U_{\varphi_{y,2}}\ \delta U_{\varphi_{z,2}}\}^T. \tag{24}$$

Possible displacements of finite element nodes in the global coordinate system, in the same order, are presented by square diagonal matrix $[\delta y_e]$.

$$[\delta y_e] = \begin{bmatrix} \delta u_1 & \cdots & 0 \\ \vdots & \ddots & \vdots \\ 0 & \cdots & \delta\varphi_{z,2} \end{bmatrix}. \tag{25}$$

Using the vector of unknown nodal forces $\{S_e\}$, introduced in (7), we can write the following expression:

$$\{\delta U_e\} = [\delta y_e][L_e]\{S_e\}. \tag{26}$$

Matrix $[L_e]$, which may be called as matrix of equilibrium of finite element, considering the expressions (14–15), (20–23) is as follows:

$$\begin{bmatrix}
\frac{-t_{31}}{l} & \frac{t_{31}}{l} & \frac{t_{21}}{l} & \frac{-t_{21}}{l} & 0 & 0 & \frac{-t_{11}}{2} & \frac{-t_{11}}{2} \\
\frac{-t_{32}}{l} & \frac{t_{32}}{l} & \frac{t_{22}}{l} & \frac{-t_{22}}{l} & 0 & 0 & \frac{-t_{12}}{2} & \frac{-t_{12}}{2} \\
\frac{-t_{33}}{l} & \frac{t_{33}}{l} & \frac{t_{23}}{l} & \frac{-t_{23}}{l} & 0 & 0 & \frac{-t_{13}}{2} & \frac{-t_{13}}{2} \\
-t_{21} & 0 & -t_{31} & 0 & \frac{-t_{11}}{2} & \frac{-t_{11}}{2} & 0 & 0 \\
-t_{22} & 0 & -t_{32} & 0 & \frac{-t_{12}}{2} & \frac{-t_{12}}{2} & 0 & 0 \\
-t_{23} & 0 & -t_{33} & 0 & \frac{-t_{13}}{2} & \frac{-t_{13}}{2} & 0 & 0 \\
\frac{t_{31}}{l} & \frac{-t_{31}}{l} & \frac{-t_{21}}{l} & \frac{t_{21}}{l} & 0 & 0 & \frac{t_{11}}{2} & \frac{t_{11}}{2} \\
\frac{t_{32}}{l} & \frac{-t_{31}}{l} & \frac{-t_{22}}{l} & \frac{t_{22}}{l} & 0 & 0 & \frac{t_{12}}{2} & \frac{t_{12}}{2} \\
\frac{t_{33}}{l} & \frac{-t_{33}}{l} & \frac{-t_{23}}{l} & \frac{t_{23}}{l} & 0 & 0 & \frac{t_{13}}{2} & \frac{t_{13}}{2} \\
0 & t_{21} & 0 & t_{31} & \frac{t_{11}}{2} & \frac{t_{11}}{2} & 0 & 0 \\
0 & t_{22} & 0 & t_{32} & \frac{t_{12}}{2} & \frac{t_{12}}{2} & 0 & 0 \\
0 & t_{23} & 0 & t_{33} & \frac{t_{13}}{2} & \frac{t_{13}}{2} & 0 & 0
\end{bmatrix}. \quad (27)$$

From the local equilibrium matrices $[L_e]$, in accordance with the numbering of nodes and finite elements, global matrix $[L]$ of the system equilibrium equations of nodes will be formed. If the number of finite elements is equal to *n*, number of nodes – *k*, and number of kinematic links – *s*, the matrix [L] would be having $(6k-s)$ lines and *8n* columns. From the vector of unknown nodal forces of finite element $\{S_e\}$ vector of unknown forces for the whole system $\{S\}$ is formed. It consists of *8n* elements.

In order to form the equilibrium equations it is also necessary to get expression of the work of external forces from the possible displacements. At possible node displacements, the work is performed by concentrated vertical forces and moments in the nodes and by loads, that is distributed along the element. If evenly distributed along the finite element loads q_x, q_y, q_z are defined in the global coordinate system, then they should be reformed into local loads using expression (28):

$$\begin{Bmatrix} \overline{q}_x \\ \overline{q}_y \\ \overline{q}_z \end{Bmatrix} = [t]^T \begin{Bmatrix} q_x \\ q_y \\ q_z \end{Bmatrix}. \quad (28)$$

Next, we form the vector $\{\overline{F}_e\}$ that consists of concentrated forces and moments in the nodes:

$$\{\overline{F}_e\}^T = \left\{\frac{\overline{q}_x l}{2} \quad \frac{\overline{q}_y l}{2} \quad \frac{\overline{q}_z l}{2} \quad \frac{\overline{q}_x l^2}{12} \quad \frac{\overline{q}_y l^2}{12} \quad \frac{\overline{q}_z l^2}{12} \quad \frac{\overline{q}_x l}{2} \quad \frac{\overline{q}_y l}{2} \quad \frac{\overline{q}_z l}{2} \quad \frac{-\overline{q}_x l^2}{12} \quad \frac{-\overline{q}_y l^2}{12} \quad \frac{-\overline{q}_z l^2}{12}\right\}^T. \quad (29)$$

Vector $\{\overline{F}_e\}$, obtained in local coordinate system, should be transformed into the vector $\{F_e\}$ in global coordinate system:

$$\{F_e\} = [t_e]\{\overline{F}_e\},$$
$$[t_e] = \begin{bmatrix} [t] & 0 & 0 & 0 \\ 0 & [t] & 0 & 0 \\ 0 & 0 & [t] & 0 \\ 0 & 0 & 0 & [t] \end{bmatrix} \quad (30)$$

From the local vectors $\{F_e\}$, according to the numbering of nodes and elements, we form the global vector of the nodal loads $\{F\}$ for all finite elements. Next, the forces and moments, that are concentrated at the nodes, are added to elements of vector $\{F\}$. Obviously, the work of the external forces is calculated as product of the elements of the vector $\{F\}$ and the corresponding possible node displacements. Thus, the system of equilibrium equations for the whole system can be written in the following form:

$$\{F\} - [L]\{S\} = 0. \tag{31}$$

For the finite element, we introduce the notation for the vector of nodal unknowns in the local coordinate system

$$\{\overline{y}_e\}^T = \{\overline{u}_1 \ \overline{v}_1 \ \overline{w}_1 \ \overline{\varphi}_{x,1} \ \overline{\varphi}_{y,1} \ \overline{\varphi}_{z,1} \ \overline{u}_2 \ \overline{v}_2 \ \overline{w}_2 \ \overline{\varphi}_{x,2} \ \overline{\varphi}_{y,2} \ \overline{\varphi}_{z,2}\}^T \tag{32}$$

and the global vector of the nodal unknowns for whole system $\{y\}$, which is the vector of Lagrange's multipliers for the equilibrium equations of the system (30). By means of Lagrange's multipliers, we include the equations (30) into the functional (11) and obtain:

$$\Pi^c = \frac{1}{2}\{S\}^T[D]\{S\} + \{y\}^T(\{F\} - [L]\{S\}) \to min. \tag{33}$$

Equating to zero the derivatives Π^c from vector $\{S\}$, we obtain the equations of compatibility of strains in terms of stresses:

$$[D]\{S\} - [L]^T\{y\} = 0. \tag{34}$$

The derivatives Π^c on elements of the vector $\{y\}$ are systems of equilibrium equations of nodes (31). Combining (31) and (34), we obtain the final system of linear algebraic equations:

$$\begin{bmatrix} [D] & -[L]^T \\ -[L] & [0] \end{bmatrix} \begin{Bmatrix} \{S\} \\ \{y\} \end{Bmatrix} = \begin{Bmatrix} 0 \\ -\{F\} \end{Bmatrix}. \tag{35}$$

Expressing vector $\{S\}$ from the first matrix equation and using it in the second, we get

$$[L][D]^{-1}[L]^T\{y\} = \{F\}, \tag{36}$$

$$\{S\} = [D]^{-1}[L]^T\{y\}. \tag{37}$$

Let us note that for getting (35) the approximation functions for the displacements are not used. Only, there were introduced approximations for possible displacements that can be of any shape, but must satisfy the kinematic relations. The solution was based on the introduction of approximations for the internal forces (stresses). By using linear approximations, we will get the values of forces and displacements of nodes that equal to the values, obtained by the method of finite elements in displacements. Since the matrix $[D]$ has simple structure, calculating product of the matrices in (36) does not require extensive computational resources.

Let us consider the problem of determining the critical load, which leads to the loss of stability in form of the rods bulging. In this paper, more complicated flexural-torsional buckling forms are not considered. As is well known [1–4], in solving problems of rod systems stability must be counted the stretching deformations that are associated with bending:

$$\varepsilon_0 = \frac{1}{2}\left(\frac{dv}{dx}\right)^2 + \frac{1}{2}\left(\frac{dw}{dx}\right)^2. \tag{38}$$

After buckling, the function of the transverse displacements of axis of the finite element is approximated by the linear function in the local coordinate system

$$v(x) = \overline{v}_1\left(1 - \frac{x}{l}\right) + \overline{v}_2\frac{x}{l}, \ \ w(x) = \overline{w}_1\left(1 - \frac{x}{l}\right) + \overline{w}_2\frac{x}{l}. \tag{39}$$

Then

$$\varepsilon_0 = \frac{1}{2}\frac{(\overline{v}_2 - \overline{v}_1)^2}{l^2} + \frac{1}{2}\frac{(\overline{w}_2 - \overline{w}_1)^2}{l^2}. \tag{40}$$

The additional energy of deformations

$$U^*_{\varepsilon_0} = \int_0^l N(x)\varepsilon_0 dx. \tag{41}$$

Setting in (41), any (5) or (6), approximation for $N(x)$ we obtain the following matrix expression for the energy of deformations

$$U^*_{\varepsilon_0} = \frac{1}{2}\{\overline{y}_e\}^T[\overline{G}_e]\{\overline{y}_e\}, \tag{42}$$

$$\left[\overline{G}_e\right] = \frac{(N_1+N_2)}{2l}\begin{bmatrix} 0 & 0 & 0 & 0 & 0 & 0 & 0 & 0 & 0 & 0 & 0 & 0 \\ 0 & 1 & 0 & 0 & 0 & 0 & 0 & -1 & 0 & 0 & 0 & 0 \\ 0 & 0 & 1 & 0 & 0 & 0 & 0 & 0 & -1 & 0 & 0 & 0 \\ 0 & 0 & 0 & 0 & 0 & 0 & 0 & 0 & 0 & 0 & 0 & 0 \\ 0 & 0 & 0 & 0 & 0 & 0 & 0 & 0 & 0 & 0 & 0 & 0 \\ 0 & 0 & 0 & 0 & 0 & 0 & 0 & 0 & 0 & 0 & 0 & 0 \\ 0 & 0 & 0 & 0 & 0 & 0 & 0 & 0 & 0 & 0 & 0 & 0 \\ 0 & -1 & 0 & 0 & 0 & 0 & 0 & 1 & 0 & 0 & 0 & 0 \\ 0 & 0 & -1 & 0 & 0 & 0 & 0 & 0 & 1 & 0 & 0 & 0 \\ 0 & 0 & 0 & 0 & 0 & 0 & 0 & 0 & 0 & 0 & 0 & 0 \\ 0 & 0 & 0 & 0 & 0 & 0 & 0 & 0 & 0 & 0 & 0 & 0 \\ 0 & 0 & 0 & 0 & 0 & 0 & 0 & 0 & 0 & 0 & 0 & 0 \end{bmatrix}. \quad (43)$$

For getting the geometric matrix of the finite elements in the global coordinate system, the following conversions must be done:

$$[G_e] = [t_e]\left[\overline{G}_e\right][t_e]^T. \quad (44)$$

From the local matrices $[G_e]$ of the finite elements we generate geometric global matrix $[G]$ for the whole system. Using $U^*_{\varepsilon_0}$, the functional (33), for solving buckling problems will be as follows:

$$\Pi^c = \frac{1}{2}\{S\}^T[D]\{S\} + \frac{1}{2}\lambda\{y\}^T[G]\{y\} - \{y\}^T[L]\{S\} \to min. \quad (45)$$

In the expression (45) the parameter λ, which is interpreted as the buckling safety factor, are introduced. Minimum of functional (45) corresponds to the existence the equilibrium of the system in deflected shape. Equating the derivatives Π^c along the vector of forces $\{S\}$ to zero, we obtain the equations the compatibility of deformations (34). The derivatives of the (45) along the vector of displacements $\{y\}$ create the equations equilibrium of the nodes after buckling with adding the influence of longitudinal forces to bending:

$$-[L]\{S\} + \lambda[G]\{y\} = 0. \quad (46)$$

Combining (34) and (46), we obtain a system of homogeneous linear algebraic equations

$$\begin{bmatrix} [D] & -[L]^T \\ -[L] & \lambda[G] \end{bmatrix}\begin{Bmatrix} \{S\} \\ \{y\} \end{Bmatrix} = \begin{Bmatrix} 0 \\ 0 \end{Bmatrix}. \quad (47)$$

Let us express vector of forces $\{S\}$, from the first matrix equation, and put it into the second equation. Introducing the notation for the matrix product $[K] = [L][D]^{-1}[L]^T$, we get:

$$-[K]\{y\} + \lambda[G]\{y\} = 0. \quad (48)$$

To determine the critical value of the parameter λ_{cr} we apply the method of inverse iterations, which includes the following steps. After solving (36) and (37), we obtain the vectors $\{y_0\}$ and $\{S_0\}$. Next, we must perform the iterations:

$$\begin{cases} i = 1,2,\cdots m; \\ \{y_i\} = [K]^{-1}[G]\{y_{i-1}\}, \\ y_{max} = \max\limits_{j=1..(6k-s)}\left|y_{i,j}\right|, \\ \lambda_{cr,i} = \dfrac{1}{|y_{max}|}. \end{cases} \quad (49)$$

In (49) y_{max} – maximum in modulus element of vector $\{y_i\}$. The iterative procedure is finished after achieving the necessary accuracy of calculating $\left|\lambda_{cr,i} - \lambda_{cr,i-1}\right| < \varepsilon$.

Results and Discussion

As examples calculations stability of the spatial frameworks, shown in Figures 4–6, were performed. The calculations were performed in Mathcad 14.0. The following characteristics of cross

sections stiffness have been taken: $EI_y = 10\ kNm^2, EI_z = 10\ kNm^2, GI_k = 10\ kNm^2, EA = 1000\ kN$. Geometric dimensions in meters are indicated in the figures. The critical loads were calculated as functions of the finite elements number, which divide each rod, shown in the figures.

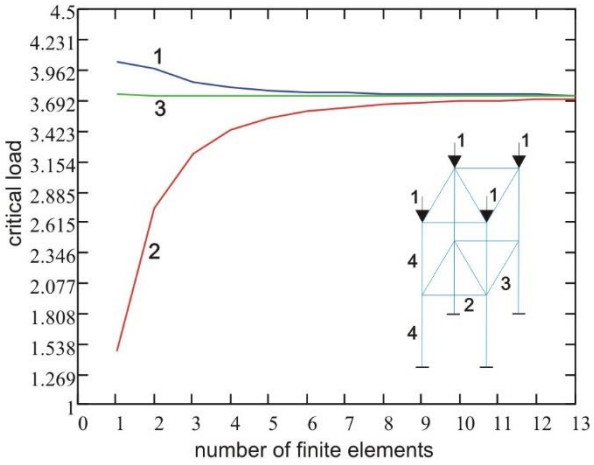

Figure 4. The critical load for rectangular framework with clamped supports

The graphs in Figures 4–6 are built on values of the critical forces, given in Tables 1–3.

Table 1. Values of the critical loads for the rectangular framework (kN). (Fig. 4)

Approximation	Number of finite elements												
	1	2	3	4	5	6	7	8	9	10	11	12	13
Linear	4.038	3.976	3.850	3.80	3.776	3.762	3.755	3.749	3.746	3.743	3.741	3.740	3.733
Piecewise constant	1.464	2.733	3.221	3.430	3.534	3.592	3.628	3.652	3.669	3.681	3.689	3.696	3.701
LIRA-SAPR	3.748	3.738	3.733	3.732	3.732	3.732	3.732	3.732	3.732	3.732	3.732	3.732	3.732

On figures: the number 1 (blue line) – indicate the results obtained by the linear approximations of the internal forces; number 2 (red line) – using piecewise constant approximations forces; number 3 (green line) – the results obtained by the finite elements method in the displacements on the program LIRA-SAPR 2013.

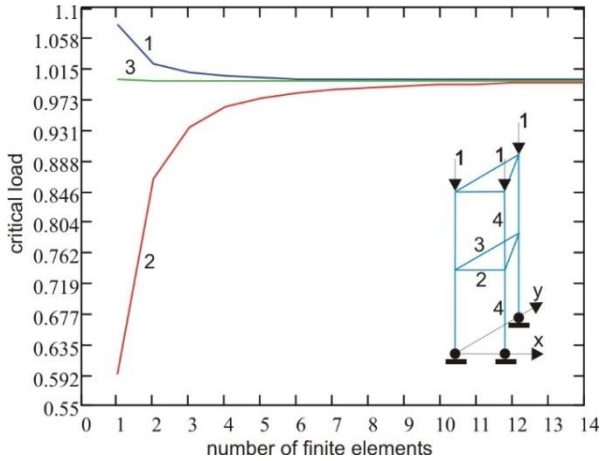

Figure 5. The critical load for the triangular framework with hinged supports

Table 2. The values of the critical loads for triangular framework with hinged supports (kN). (Fig. 5)

Approximation	Number of finite elements													
	1	2	3	4	5	6	7	8	9	10	11	12	13	14
Linear	1.075	1.021	1.009	1.005	1.003	1.001	1.0008	1.0004	1.0001	0.9999	0.9997	0.9996	0.9995	0.9994
Piecewise constant	0.593	0.862	0.935	0.962	0.975	0.982	0.986	0.990	0.9915	0.9929	0.9940	0.9948	0.9954	0.9959
LIRA-SAPR	1.0009	0.9991	0.9990	0.9990	0.9990	0.9990	0.9990	0.9990	0.9990	0.9990	0.9990	0.9990	0.9990	0.9990

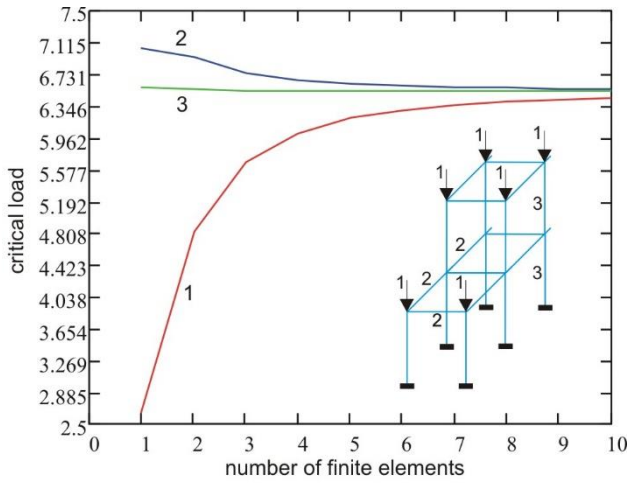

Figure 6. Critical load for the stepped framework with clamped supports

Table 3. The values of the critical load for the stepped framework with clamped supports (kN). (Fig. 6)

Approximation	Number of finite elements									
	1	2	3	4	5	6	7	8	9	10
Linear	7.0531	6.9479	6.7372	6.6526	6.6118	6.5892	6.5754	6.5665	6.5603	6.5559
Piecewise constant	2.6228	4.8323	5.6690	6.0234	6.2003	6.3000	6.3614	6.4019	6.4298	6.4499
LIRA-SAPR	6.5644	6.5465	6.5388	6.5373	6.5369	6.5368	6.5368	6.5367	6.5367	6.5366

Analysis of the results of the calculations shows that the use of piecewise constant approximations of internal forces lead to the convergence of the calculated values of critical forces (loads) to the exact values of strictly from bottom and allows you to get solutions to the stability reserve. At the same time, compared to the finite element method in the displacements, it is necessary to use the finer grids. The finite element method in displacements provides more accurate solutions with coarse grids. Necessary to consider, that the solution in displacements is more "rigid" and converges to the exact value from above as in the case of the use of linear approximations for the internal forces on the proposed method. It is known, by dividing of the finite elements grid we get values of stresses, which will tend to constant values, so for the convergence of solutions is necessary to ensure representation of the constant stresses or deformations. If solutions are get by proposed method, then this condition is performed. In the Fig. 7 shows graphs of the relative difference, in percentages, between the solutions, obtained for different approximations of internal forces, for the above examples. In the figure introduced the notation: $P_{cr,1}$ – linear approximations of internal forces; $P_{cr,2}$ – piecewise constant approximations of forces; $P_{cr,1*}$ – the minimum value, obtained by the linear approximations of forces; 1 (red line) – the results for the framework in Figure 4; 2 (blue line) – the results for the framework in Figure 5; 3 (green line) – the results for the framework in Figure 6. Reducing the difference between two solutions by the crushing of finite element mesh indicates to the convergence of solutions to the exact value. Note, that graphics for the 1st and 3rd schemes are practically the same (Table 4). Per the difference of two solutions we can assume the accuracies of calculation critical forces.

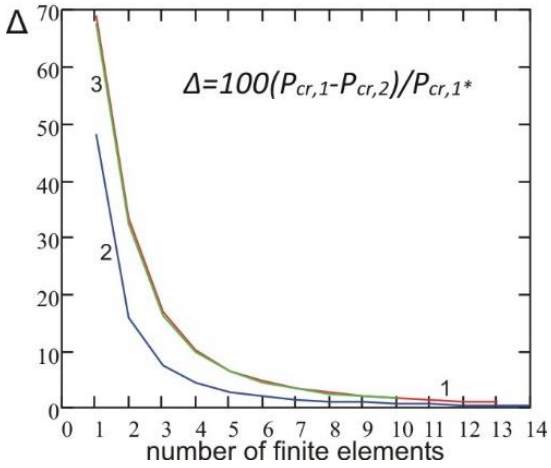

Figure 7. The relative difference between the values of the critical forces

Table 4. The relative difference of critical forces values in percentage (Fig. 7)

Scheme	Number of the crushing elements													
	1	2	3	4	5	6	7	8	9	10	11	12	13	14
Fig. 4	68.9	33.3	16.8	9.9	6.5	4.6	3.4	2.6	2.1	1.7	1.4	1.2	0.85	-
Fig. 5	48.2	15.8	7.4	4.3	2.7	1.9	1.4	1.1	0.9	0.7	0.57	0.48	0.41	0.39
Fig. 6	67.6	32.3	16.3	9.6	6.3	4.4	3.3	2.5	2.0	1.6	-	-	-	-

To evaluate the accuracy and convergence of the approximate solution by proposed method, the critical forces were defined for straight rods with different types of ends fixing and for different number of finite elements. To simplify the analysis, the bending stiffness and length of the rods have been taken equal to unity. We considered the following variants of the rods: 1 – hinged rod; 2 – cantilever rod; 3 – rod with hinge and with clamped end; 4 – rod with clamped ends. The calculation results are shown in Table 5. Exact, analytically derived, values of the critical forces are taken from [37].

Table 5. Critical forces for straight rods

Variants of rods	Approximations	Number of finite elements								Exact values
		2	4	5	10	20	40	80	100	
1	Linear	12.0	10.4	10.2	9.951	9.8999	9.8746	9.87087	9.87042	9.86960
	Piecewise constant	8.0	9.38	9.55	9.789	9.8493	9.8645	9.86834	9.86879	
2	Linear	3.0	2.50	2.49	2.472	2.4687	2.4677	2.46748	2.46745	2.46740
	Piecewise constant	2.0	2.41	2.45	2.462	2.4661	2.4671	2.46732	2.46735	
3	Linear	27.4	22.4	21.6	20.53	20.275	20.212	20.1960	20.1941	20.19064
	Piecewise constant	12.0	17.8	18.6	19.79	20.089	20.165	20.1844	20.1867	
4	Linear	48.0	48.0	44.9	40.79	39.804	39.560	39.4987	39.4914	39.47842
	Piecewise constant	16.0	32.0	34.6	38.20	39.155	39.397	39.4581	39.4654	

The calculation results of the stability of straight rods confirm, as was noted above, characteristic features of the proposed method of calculation, which is based on the functional of additional energy. These characteristics allow to note the following possible fields of application of the method: getting the lower limit of the critical forces; calculation the stability of the structures such as plates, which can be strengthen by rods; the curvilinear constructions or constructions on elastic foundation; getting the solutions, which are alternative to the solutions on method of finite elements in displacements.

Conclusions

1. For problems of stability the spatial rod systems there are proposed the method, which is based on functional of the additional energy and the principle of virtual displacements. Equations for static analysis of spatial rod systems based on the approximation of the forces (stress) were obtained.

2. The examples of the calculations the critical forces for straight rods and three-dimensional frameworks for different finite element grids show that using of piecewise constant approximations of internal forces provides a lower bound of the critical forces. It is necessary to use a fine grid of finite elements. For the above examples, the required number of finite elements for achieving the same accuracy as accuracy of the solutions by finite elements method in displacements is about 5 times more. Accuracy solutions, lot less than 1 percent, can be obtained, if very fine grid of the finite elements (Table 4) is used.

3. By using linear approximations of the internal forces, we get the solutions which converge to the exact values of the critical forces from above and give an upper bound. It is possible to define accuracies of calculation of the critical forces per the difference of two solutions with linear and piecewise constant approximations.

4. Possible fields of application of the method are getting the lower limit of the critical forces; calculation the stability of the structures such as plates, which can be strengthen by rods; calculation the stability of the curvilinear constructions or constructions on an elastic foundation; getting the solutions, which are alternative to the solutions getting on method of finite elements in displacements.

References

1. Zenkevich O. *Metod konechnykh elementov v tekhnike* [The finite element method in the technique]. M.: Mir, 1975. 541 p. (rus)
2. Zenkevich O., Morgan K. *Konechnyye elementy i approksimatsiya* [Finite Elements and Approximation]. M.: Mir, 1986. 318 p. (rus)
3. Gallager R. *Metod konechnykh elementov. Osnovy* [Finite elements and approximation. foundation]. M.: Mir, 1984. 428 p. (rus)
4. Slivker V.I. *Stroitelnaya mekhanika. Variatsionnyye osnovy* [Construction mehanika. Variatsionnye bases]. M.: Izdatelstvo Assotsiatsii stroitelnykh vuzov. 2005. 736 p. (rus)
5. Rozin L.A. *Metod konechnykh elementov v primenenii k uprugim sistemam* [Finite element method, as applied to an elastic system]. M.: Stroyizdat, 1977. 129 p. (rus)
6. Senjanović I., Vladimir N., Cho D.-S. A simplified geometric stiffness in stability analysis of thin-walled structures by the finite element method. *Inter J. Nav. Archit. Oc. Engng*. 2012. Vol. 4. Pp. 313-321.
7. Ibearugbulem O.M., Eziefula U.G., Onwuka D.O. Stability analysis of uniaxially compressed flat rectangular isotropic CCSS plate. *International Journal of Applied Mechanics and Engineering.* 2015. Vol. 20. No. 3. Pp. 637–646.
8. Yevzerov I.D. Zadachi ustoychivosti dlya sterzhney i plastin [Stability problems for rods and plates]. *Magazine of Civil Engineering.* 2014. No. 1(45). Pp. 6–11. (rus)
9. Lalin V.V., Rozin L.A., Kushova D.A. Variatsionnaya postanovka ploskoy zadachi geometricheski nelineynogo deformirovaniya i ustoychivosti uprugikh sterzhney [The variational formulation of the plane problem of geometrically nonlinear deformation and stability of elastic rods]. *Magazine of Civil Engineering.* 2013. No. 1(36). Pp. 87–96. (rus)
10. Lalin V.V. Razlichnyye formy uravneniy ravnovesiya nelineynoy dinamiki uprugikh sterzhney [Various forms of the equilibrium equations of the nonlinear dynamics of elastic rods]. *Trudy SPbGPU.* 2004. No. 489. Pp. 121–128. (rus)
11. Lalin V.V., Zdanchuk Ye.V., Kushova D.A., Rozin L.A. Variatsionnyye postanovki nelineynykh zadach s nezavisimymi vrashchatelnymi stepenyami svobody [Variational formulation of nonlinear problems with independent rotational degrees of freedom]. *Magazine of*

Литература

1. Зенкевич О. Метод конечных элементов в технике. М.: Мир, 1975. 541 с.
2. Зенкевич О., Морган К. Конечные элементы и аппроксимация. М.: Мир, 1986. 318 с.
3. Галлагер Р. Метод конечных элементов. Основы. М.: Мир, 1984. 428 с.
4. Сливкер В. И. Строительная механика. Вариационные основы. М.: Издательство Ассоциации строительных вузов. 2005. 736 с.
5. Розин Л. А. Метод конечных элементов в применении к упругим системам. М.: Стройиздат, 1977. 129 с.
6. Senjanović I., Vladimir N., Cho D.-S. A simplified geometric stiffness in stability analysis of thin-walled structures by the finite element method // Inter J. Nav. Archit. Oc. Engng. 2012. Vol. 4. Pp. 313–321.
7. Ibearugbulem O.M., Eziefula U.G., Onwuka D.O. Stability analysis of uniaxially compressed flat rectangular isotropic CCSS plate // International Journal of Applied Mechanics and Engineering. 2015. Vol. 20. № 3. Pp. 637–646.
8. Евзеров И.Д. Задачи устойчивости для стержней и пластин // Инженерно-строительный журнал. 2014. № 1(45). С. 6–11.
9. Лалин В.В., Розин Л.А., Кушова Д.А. Вариационная постановка плоской задачи геометрически нелинейного деформирования и устойчивости упругих стержней // Инженерно-строительный журнал. 2013. № 1(36). С. 87–96.
10. Лалин В.В. Различные формы уравнений равновесия нелинейной динамики упругих стержней // Труды СПбГПУ. 2004. № 489. С. 121–128.
11. Лалин В.В., Зданчук Е.В., Кушова Д.А., Розин Л.А. Вариационные постановки нелинейных задач с независимыми вращательными степенями свободы // Инженерно-строительный журнал. 2015. № 4(56). С. 54–65.
12. Лалин В.В., Беляев М.О. Изгиб геометрически нелинейного консольного стержня. Решение по теориям Кирхгофа и Коссера – Тимошенко // Инженерно-строительный журнал. 2015. № 1(53). С. 39–55.
13. Lalin V., Rybakov V., Alexander S. The finite elements for design of frame of thin-walled beams // Applied Mechanics

Tyukalov Yu.Ya. The functional of additional energy for stability analysis of spatial rod systems. *Magazine of Civil Engineering*. 2017. No. 2. Pp. 18–32. doi: 10.18720/MCE.70.3

Civil Engineering. 2015. No. 4(56). Pp. 54–65. (rus)

12. Lalin V.V., Belyayev M.O. Izgib geometricheski nelineynogo konsolnogo sterzhnya. Resheniye po teoriyam Kirkhgofa i Kossera – Timoshenko [Bending geometrically nonlinear cantilever beam. The decision on the theories of Kirchhoff and Cosserat – Tymoshenko]. *Magazine of Civil Engineering.* 2015. No. 1(53). Pp. 39–55. (rus)
13. Lalin V., Rybakov V., Alexander S. The finite elements for design of frame of thin-walled beams. *Applied Mechanics and Materials.* 2014. Vol. 578–579. Pp. 858–863.
14. Perelmuter A.V., Slivker V.I. *Ustoychivost ravnovesiya konstruktsiy i rodstvennyye problemy* [Stability of equilibrium structures and related problems]. Vol. 1. M.: SKAD SOFT, 2010. 704 p. (rus)
15. Chepurenko A.S., Andreyev V.I., Yazyyev B.M. Energeticheskiy metod pri raschete na ustoychivost szhatykh sterzhney s uchetom polzuchesti [Energy method, with respect to stability in view of the rods of compressed creep]. *Vestnik MGSU.* 2013. No. 1. Pp. 101–108. (rus)
16. Kagan-Rozentsveyg L.M. O raschete uprugikh ram na ustoychivost [On calculation of the elastic frame for stability]. *Magazine of Civil Engineering.* 2012. No. 1(27). Pp. 74–78. (rus)
17. Chernov S.A. Modelirovaniye ustoychivosti podkreplennoy tonkostennymi sterzhnyami plastiny [Simulation of the stability of thin-walled stiffened plate]. *Programmnyye produkty i sistemy.* 2014. No. 4. Pp. 183–187. (rus)
18. Manuylov G.A., Kositsyn S.B., Begichev M. M. Chislennoye issledovaniye prostranstvennoy ustoychivosti uprugikh krugovykh zashchemlennykh arok [Numerical study of spatial stability of elastic clamped circular arches]. *International Journal for Computational Civil and Structural Engineering.* 2013. Vol. 9. No 1. Pp. 78–84. (rus)
19. Chamekh M., Mani-Aouadi S., Moakher M. Stability of elastic rods with self-contact. *Computer Methods in Applied Mechanics and Engineering.* 2014. Vol. 279. Pp. 227–246.
20. Dubrovin V.M., Butina T.A. Modelirovaniye ustoychivosti szhatogo i skruchennogo sterzhnya v tochnoy postanovke zadachi [Simulation of the stability of compressed and twisted rod in the exact formulation of the problem]. *Matematicheskoye modelirovaniye i chislennyye metody.* 2015. No. 3. Pp. 3–16. (rus)
21. Blyumin S.L., Zverev V.V., Sotnikova I.V., Sysoyev A.S. Resheniye zadachi ustoychivosti szhato-izgibayemykh zhestko opertykh sterzhney peremennoy zhestkosti [Solution of the problem of stability of compressed-bent rigidly simply supported rods of variable stiffness]. *Vestnik MGSU.* 2015. No. 5. Pp. 18–26. (rus)
22. Yuan W.B., Kim B., Li L.Y. Buckling of axially loaded castellated steel columns. *J. Construct. Steel Res.* 2014. No. 92. Pp. 40–45.
23. Kim B., Li L., Edmonds A. Analytical Solutions of Lateral–Torsional Buckling of Castellated Beams. *International Journal of Structural Stability and Dynamics.* 2016. Vol. 16. No. 8. Pp. 443–455.
24. Gorbachev V.I., Moskalenko O.B. Ustoychivost sterzhney s peremennoy zhestkostyu pri szhatii raspredelennoy nagruzkoy [Stability of rods with variable stiffness in compression load distributed]. *Vestnik Moskovskogo gosudarstvennogo universiteta. Seriya 1. Matematika. Mekhanika.* 2012. No. 1. Pp. 41–47. (rus)
25. Galkin A.V., Sysoyev A.S., Sotnikova I.V. Zadacha ustoychivosti szhato-izgibayemykh sterzhney so stupenchatym izmeneniyem zhestkosti [The problem of stability of compressed-bent rods with a step change in stiffness]. *Vestnik MGSU.* 2015. No. 2. Pp. 38–44. (rus)
26. Kucukler M., Gardner L., Macorini L. Flexural–torsional buckling assessment of steel beam–columns through a stiffness reduction method. *Engineering Structures*. 2015. Vol. 101. Pp. 662–676.
27. Pokrovskiy A.A. Ustoychivost sterzhnya peremennogo and Materials. 2014. Vol. 578–579. Pp. 858–863.
14. Перельмутер А.В., Сливкер В.И. Устойчивость равновесия конструкций и родственные проблемы. Том 1. М.: СКАД СОФТ, 2010. 704 с.
15. Чепуренко А.С., Андреев В.И., Язьев Б.М. Энергетический метод при расчете на устойчивость сжатых стержней с учетом ползучести// Вестник МГСУ. 2013. № 1. С. 101–108.
16. Каган-Розенцвейг Л. М. О расчете упругих рам на устойчивость // Инженерно-строительный журнал. 2012. № 1(27). С. 74–78.
17. Чернов С.А. Моделирование устойчивости подкрепленной тонкостенными стержнями пластины// Программные продукты и системы. 2014. № 4. С. 183–187.
18. Мануйлов Г.А., Косицын С.Б., Бегичев М.М. Численное исследование пространственной устойчивости упругих круговых защемленных арок // International Journal for Computational Civil and Structural Engineering. 2013. Vol. 9. № 1. Pp. 78–84.
19. Chamekh M., Mani-Aouadi S., Moakher M. Stability of elastic rods with self-contact// Computer Methods in Applied Mechanics and Engineering. 2014. Vol. 279. Pp. 227–246.
20. Дубровин В.М., Бутина Т.А. Моделирование устойчивости сжатого и скрученного стержня в точной постановке задачи // Математическое моделирование и численные методы. 2015. № 3. С. 3–16.
21. Блюмин С.Л., Зверев В.В., Сотникова И.В., Сысоев А.С. Решение задачи устойчивости сжато-изгибаемых жестко опертых стержней переменной жесткости // Вестник МГСУ. 2015. № 5. С. 18–26.
22. Yuan W. B., Kim B., Li L. Y. Buckling of axially loaded castellated steel columns // J. Construct. Steel Res. 2014. № 92. Pp. 40–45.
23. Kim B., Li L., Edmonds A. Analytical Solutions of Lateral–Torsional Buckling of Castellated Beams // International Journal of Structural Stability and Dynamics. 2016. Vol. 16. № 8. Pp. 443–455.
24. Горбачев В.И., Москаленко О.Б. Устойчивость стержней с переменной жесткостью при сжатии распределенной нагрузкой // Вестник Московского государственного университета. Серия 1. Математика. Механика. 2012. № 1. С. 41–47.
25. Галкин А.В., Сысоев А.С., Сотникова И.В. Задача устойчивости сжато-изгибаемых стержней со ступенчатым изменением жесткости // Вестник МГСУ. 2015. № 2. С. 38–44.
26. Kucukler M., Gardner L., Macorini L. Flexural–torsional buckling assessment of steel beam–columns through a stiffness reduction method // Engineering Structures. 2015. Vol. 101. Pp. 662–676.
27. Покровский А.А. Устойчивость стержня переменного сечения по длине и его применение в структурных конструкциях // Строит. механика и расчёт сооружений. 2007. № 4. С. 39–40.
28. Yong-Lin Kuo. Stress-based Finite Element Analysis of Sliding Beams // Appl. Math. Inf. Sci. 2015. Vol. 9. № 2. Pp. 609–616.
29. Qiu W., Demkowicz L. Mixed hp-finite element method for linear elasticity with weakly imposed symmetry: stability analysis // SIAM J. Numer. Anal. 2011. Vol. 49. № 2. Pp. 619–641.
30. Guzman J. A unified analysis of several mixed methods for elasticity with weak stress symmetry // J. Sci. Comput. 2010. Vol. 44. Pp. 156–169.
31. Суходолова Ю.С., Труфанов Н.А. О конечном элементе на основе вариационного принципа Кастильяно для плоских задач теории упругости // Вестник Пермского национального исследовательского политехнического

secheniya po dline i yego primeneniye v strukturnykh konstruktsiyakh [Stability rod of variable cross section along the length of its use and structural designs]. Stroit. mekhanika i raschet sooruzheniy. 2007. No. 4. Pp. 39–40. (rus)

28. Yong-Lin Kuo. Stress-based Finite Element Analysis of Sliding Beams. *Appl. Math. Inf. Sci.* 2015. Vol. 9. No. 2. Pp. 609–616.
29. Qiu W., Demkowicz L. Mixed hp-finite element method for linear elasticity with weakly imposed symmetry: stability analysis. *SIAM J. Numer. Anal.* 2011. Vol. 49. No. 2. Pp. 619–641.
30. Guzman J. A unified analysis of several mixed methods for elasticity with weak stress symmetry. *J. Sci. Comput.* 2010. Vol. 44. Pp. 156–169.
31. Sukhodolova Yu.S., Trufanov N.A. O konechnom elemente na osnove variatsionnogo printsipa Kastilyano dlya ploskikh zadach teorii uprugosti [On the finite element based on Castigliano variational principle for plane elasticity problems]. *Vestnik Permskogo natsionalnogo issledovatelskogo politekhnicheskogo universiteta. Mekhanika.* 2012. No. 1. Pp. 168–178. (rus)
32. Tyukalov Yu.Ya. Raschet plit na dinamicheskiye vozdeystviya s uchetom plasticheskikh deformatsiy [Calculation of the plates on the dynamic effects of considering plastic deformation]. *Seysmostoykoye stroitelstvo. Bezopasnost sooruzheniy*. 2005. No. 2. Pp. 24–26. (rus)
33. Tyukalov Yu.Ya. Raschet obolochek proizvolnoy formy metodom konechnykh elementov v napryazheniyakh [Calculation of shells of arbitrary shape by finite element method in stresses]. *Stroitelnaya mekhanika i raschet sooruzheniy.* 2006. No. 1. Pp. 65–74. (rus)
34. Tyukalov Yu.Ya. Resheniye ploskoy zadachi teorii uprugosti metodom konechnykh elementov v napryazheniyakh [The solution of the plane problem of elasticity theory of finite elements method in stresses]. *Stroitelnaya mekhanika i raschet sooruzheniy.* 2006. No. 2. Pp. 34–38. (rus)
35. Tyukalov Yu.Ya. Variatsionno-setochnyy metod resheniya zadach izgiba plit v napryazheniyakh[Variational-grid method for solving the problems of plate bending in stresses]. *Izvestiya vuzov. Stroitelstvo.* 2006. No. 8. Pp. 13–20. (rus)
36. Tyukalov Yu.Ya. Ispolzovaniye kusochno-postoyannykh napryazheniy dlya resheniya obyemnykh zadach teorii uprugosti [Using the piecewise constant stresses for solutions of the volume elasticity problems]. *Izvestiya vuzov. Stroitelstvo.* 2008. No. 4. Pp. 4–9. (rus)
37. Kiselev V.A. *Stroitelnaya mekhanika. Dinamika i ustoychivost sooruzheniy* [Structural mechanics. The dynamics and stability of structures]. M.: Stroyizdat, 1980. 616 p. (rus)
38. Chiras A.A. *Stroitelnaya mekhanika: Teoriya i algoritmy* [Structural Mechanics: Theory and Algorithms]. M.: Stroyizdat, 1989. 255 p.(rus)

университета. Механика. 2012. № 1. С. 168–178.

32. Тюкалов Ю.Я. Расчет плит на динамические воздействия с учетом пластических деформаций // Сейсмостойкое строительство. Безопасность сооружений. 2005. № 2. С. 24–26.
33. Тюкалов Ю.Я. Расчет оболочек произвольной формы методом конечных элементов в напряжениях // Строительная механика и расчет сооружений. 2006. № 1. С. 65–74.
34. Тюкалов Ю.Я. Решение плоской задачи теории упругости методом конечных элементов в напряжениях // Строительная механика и расчет сооружений. 2006. № 2. С. 34–38.
35. Тюкалов Ю.Я. Вариационно-сеточный метод решения задач изгиба плит в напряжениях // Известия вузов. Строительство. 2006. № 8. С. 13–20.
36. Тюкалов Ю.Я. Использование кусочно-постоянных напряжений для решения объемных задач теории упругости // Известия вузов. Строительство. 2008. № 4. С. 4–9.
37. Киселев В.А. Строительная механика. Динамика и устойчивость сооружений. М.: Стройиздат, 1980. 616 с.
38. Чирас А.А. Строительная механика: Теория и алгоритмы. М.: Стройиздат, 1989. 255 с.

Yury Tyukalov,
+7(912)8218977; yutvgu@mail.ru

Юрий Яковлевич Тюкалов,
+7(912)8218977; эл. почта: yutvgu@mail.ru

Tyukalov Yu.Ya. The functional of additional energy for stability analysis of spatial rod systems. *Magazine of Civil Engineering*. 2017. No. 2. Pp. 18–32. doi: 10.18720/MCE.70.3

doi: 10.18720/MCE.70.4

Stress state of protective shells in the area of holes due to prestressed reinforcement curvature

Напряженное состояние защитных оболочек в зоне отверстий вследствие кривизны преднапряженных элементов

V.A. Sokolov,
D.A. Strachov,
L.N. Sinyakov,
S.V. Vasiutina,
Peter the Great St. Petersburg Polytechnic University, St. Petersburg, Russia

Канд. техн. наук, доцент В.А. Соколов,
канд. техн. наук, доцент Д.А. Страхов,
канд. техн. наук, доцент Л.Н. Синяков,
студент С.В. Васютина,
Санкт-Петербургский политехнический университет Петра Великого, г. Санкт-Петербург, Россия

Key words: prestressed concrete shell; reinforcement; holes in shell; curvature of reinforcement elements; stress concentration; complex functions; Fourier series; approximate solution

Ключевые слова: предварительно напряженная бетонная оболочка; арматура; отверстия в оболочке; кривизна арматурных элементов; концентрация напряжений; комплексные функции; ряды Фурье; приближенное решение

Abstract. The stress state around the holes in cylindrical part of prestressed concrete protective shells is examined in this paper. This stress state is caused by general shell prestressing having the aim to compensate internal emergency pressure and the curvature of the reinforcement elements near technological holes in cylindrical part of shell. Presence of technological holes predetermines occurrence of so called “disturbed” stress state of a local nature (stress concentration). The exact solution of the stress concentration problem at any load does not exist even for a plate. So the approximate solution using complex functions and Fourier series for a plate with a hole is proposed. It can be concluded on the basis of the calculation results that the stress concentration due to curvature of reinforcement elements near hole has to be taken into account, since in this case the maximum compressive stress is considerable.

Аннотация. В данной работе рассматривается напряженное состояние конструкции вокруг отверстий в цилиндрической части предварительно напряженных бетонных защитных оболочек. Это напряженное состояние вызвано общим предварительным напряжением оболочки, необходимым для компенсации внутреннего аварийного давления, и кривизной арматурных элементов вблизи технологических отверстий в цилиндрической части оболочки. Наличие технологических отверстий предопределяет возникновение так называемого «возмущенного» напряженного состояния локального характера (концентрация напряжений). Точного решения проблемы концентрации напряжений при любой нагрузке не существует даже для пластины. Поэтому предлагается приближенное решение с использованием комплексных функций и рядов Фурье для пластины с отверстием. На основании результатов расчета можно сделать вывод о том, что необходимо учитывать концентрацию напряжений, вызванную искривлением арматурных элементов вблизи отверстия, поскольку в этом случае максимальное сжимающее напряжение является значительным.

Introduction

Cylindrical part of prestressed concrete protective shells for nuclear power plants with a helical scheme of reinforcement is compressed by two groups of reinforcement elements, oriented over the counter spirals and directed at an angle of 55 degrees to meridian.

The general stress state of the cylindrical part of the shell caused by the preliminary compression forces in areas, sufficiently distant from the bottom and the support ring, is momentless and can be determined in accordance with the membrane theory of thin shells [1–8].

Соколов В.А., Страхов Д.А., Синяков Л.Н., Васютина С.В. Напряженное состояние защитных оболочек в зоне отверстий вследствие кривизны преднапряженных элементов // Инженерно-строительный журнал. 2017. № 2(70). С. 33–41.

In areas of technological holes, the largest of which reaches a diameter of 4 m (at elev. 38.1 m), it is necessary to bend the reinforcement elements around the hole. To reduce the prestressing losses from friction trajectory of the reinforcement is made fairly smooth; nevertheless there is considerable pressure of the reinforcement elements (Fig. 1) and the additional stress state in concrete. Of course, in Figure 1 for illustration a simplified scheme of the fragment of rather complicated reinforcement system around the circular hole is presented.

Presence of technological holes predetermines occurrence of so called “disturbed” stress state of a local nature (stress concentration). Thus the stress concentration around the holes is caused by the general compression and by the influence of the curvature of the reinforcement around these holes.

The concentration of the stress caused by a general shells compression is sufficiently investigated [9–23], so the aim of this article is the research of effect of the reinforcement elements curvature for the stress state near the holes , because only a few studies is devoted to this problem [24–25].

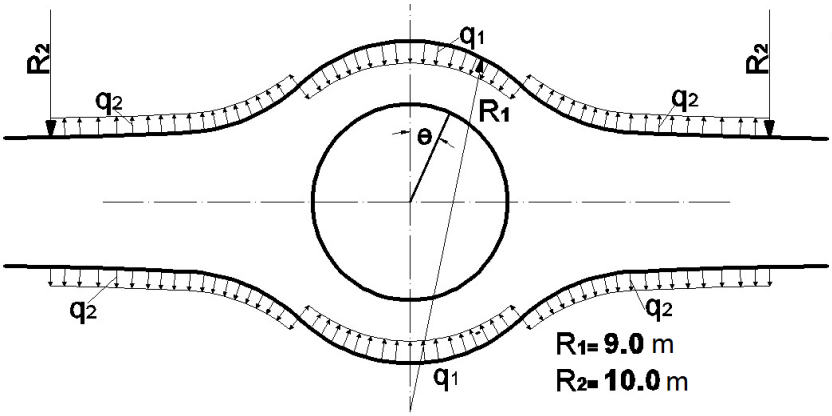

Figure 1. Loads due to curvature of the reinforcement elements

Methods

In the framework of the theory of elasticity a number of special problems of shell theory is currently still not resolved taking into account the complicating factors connected with the mathematical nature of the difficulties. One of such problem is the determination of the stress-strain condition of shells in the area of technological holes. So one has to substitute shell fragment around the hole by the plane fragment in order to solve many engineering problems and consider the plane task. The latter does not lead to significant errors if the fragment is characterized by small curvature, and the hole can be considered as "small". Methods for solving some problems for thin isotropic cylindrical shells (membranes) are described for example in [8, 9, 11]. The holes in these membranes is called small if the following condition take place:

$$\beta a < 1, \tag{1}$$

where $\beta = \sqrt[4]{3(1-\upsilon^2)} / 2\sqrt{Rh}$; R, h – radius and thickness of the shell; a – radius of the hole.

For this problem solution the following sizes are accepted: R = 23.1 m; h = 1.2 m; a = 2.0 m, which corresponds to βa = 0.25, that is, the hole is certainly small. Note that, if in the above formulas for the stresses around the holes [9, 11] to accept βa = 0, one gets the corresponding formula for a plate of unlimited size.

Comparative calculations show that for the shell with accepted parameters in case of uniaxial tension (or compression) along the cylinder the maximum stress for the shell near hole exceeds corresponding stress for the plate by only 3 % and in case of internal pressure – by 18 %. It can be assumed, that in case of the reinforcement curvature influence the error is less than above.

However, even for plates stress concentration around the holes is one of the most difficult sections of the theory of elasticity, so here analytical solutions in its final form have been obtained for comparatively simple cases of loading [12].

Solution of the problem of stress concentration around the hole can be realized as follows. Due to the task linearity the overall stress-strain state of the plate or membrane can be taken as the sum of

"background" stress-strain state and "disturbed" stress-strain state. The state of the plate (or membrane) without holes loaded with an arbitrary system of forces and moments is considered as "background" stress-strain state.

In determining the disturbed state of stress a plate with a hole is considered, and this plate is under influence of the load applied to the hole contour. This load has to be taken equal to stress of the background state, but has to have the opposite direction in order to get zero stress on the hole contour, as well as it should be within the meaning of the problem.

When the superposition of background and disturbed states is realized, the result stress state of the plate with the hole will take place.

In this paper the pressure of the reinforcement elements, caused by its curvature (Fig. 1), for the plate without hole is taken as a background stress state. The intensity of this pressure can be calculated as:

$$q_i = N / R_i, \tag{2}$$

where N – tension force in the reinforcement elements, R_i – radius of curvature of these elements in the plane of the plate. To calculate stress state the actual distribution of the load was replaced by an equivalent in the form of a large number of concentrated forces oriented at different angles to the vertical axis (Fig. 1).

Calculation of the background state of stress from the effects of each of the concentrated forces was carried out according to formulas derived by Melan [1] for the force acting within an infinite plate (without holes) in its plane:

$$\sigma_x = \frac{P}{4\pi}\frac{\cos\theta}{r}\left[-(3+\upsilon)+2(1+\upsilon)\sin^2\theta\right]; \tag{3}$$

$$\sigma_y = \frac{P}{4\pi}\frac{\cos\theta}{r}\left[1-\upsilon-2(1+\upsilon)\sin^2\theta\right]; \tag{4}$$

$$\tau_{xy} = \frac{-P}{4\pi}\frac{\sin\theta}{r}\left[1-\upsilon+2(1+\upsilon)\cos^2\theta\right]. \tag{5}$$

In the above formulas: r – distance from the force to the point at which the stress is determined; θ – angle is measured from the vertical axis.

The state of stress from all the concentrated forces approximating a distributed load is determined by a superposition of solutions for each of the concentrated forces. Then the transition from Cartesian coordinates to polar has to be fulfilled.

To solve the problem of the second stage (the calculation of the disturbed state) it is advisable to apply the solution of the plane task of elasticity theory with complex variables, which in some cases leads to significant simplifications.

The components of stresses for plane stress state in polar coordinates can be expressed as follows [6]:

$$\sigma_r + \sigma_\theta = 4\,\mathrm{Re}\,F'(Z) = 2\left[F'(Z)+\overline{F}'(\overline{Z})\right]; \tag{6}$$

$$\sigma_\theta - \sigma_r + 2i\tau_{r\theta} = 2\left[\overline{Z}F''(Z)+\chi''(Z)\right]e^{2i\theta}, \tag{7}$$

where $Z = r(\cos\theta + i\sin\theta) = re^{i\theta}$; $\overline{Z} = r(\cos\theta - i\sin\theta) = re^{-i\theta}$; $\overline{Z}$ – conjugate function Z, $F'(Z)\ u\ \chi'(Z)$ – some analytic functions. Subtracting (7) from (6) we obtain:

$$\sigma_r - i\tau_{r\theta} = F'(Z)+\overline{F}'(\overline{Z})-\left[\overline{Z}F''(Z)+\chi''(Z)\right]e^{2i\theta}. \tag{8}$$

Соколов В.А., Страхов Д.А., Синяков Л.Н., Васютина С.В. Напряженное состояние защитных оболочек в зоне отверстий вследствие кривизны преднапряженных элементов // Инженерно-строительный журнал. 2017. № 2(70). С. 33–41.

Let us consider the general solution for unlimited size plate with a circular hole with the origin in the center of the hole. If to run the boundary conditions on the contour of the hole, then σ_r and $\tau_{r\theta}$ will be known when $z = ae^{i\theta}$, where *a* – the radius of the hole, r – distance from the center of the hole (on the contour r = *a*).

Analytic functions $F'(Z), \chi''(Z)$ – can be expanded in power series, so that the functions remain finite at $r \to \infty$

$$F'(Z) = \sum_{n=0}^{\infty} A_n Z^{-n} = A_0 + A_1 \frac{1}{Z} + A_2 \frac{1}{Z^2} + \ldots ; \tag{9}$$

$$\chi''(Z) = \sum_{n=0}^{\infty} B_n Z^{-n} = B_0 + B_1 \frac{1}{Z} + B_2 \frac{1}{Z^2} + \ldots , \tag{10}$$

where A_n and B_n − complex constants (independing from *Z*).

$$F'(Z) = \sum_{n=0}^{\infty} \overline{A_n}\,\overline{Z}^{-n} = \overline{A_0} + \overline{A_1} \frac{1}{\overline{Z}} + \overline{A_2} \frac{1}{\overline{Z}^2} + \ldots ; \tag{11}$$

$$F''(Z) = -A_1 Z^{-2} - 2A_2 Z^{-3} - \ldots . - nA_n Z^{-n-1}. \tag{12}$$

Since the stresses σ_r and $\tau_{r\theta}$ must be known on the hole contour ($r = a$), the expression $(\sigma_r - i\tau_{r\theta})_{r=a}$ can be expanded in a complex Fourier series [6]:

$$(\sigma_r - i\tau_{r\theta})_{r=a} = \sum_{n=-\infty}^{\infty} C_n e^{in\theta}; \tag{13}$$

the coefficients of which are determined by the formula:

$$C_n = \frac{1}{2\pi} \int_0^{2\pi} \left[\sigma_r(\theta) - i\tau_{r\theta}\right]_{r=a} e^{-in\theta} d\theta; \tag{14}$$

where $n = 0; 1; -1; 2; -2; \ldots$

Equating the right-hand side of the equation (8), expressed in terms of (9)–(12) and the expression (13), we obtain:

$$\sum_{n=-\infty}^{\infty} C_n e^{in\theta} = \sum_{n=0}^{\infty} \frac{A_n}{a^n} e^{-in\theta} + \sum_{n=0}^{\infty} \frac{\overline{A_n}}{a^n} e^{in\theta} + \sum_{n=0}^{\infty} \frac{nA_n}{a^n} e^{-in\theta} - \sum_{n=0}^{\infty} \frac{B_n}{a^n} e^{-i(n-2)\theta}, \tag{15}$$

since at the hole contour $z = ae^{i\theta}$; $Z^{-n} = \frac{1}{a^n} e^{-in\theta}$.

The last expression can be written as follows:

$$\begin{aligned}
&C_0 + C_1 e^{i\theta} + C_{-1} e^{-i\theta} + C_2 e^{2i\theta} + C_{-2} e^{-2i\theta} + C_3 e^{3i\theta} + \ldots . = \\
&A_0 + \frac{A_1}{a} e^{-i\theta} + \frac{A_2}{a^2} e^{-2i\theta} + \frac{A_3}{a^3} e^{-3i\theta} + \ldots . \\
&+ \overline{A_0} + \frac{\overline{A_1}}{a} e^{i\theta} + \frac{\overline{A_2}}{a^2} e^{2i\theta} + \frac{\overline{A_3}}{a^3} e^{3i\theta} + \ldots . \\
&+ \frac{A_1}{a} e^{-i\theta} + \frac{2A_2}{a^2} e^{-2i\theta} + \frac{3A_3}{a^3} e^{-3i\theta} + \ldots . \\
&- B_0 e^{2i\theta} - \frac{B_1}{a} e^{i\theta} - \frac{B_2}{a^2} e^{0} - \frac{B_3}{a^3} e^{-i\theta} - \frac{B_4}{a^4} e^{-2i\theta} + \ldots .
\end{aligned} \tag{16}$$

Sokolov V.A., Strachov D.A., Sinyakov L.N., Vasiutina S.V. Stress state of protective shells in the area of holes due to prestressed reinforcement curvature. *Magazine of Civil Engineering*. 2017. No. 2. Pp. 33–41. doi: 10.18720/MCE.70.4

Equating the coefficients before the same powers of *e* in both parts of the equality, we get:

$$A_0 + \overline{A_0} - \frac{B_2}{a^2} = C_0 \quad \text{(when n = 0);} \tag{17}$$

$$\frac{\overline{A_1}}{a} - \frac{B_1}{a} = C_1 \quad \text{(when n = 1);} \tag{18}$$

$$\frac{\overline{A_2}}{a^2} - B_0 = C_2 \quad \text{(when n = 2);} \tag{19}$$

$$\frac{\overline{A_n}}{a^n} = C_n \quad \text{(when } n \geq 3\text{);} \tag{20}$$

$$\frac{2A_1}{a} - \frac{B_3}{a^3} = C_{-1} \quad \text{(when n = −1);} \tag{21}$$

$$\frac{1+n}{a^n} A_n - \frac{B_{n+2}}{a^{n+2}} = C_{-n}. \tag{22}$$

Constants A_0, $\overline{A_0}$ equal to each other, since the imaginary part determines the displacement of a rigid body, and in the analysis of strain and stress can be assumed to be equal zero [6]:

$$r\left(\cos\theta + i\sin\theta\right) = r\left(\cos\theta - i\sin\theta\right) = r\left(\cos\theta\right), \tag{23}$$

that is $A_0 + \overline{A_0} = 2A_0$.

From the condition of the uniqueness of the value of the displacement $\vartheta_r + i\vartheta_\theta$, should be

$$A_1 = -\frac{1+\upsilon}{3-\upsilon}\overline{B_1}; \tag{24}$$

whence

$$\overline{A_1} = -\frac{1+\upsilon}{3-\upsilon} B_1; \tag{25}$$

Substituting (25) into (18) we obtain:

$$B_1 = -\frac{(3-\upsilon)c_1 a}{4}; \tag{26}$$

Substituting (26) into (25) we obtain:

$$\overline{A_1} = -\frac{1+\upsilon}{3-\upsilon} B_1 = -\frac{1+\upsilon}{3-\upsilon}\left(-\frac{(3-\upsilon)c_1 a}{4}\right) = \frac{\left(1+\upsilon\right)c_1 a}{4}; \tag{27}$$

or

$$\overline{A_1} = \frac{\left(1+\upsilon\right)c_1 a}{4}. \tag{28}$$

From (19) we get:

$$\overline{A_2} = B_0 a^2 + C_2 a^2; \tag{29}$$

Соколов В.А., Страхов Д.А., Синяков Л.Н., Васютина С.В. Напряженное состояние защитных оболочек в зоне отверстий вследствие кривизны преднапряженных элементов // Инженерно-строительный журнал. 2017. № 2(70). С. 33–41.

$$A_2 = \overline{B_0}a^2 + \overline{C_2}a^2; \tag{30}$$

Taking into account, that $A_0 + \overline{A_0} = 2A_0$, from (17):

$$2A_0 - \frac{B_2}{a^2} = C_0 \tag{31}$$

$$B_2 = 2A_0a^2 - C_0a^2; \tag{32}$$

From equations (20) and (22):

$$A_n = C_n a^n \text{ when } n \geq 3; \tag{33}$$

$$B_n = (n-1)a^2 A_{n-2} - a^n C_{-n+2}, \text{ when } n \geq 3. \tag{34}$$

Thus, all members of the functions $F'(Z), \chi''(Z), \overline{F}'(Z), F''(Z)$, are known (expressed in terms C_n), and the problem reduces to the determination of the coefficients C_n by the formula (14), which can be written as follows:

$$\begin{aligned} C_n &= \frac{1}{2\pi}\int_0^{2\pi}\left[\sigma_r(\theta) - i\tau_{r\theta}\right]_{r=a} e^{-in\theta}d\theta = \\ &= \frac{1}{2\pi}\int_0^{2\pi}\left[\sigma_r(\theta) - i\tau_{r\theta}\right]_{r=a}(\cos n\theta - i\sin n\theta)\,d\theta. \end{aligned} \tag{35}$$

Results and Discussion

When the plate is loading by the pressure of curved near the hole reinforcing elements (Fig. 1), coefficients in the complex Fourier series were determined by numerical integration in accordance with expression (35). Convergence was studied by doubling the number of intervals between concentrated forces. The calculation results show that for the scheme of loading, which has two axes of symmetry (Fig. 1.), it is sufficient to restrict 8–10 members of series (9)–(12).

The calculations were performed for the reinforcement elements with the prestressing force of 8000 *kN.* Accordingly accepted radius of curvature distributed load intensity are $q_1 = 888,9kN/m, q_2 = 800kN/m.$ According to the calculations, the maximum value of the tangential forces near the hole, induced by curvature of two reinforcement elements, when $\theta = \frac{\pi}{2}$ is about 1900 *kN*/*m*.

Since the influence of the curvature of individual prestressed elements near holes was hardly studied by other authors, the force from curvature of two elements is compared with the vertical force of general compression which is necessary to compensate internal emergency pressure *p* = 0,4 *MPa*. This force in the shell with a hole, but excluding influence of the curvature of reinforcement elements near hole, is approximately determined as 3*pR*/2 [26–37], where *R* is the radius of the cilindrical part of the shell. This force at *R* = 23.1 m is equal to 13860 *kN/m*.

It can be concluded on the basis of the calculation results that the stress concentration due to curvature of reinforcement elements near holes has to be take into consideration, since in this case the maximum compressive stress may achieve about 15% of the maximum stresses caused by general compression.

$$3\frac{pR}{2} = 3\frac{400 \cdot 23,11}{2} = 13860kN/m. \tag{36}$$

Sokolov V.A., Strachov D.A., Sinyakov L.N., Vasiutina S.V. Stress state of protective shells in the area of holes due to prestressed reinforcement curvature. *Magazine of Civil Engineering*. 2017. No. 2. Pp. 33–41. doi: 10.18720/MCE.70.4

Conclusions

1. Analysis of existing analytical solutions related to the study of stresses around the holes in the cylindrical shells and plates, showed that, when examined relations between the radius of the shell and the radius of the hole take place, solutions for the plates is allowed to use.

2. It can be concluded on the basis of the calculation results that the stress concentration due to curvature of reinforcement elements near hole has to be take into account, since in this case the maximum compressive stress may achieve about 15 % of the maximum stresses caused by general compression. At the same time, a significant value of tensile stresses, caused by curvature of reinforcement, may result in inadequate general compression in some areas of the shell around the holes.

3. The method developed for calculation of the stress state near the holes of plates using complex functions with some improvements can be used in any case of the load distribution in plane of the plate.

References

1. Timoshenko S.P., Gudyer Dzh. *Teoriya uprugosti* [Elasticity theory]. Moscow: Nauka, 1979. 576 p. (rus)
2. Timoshenko S.P., Voynovskiy-Kriger S. *Plastinki i obolochki* [Plates and Shells]. Moscow: Nauka, 1966. 636 p. (rus)
3. Sokolov V.A. *Zashchitnyye obolochki reaktornykh otdeleniy AES* [Protective shells of NPP reactor compartment]. St. Petersburg: Izdatelstvo Politekhnicheskogo universiteta Petra Velikogo, 2007. 106 p. (rus)
4. Musabayev T.T. *Nelineynaya teoriya rascheta zhelezobetonnykh obolochek i plastin* [The nonlinear theory of concrete shells and plates calculation]. PhD dissertation. Saint-Petersburg State University of Architecture and Civil Engineering. St. Petersburg. 1999. (rus)
5. Medvedev V.N., Ulyanov A.N., Kiselev A.S., Kiselev A.S., Lopanchuk A.A., Nefedov S.S. *Analiz predelnoy prochnosti zashchitnoy obolochki energobloka VVER-1000* [Analysis of protective shell ultimate strength of power block VVER-1000]. Proceedings of IBRAE RAS. 2008. No. 6. Pp. 122–130. (rus)
6. Van Tszi-De. *Prikladnaya teoriya uprugosti* [Applied elasticity]. Moscow: Fizmatgiz, 1959. 400 p. (rus)
7. Korobov L.A., Zharkov A.F., Shernik A.O. *Issledovanie zhelezobetonnykh zashchitnykh obolochek AES. Preduprezhdenie o vozmozhnykh avariyakh na AES Rossii* [Research of concrete protective shell of NPP. Warning of possible accidents at Russian NPP]. Moscow: Sputnik plyus, 2011. 256 p. (rus)
8. Lurye A.I. *Statika tonkostennykh uprugikh obolochek* [Statics of thin elastic shells]. Moscow : Gostekhizdat, 1947. 252 p. (rus)
9. Pirogov I.M. Vliyanie krivizny naraspredelenie napriazhenij okolo otverstiya v tsilindricheskoj obolochke [Effect of curvature on the stress distribution near the hole inthe cylindrical shell]. *Applied Mechanics.* 1965. Vol. 1. No. 12. Pp. 116–119. (rus)
10. Solovey N.A., Krivenko O.P., Malygina O.A. Konechnoelementnye modeli issledovaniya nelineynogo deformirovaniya obolochek stupenchato-peremennoy tolshchiny s otverstiyami, kanalami i vyemkami [Finite element models for the analysis of nonlinear deformation of shells stepwise-variable thickness with holes, channels and cavities]. *Magazine of Civil Engineering.* 2015. No. 1. Pp. 56–69. (rus)
11. Guz A.N., Chernyshenko I.S., Chekhov Val.N., Chekhov Vik.N., Shnerenko K.I. *Tsilindricheskie obolochki, oslablennye otverstiyami* [Impaired by holes cylindrical shell]. Kiev: Naukova Dumka, 1974. 272 p. (rus)
12. Savin G.N. *Raspredelenie napryazheniy okolo otverstiy* [Stress distribution around holes]. Kiev: Naukova Dumka, 1968. 891 p. (rus)
13. Sigova E.M. *Chislennoe reshenie geometricheski*

Литература

1. Тимошенко С.П., Гудьер Дж. Теория упругости. М.: Наука, 1979. 576 с.
2. Тимошенко С.П., Войновский-Кригер С. Пластинки и оболочки. М.: Наука, 1966. 636 с.
3. Соколов В.А. Защитные оболочки реакторных отделений АЭС. СПб: Издательство Политехнического университета Петра Великого, 2007. 106 с.
4. Мусабаев Т.Т. Нелинейная теория расчета железобетонных оболочек и пластин. Дисс. на соиск. учен. степ. к.т.н.: Спец. 05.23.17. СПб, 1999. 421 с.
5. Медведев В.Н., Ульянов А.Н., Киселев А.С., Киселев А.С., Лопанчук А.А., Нефедов С.С. Анализ предельной прочности защитной оболочки энергоблока ВВЭР-1000 // Труды ИБРАЭ РАН. 2008. № 6. С. 122–130.
6. Ван Ц.-Д. Прикладная теория упругости. М. Государственное издательство физико-математической литературы, 1959. 400 с.
7. Коробов Л.А., Жарков А.Ф., Шерник А.О. Исследование железобетонных защитных оболочек АЭС. Предупреждения о возможных авариях на АЭС России. М.: Спутник плюс, 2011. 256 с.
8. Лурье А.И. Статика тонкостенных упругих оболочек. М.: Гостехиздат, 1947. 252 с.
9. Пирогов И.М. Влияние кривизны на распределение напряжений около отверстия в цилиндрической оболочке // Applied Mechanics. 1965. Vol. 1. № 12. С. 116–119.
10. Соловей Н.А., Кривенко О.П., Малыгина О.А. Конечноэлементные модели исследования нелинейного деформирования оболочек ступечато-переменной толщины с отверстиями, каналами и выемками // Инженерно-строительный журнал. 2015. № 1. С. 56–69.
11. Гуз А.Н., Чернышенко И.С., Чехов Вал.Н., Чехов Вик.Н. Шнеренко К.И. Цилиндрические оболочки, ослабленные отверстиями. Киев: Наукова Думка, 1974. 272 с.
12. Савин Г.Н. Распределение напряжений около отверстий. Киев: Наукова Думка, 1968. 891 с.
13. Сигова Е.М. Численное решение геометрически нелинейной задачи о напряженно-деформируемом состоянии цилиндрической облочки с отверстием. Томск: Издательство Томского политехнического университета, 2013. 468 с.
14. Довбня Е.Н., Крупко Н.А. Влияние кругового отверстия на напряженное состояние оболочки произвольной гауссовской кривизны // Вестник ПНИПУ. № 1. С. 108–125.
15. Васильев В.В., Федоров Л.В. Задача геометрической теории упругости о концентрации напряжений в пластине с круговым отверстием // Механика твердого тела. 2008. № 4. С. 6–18.

Соколов В.А., Страхов Д.А., Синяков Л.Н., Васютина С.В. Напряженное состояние защитных оболочек в зоне отверстий вследствие кривизны преднапряженных элементов // Инженерно-строительный журнал. 2017. № 2(70). С. 33–41.

nelineynoy zadachi o napryazhenno-deformirovannom sostoyanii tsilindricheskoy obolochki s otverstiem [numerical solution geometrically nonlinear problem of stress strain behavior of cylindrical shell with a hole]. Tomsk : Izdatelstvo Tomskogo politekhnicheskogo universiteta, 2013. 468 p. (rus)

14. Dovbnya Ye.N., Krupko N.A. Vliyaniye krugovogo otverstiya na napryazhennoye sostoyaniye obolochki proizvolnoy gaussovoy krivizny [Influence of circular hole on the shell stress state for arbitrary Gaussian curvature]. *PNRPU Mechanics Bulletin.* 2014. No. 1. Pp. 108–125. (rus)
15. Vasilyev V.V., Fedorov L.V. Zadacha geometricheskoy teorii uprugosti o kontsentratsii napryazheniy v plastine s krugovym otverstiyem [The geometric theory problem of elasticity of the stress concentration at the plate with a circular hole]. *Mechanics of Solids.* 2008. No. 4. Pp. 6–18. (rus)
16. Trofimov V.N., Abdulova A.S., Isayeva Yu.A., Podkina N.S. Issledovaniye kontsentratsii napryazheniy sostoyaniya v plastinakh s otverstiyami [Research of stress concentration of state in plates with holes]. *Proceedings of the XI International Scientific and Practical Conference.* Kursk: University Book, 2014. Vol. 4. Pp. 205–208. (rus)
17. Nizomov D.N. Khodzhiboyev A.A. Khodzhiboyev O.A. Napryazhenno-deformirovannoye sostoyaniye anizotropnoy plastiny, oslablennoy otverstiyem [Stress-strain state of anisotropic plate weakened by a hole]. *Structural Mechanics of Engineering Constructions and Buildings.* 2013. No. 4. Pp. 22–28. (rus)
18. Timerbayev R.M., Khayrullin F.S., Khakimov R.G. Zadacha o deformirovanii krugloy plastiny s otverstiyem [The problem of the deformation of the circular plate with hole]. *Vestnik Kazanskogo Tekhnologicheskogo Universiteta.* 2013. Vol. 16. No. 6. Pp. 179–182. (rus)
19. Semykina T.D., Vulman S.A. Vliyaniye na napryazhennoye sostoyaniye beskonechnoy plastiny kasatelnykh napryazheniy, raspredelennykh po krugovomu otverstiyu [Influence of shear stresses distributed over a circular hole to the stress state of an infinite plate]. *Vestnik ChGPU im. I.Ya. Yakovleva.* 2012. Vol. 12. No 2. Pp. 83–87.
20. Nizomov D.N., Khodzhiboyev A.A., Khodzhiboyev O.A. Kontsentratsiya napryazheniy vokrug otverstiya v anizotropnoy plastine [Simulation of the stress-strain state of excavation boundaries in fractured massifs]. *Scientific and Technical Journal on Construction and Architecture.* 2011. No. 6. Pp. 307–311.
21. Makarov E.V., Monahov I.A., Nefedova I.V. Dvuosnoye rastyazheniye plastiny s krugovym otverstiyem [Biaxial stretching of the plate a circular hole]. *Bulletin of Russian Peoples' Friendship University. Series Engineering Researches.* 2015. No 3. Pp. 17–22.
22. Poluektov V.A., Mirenkov V.Ye., Shutov V.A. Napryazhennoye sostoyaniye plastin s otverstiyem [Stress state of plates with a hole]. *News of higher educational institutions. Construction.* 2014. Vol. 671. No .11. Pp. 5–9.
23. Bok Kh.K.A. *Konstruirovaniye i issledovaniye napryazhenno-deformirovannogo sostoyaniya plastin i obolochek s otverstiyami variatsionno-raznostnym metodom* [Design and research of stress-strain state of plates and shells with holes by variational-difference method]. PhD dissertation. RUDN University. Moscow. 2005. (rus)
24. Ulyanov A.N., Medvedev V.N Printsipy konstruirovaniya zon tekhnologicheskikh prokhodok [Design principles of technological holes areas]. *Proceedings of IBRAE RAS.* 2008. No. 6. Pp. 8–10. (rus)
25. Ulyanov A.N., Medvedev V.N., Kiselev A.S. Vliyaniye otgibov armaturnykh elementov na napryazhennoye sostoyaniye zashchitnykh obolochek AES v zone tekhnologicheskikh prokhodok [Influence of offset bend to the NPP protective shell stress state in technological holes areas]. *Proceedings of IBRAE RAS.* 2008. No. 6. Pp. 11–
16. Трофимов В.Н., Абдулова А.С., Исаева Ю.А. Исследование концентраций напряженний состояния в пластинах с отверстиями // Сборник научных трудов XI Международной научно-практической конференции. Курск: Университетская книга, 2014. Т. 4. С. 205–208.
17. Низомов Д.Н., Ходжибоев А.А., Ходжибоев О.А. Напряженно-деформированное состояние анизотропной пластины, ослабленной отверстием // Строительная механика иженерных конструкций и сооружений. 2013. № 4. С. 22–28.
18. Тимербаев Р.М. Хайруллин Ф.С., Хакимов Р.Г. Задача о деформировании круглой пластины с отверстием // Вестник Казанского технологического унвиерситета. 2013. Т. 16. № 6. С. 179–182.
19. Семыкина Т.Д., Вульман С.А. Влияние на напряженное состояние бесконечной пластины касательных напряжений, распределенных по круговому отверстию // Вестник Чувашского государственного педагогического университета им. И.Я. Яковлева. 2012. Т. 12. № 2. С. 83–87.
20. Низомов Д.Н., Ходжибоев А.А., Ходжибоев О.А. Концентрация напряжений вокруг отверстия в анизотропной пластине // Вестник МГСУ. 2011. № 6. С. 307–311.
21. Макаров Е.В., Монахов И.А., Нефедова И.В. Двуосное растяжение пластины с круговым отверстием // Вестник РУДН. Серия: Инженерные исследования. 2015. № 3. С. 17–22.
22. Полуэктов В.А., Миренков В.Е., Шутов В.А. Напряженное состояние пластин с отверстием // Известия ВУЗов. Строительство. 2014. № 11. С. 5–9.
23. Бок Х.К.А. Конструирование и исследование напряженно-деформируемого состояния пластин и оболочек с отверстиями вариационно-разностным методом. Дисс... на соиск. учен. степ. к.т.н.: Спец. 05.23.17.Москва, 2005. 231 с.
24. Ульянов А.Н., Медведев В.Н. Принципы конструирования зон технологичеких проходок // Труды ИБРАЭ РАН. 2008. № 6. С. 8–10.
25. Ульянов А.Н., Медведев В.Н., Киселев А.С. Влияние отгибов арматурных элементов на напряженное состояние защитных оболочек АЭС в зоне технологических проходок // Труды ИБРАЭ РАН. 2008. № 6. С. 11–14.
26. Kulka F. Prestressing systems for secondary and primary containment structures // Nuclear Engineering and Design. 1968. Vol. 8. № 4. Pp. 435–439.
27. Walser A. Capability of a prestressed concrete containment for internal pressure load // Nuclear Engineering and Design. 1984. Vol. 82. № 1. Pp. 25–35.
28. Ashar H., Naus D.J. Overview of the use of prestressed concrete in U.S. nuclear power plants. Nuclear Engineering and Design. 1983. Vol. 75. № 3. Pp. 425–437
29. Prinja N.K., Ogunbadejo A., Jonathan Sadeghi, Edoardo Patelli. Structural reliability of pre-stressed concrete containments // Nuclear Engineering and Design. 2016. Vol. 82. № 1. Pp. 36–46.
30. Noh S.-H., Kwak H.-G., Jung R. Effects of No Stiffness Inside Unbonded Tendon Ducts on the Behavior of Prestressed Concrete Containment Vessels // Nuclear Engineering and Technology. Vol. 48. № 3. Pp. 805–819.
31. Takeda H., Kusabuka M., Imoto K., Takumi K., Soejima M.. Numerical algorithm for local failure mechanism of pre-stressed concrete containment vessel wall with penetration // Nuclear Engineering and Design. 1996. Vol. 166. № 3. Pp. 389–401.
32. Sun Z., Liu S., Lin S., Xie Yo. Strength monitoring of a prestressed concrete containment with grouted tendons // Nuclear Engineering and Design. 2002. Vol. 216. № 1–3.

Sokolov V.A., Strachov D.A., Sinyakov L.N., Vasiutina S.V. Stress state of protective shells in the area of holes due to prestressed reinforcement curvature. *Magazine of Civil Engineering*. 2017. No. 2. Pp. 33–41. doi: 10.18720/MCE.70.4

14. (rus)
26. Kulka F. Prestressing systems for secondary and primary containment structures. *Nuclear Engineering and Design.* 1968. Vol. 8. No. 4. Pp. 435–439.
27. Walser A. Capability of a prestressed concrete containment for internal pressure load. *Nuclear Engineering and Design*. 1984. Vol. 82. No. 1. Pp. 25–35.
28. Ashar H., Naus D.J. Overview of the use of prestressed concrete in U.S. nuclear power plants. *Nuclear Engineering and Design.* 1983. Vol. 75. No. 3. Pp. 425–437
29. Prinja N.K., Ogunbadejo A., Jonathan Sadeghi, Edoardo Patelli. Structural reliability of pre-stressed concrete containments. *Nuclear Engineering and Design.* 2016. Vol. 82. No. 1. Pp. 36–46.
30. Noh S.-H., Kwak H.-G., Jung R. Effects of No Stiffness Inside Unbonded Tendon Ducts on the Behavior of Prestressed Concrete Containment Vessels. *Nuclear Engineering and Technology.* Vol. 48. No. 3. Pp. 805–819.
31. Takeda H., Kusabuka M., Imoto K., Takumi K., Soejima M.. Numerical algorithm for local failure mechanism of pre-stressed concrete containment vessel wall with penetration. *Nuclear Engineering and Design.* 1996. Vol. 166. No. 3. Pp. 389–401.
32. Sun Z., Liu S., Lin S., Xie Yo. Strength monitoring of a prestressed concrete containment with grouted tendons. *Nuclear Engineering and Design*. 2002. Vol. 216. No. 1-3. Pp. 213–220.
33. Kwak H.-G., Kwon Ya. Nonlinear analysis of containment structure based on modified tendon model. *Annals of Nuclear Energy.* 2016. Vol. 92. Pp. 113–126.
34. Bílý P., Kohoutková A. Sensitivity analysis of numerical model of prestressed concrete containment. *Nuclear Engineering and Design.* 2015. Vol. 295. Pp. 204–214.
35. Hu Hs.-T., Lin Yu-H. Ultimate analysis of PWR prestressed concrete containment subjected to internal pressure. *International Journal of Pressure Vessels and Piping.* 2006. Vol. 83. No. 3. Pp. 161–167.
36. Hofstetter G., Mang H.A. Collapse load analysis of prestressed concrete surface structures with unbonded tendons by the finite element method. *Finite Elements in Analysis and Design.* 1989. Vol. 5. No. 2. Pp. 141–165.
37. Pandey M.D. Reliability-based assessment of integrity of bonded prestressed concrete containment structures. *Nuclear Engineering and Design.* 1997. Vol. 176. No. 3. Pp. 247–260.

Pp. 213–220.
33. Kwak H.-G., Kwon Ya. Nonlinear analysis of containment structure based on modified tendon model // Annals of Nuclear Energy. 2016. Vol. 92. Pp. 113–126.
34. Bílý P., Kohoutková A. Sensitivity analysis of numerical model of prestressed concrete containment // Nuclear Engineering and Design. 2015. Vol. 295. Pp. 204–214.
35. Hu Hs.-T., Lin Yu-H. Ultimate analysis of PWR prestressed concrete containment subjected to internal pressure // International Journal of Pressure Vessels and Piping. 2006. Vol. 83. № 3. Pp. 161–167.
36. Hofstetter G., Mang H.A. Collapse load analysis of prestressed concrete surface structures with unbonded tendons by the finite element method // Finite Elements in Analysis and Design. 1989. Vol. 5. № 2. Pp. 141–165.
37. Pandey M.D. Reliability-based assessment of integrity of bonded prestressed concrete containment structures // Nuclear Engineering and Design. 1997. Vol. 176. № 3. Pp. 247–260.

Vladimir Sokolov,
+7(812)5526087; sva0808@rambler.ru

Dmitriy Strachov,
+7(812)5526087; sdaleks2008@rambler.ru

Leonid Sinyakov,
+7(812)5526087; cbyzrjd_45@mail.ru

Sofia Vasiutina,
+7(965)0822433; sofi-le@yandex.ru

Владимир Алексеевич Соколов,
+7(812)5526087;
эл. почта: sva0808@rambler.ru

Дмитрий Александрович Страхов,
+7(812)5526087;
эл. почта: sdaleks2008@rambler.ru

Леонид Николаевич Синяков,
+7(812)5526087; эл. почта: cbyzrjd_45@mail.ru

Софья Васильевна Васютина,
+7(965)0822433; эл. почта: sofi-le@yandex.ru

Соколов В.А., Страхов Д.А., Синяков Л.Н., Васютина С.В. Напряженное состояние защитных оболочек в зоне отверстий вследствие кривизны преднапряженных элементов // Инженерно-строительный журнал. 2017. № 2(70). С. 33–41.

doi: 10.18720/MCE.70.5

Evaluation methods of asphalt pavement service life

Методы оценки срока службы асфальтобетонного покрытия

M.A. Zavyalov,
Lomonosov Moscow State University, Moscow, Russia
A.M. Kirillov,
Moscow Automobile and Road Construction State Technical University (MADI), Sochi, Russia

Д-р техн. наук, доцент М.А. Завьялов,
Московский государственный университет им. М.В. Ломоносова, г.Москва, Россия
канд. физ.-мат. наук, доцент А.М. Кириллов,
Сочинский филиал Московского автомобильно-дорожного государственного технического университета, г. Сочи, Россия

Key words: civil engineering; road construction; asphalt pavement; pavement evaluation; energy characteristics; thermodynamic framework

Ключевые слова: дорожное покрытие; асфальтобетон; межремонтный срок службы; мониторинг функционального состояния; термодинамические характеристики

Abstract. A functional relationship of the dynamics of asphalt concrete pavement condition and its thermodynamic and thermophysical functions and parameters (Helmholtz's energy, internal energy, entropy, specific heat, etc.) is described. Based on this functional relationship, novel approaches to the estimation of asphalt pavement lifetime are proposed. The dependence of pavement lifetime from the basic thermodynamic parameter – specific heat (for the determination of which expensive and complicated equipment is not required) is derived. The statistical approach to determination of pavement lifetime, based on the analysis of the temporal changes in the spatial distribution of the basic parameter (specific heat) is proposed. Overall, three alternative but complementary approaches are described to determine pavement service interval using either a molar weight, a change of free energy, or the uniformity of the basic parameter – specific heat based the index of thermophysical uniformity (a dimensionless coefficient). Numerical pavement lifetime values suitable for exploitation under the Russian service conditions (transportation and construction terms) are calculated analytically. Regardless of the approach used of the calculated pavement lifetimes are of the same order of magnitude. These initial results are quite promising and offer a new thermodynamic approach to the estimation of pavement condition and its useful lifetime. This practical new approach can be utilized to replace or complement the traditional "mechanical" and geo-radar methods.

Аннотация. В предыдущих исследованиях была показана возможность учета энергетических изменений, происходящих в системе дорожное покрытие – транспортное средство, и их вклад в формирование научно обоснованной системы назначения сроков ремонтных работ. В связи с этим также перспективным является развитие результатов работ, в которых приводится анализ зависимостей термодинамических функций дорожного покрытия от времени эксплуатации. Несмотря на то, что ранее был сформулирован термодинамический подход, удобные расчетные формулы для определения межремонтного срока службы покрытия отсутствуют. На основании анализа полученных соотношений, описывающих динамику состояния асфальтобетонного дорожного покрытия с помощью его термодинамических и теплофизических функций и параметров (энергия Гельмгольца, внутренняя энергия, энтропия, теплоемкость), предложены подходы к назначению межремонтного срока службы дорожного покрытия. Выведены зависимости межремонтного срока службы покрытия от базисного параметра – удельной теплоемкости. Обоснован статистический подход определения межремонтного срока службы покрытия, основанный на анализе временных изменений в пространственном распределении базисного параметра. В результате исследования получены три альтернативные по отношению друг к другу и, в то же время, взаимодополняющие подхода к нахождению времени жизни покрытия: через молярную массу; через изменение свободной энергии; через однородность базового параметра – удельной теплоемкости путем ввода безразмерного коэффициента теплофизической однородности. Аналитически получены числовые значения межремонтного срока службы покрытия адекватные российским условиям эксплуатации (транспортным и строительным условиям). Несмотря на различные подходы, полученные значения межремонтного срока службы

покрытия имеют один порядок величины. Полученные результаты развивают сравнительно новый термодинамический подход к решению задач мониторинга покрытий и их эксплуатационных режимов и нацелены на замену или дополнение традиционных «механических» методов мониторинга состояния дорожного покрытия.

Introduction

Currently, the asphalt paved road infrastructure of the Russian Federation is undergoing an extensive expansion. There has also been a significant increase in the exploitation of the existing roads in recent years. These factors necessitate the development of a practical, inexpensive, and fast method to evaluate the functional condition of a pavement. It would be highly desirable if such a method is capable of predicting future changes in pavement characteristics and determining the optimum modes of road usage. Optimization of pavement management is expected to have a positive effect on pavement longevity which in turn should lead to an increase in its service life.

In our previous article [1] we described the numerical assessment of such characteristics as vehicle dynamic forces, work of a single wheel on pavement; analytical dependences of increments of internal energy, energy of elastic deformation, and dissipative energy. The main purpose was to establish the functional relationships between mechanical and thermal parameters in the system pavement – vehicle, and also to consider the processes of vehicle energy dissipation by pavement. We envisioned that a deeper understanding of energy dissipation between pavement and vehicle should make it possible to devise a method of defining pavement functional condition at any time. This in turn should lead to better monitoring and forecasting of asphalt pavement functional condition and its remaining service life.

In our previous publications [2] we described the dependences of asphalt concrete thermodynamic functions from specific heat: change of internal energy, entropy and free energy. The main focus of our paper was to apply the thermodynamic framework to the description of changes of physical, mechanical and thermophysical parameters of a material during the lifetime of an asphalt concrete layer. Dependences of specific heat versus time for different asphalt brand, type and road category were obtained. The analysis of a nature of the obtained dependences, their comparison to the experimental data and visual evaluation allowed us to conclude that the starting time of required asphalt pavement repair is directly linked to quasilinearity loss in the function graphs of asphalt specific heat versus time. Calculations showed that this specified time point is characterized by free energy deficiency, i.e., its negative increment. Based on experimental data similar dependences were derived for various types and brands of asphalt concrete [2]. We can conclude that during the normal exploitation of asphalt pavement, internal energy and entropy of its constituent materials increase. In particular, the amount of internal energy constantly increases because of accumulation of dissipative energy from the contact with vehicle wheels. At the same time, the amount of free energy decreases (it plays a compensation role in various deformation processes).

The available scientific publications that study the relationship of physical, mechanical and thermophysical parameters in the system "pavement – vehicle" can be divided into three large groups. The first and, most representative group contains research of tire-pavement interaction with the goal of providing the optimum vehicle speed [3, 4], safety [5], motion comfort [6], and fuel economy [7]. The second group encompasses research on the thermophysical properties of asphalt concrete. Optimization of these properties has shown to help reduce thermal absorption and high temperatures of pavement surface [8, 9] to prevent rutting [10], and cracks [11]. The third group includes approaches using surface radiation properties: albedo and emissivity, surface temperature gradient [12, 13], taking into consideration hydrogeological and climatic conditions of the region [14], and urban heat island effect [15]. The main goal of these approaches is to develop a network of smart roads with possibility of energy cumulation [16, 17]. There are also a number of papers [18–24] where the results of laboratory studies demonstrated conclusively the influence of thermophysical properties on mechanical characteristics. However, to date the authors are not aware of any publications related to development of an approach of asphalt pavement condition monitoring using the thermodynamic framework.

In previous research analytical dependences of thermodynamic functions versus specific heat of asphalt concrete have been obtained [2]:

$$\delta F = -\mu T\left[C\ln T + C_0\left(\frac{T_0}{T} - 1 - \ln T_0\right)\right]; \quad (1)$$

$$\delta U = \mu(CT - C_0T_0); \quad (2)$$

Завьялов М.А., Кириллов А.М. Методы оценки срока службы асфальтобетонного покрытия // Инженерно-строительный журнал. 2017. № 2(70). С. 42–56.

$$\delta S = \mu[C(1+\ln T) - C_0(1+\ln T_0)], \quad (3)$$

where F – free energy (Helmholtz's energy); U – internal energy; S – entropy; T_0, T – initial and current values of temperature; C – specific heat; C_0 – initial value of C, at $T=T_0$; μ – value in number equal to density of material, dimension of mass.

Proceeding from experimental data, dependences of change of free energy, internal energy and entropy versus time for the different types of pavements and road types have been constructed (Fig. 1) [2].

As it is possible to see from expressions (1)–(3), changes (variations) of thermodynamic functions are more sensitive to changes of temperature (seasonal and daily fluctuations). However, these changes are reversible. On the contrary, variations of thermodynamic functions caused by changes of specific heat are irreversible. The use of "average" dependences (Fig. 1) allows us to observe the evolution of changes of thermodynamic functions depending only on specific heat.

The main result obtained by physical and mathematical models is the ability to predict the pavement lifetime. A thermodynamic simulation model of changes the material of asphalt pavement during its life cycle has been constructed. The simulation model allows us to determine pavement degradation at any time. Since the heat capacity varies over time under the certain law, then this option can be selected as the base, thereby linking the variation of the thermodynamic functions with pavement lifetime.

The coefficient of free energy deficiency was input to determine the numerical values of pavement lifetimes as the relation of the module of an increment of free energy at present time to the maximum positive value of this increment for the entire period of pavement life. Determination of pavement lifetimes is obtained by an analysis of graphs, constructed using the Eq. (1).

Despite the fact that the basis of the thermodynamic approach is formulated in previous studies, a convenient formula for calculating pavement lifetime is absent.

In order to develop an approach associated with the variation of the free energy and its deficit, consider the processes of energy exchange in the system of pavement – vehicle.

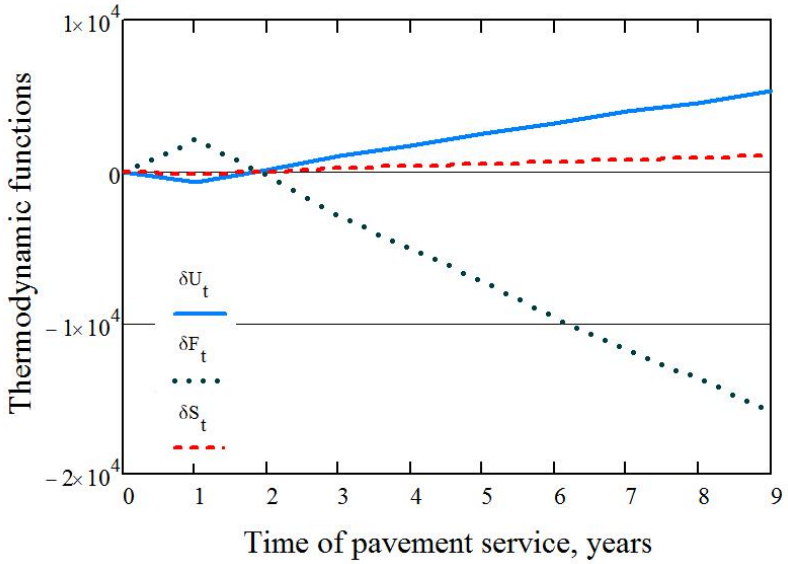

Figure 1. Dependences of change of internal energy δU, free energy δF and entropy δS versus time (fine-grained asphalt concrete of type A)

Free energy decrease is equal to the maximum full work A_{max} made by system over external solids in quasistatic thermodynamic process:

$$A_{\max} = -\Delta F. \quad (4)$$

In other words F – that part of internal energy U of system which is capable of turning into mechanical work:

$$F = U - TS \quad (5)$$

where T – the absolute (thermodynamic) temperature, S – entropy. We can define the rest of internal energy TS as the connected energy. The degradation of system (increase in its entropy ΔS) connected with internal and external processes can be slowed down by free energy reserve. The reserve of free energy is available for system at an initial stage of its usage (after the end of construction), further we can expect the replenishment of free energy level because of external forces (during service, maintenance and rehabilitation).

Since work of external forces A_{ex} over system is equal to work of system A made over external solids ($A_{ex} = -A$), from Eqs. (4) and (5) it follows that

$$\Delta S = (\Delta U - A_{\text{ex}})/T. \tag{6}$$

Thus, from Eq. (6) it is possible to assume that degradation of system is connected with increase in its internal energy and can be slowed down due to work of external forces. Eq. (6) also shows influence of temperature on degradation processes.

Opening Eq. (6), it is possible to deduce the expression for entropy increment as follows:

$$\Delta S = 3\nu R \ln\frac{T_2}{T_1} - \int_{T_1}^{T_2}\frac{\mathrm{d}A_{\text{ex}}}{T}, \tag{7}$$

where ν – amount of substance, R – gas constant, and T_1 and T_2 can be interpreted as boundary values of temperature at the time of pavement service (seasonal or daily fluctuations).

Eq. (7) allows us to draw a valid conclusion: the less the fluctuation of temperature, the less the value of the first summand in Eq. (7) and, therefore, the less entropy increment (degradation) of asphalt pavement. Eq. (7) is derived in approach of ν = const. However physical and chemical processes that go in pavement in conjunction with “destructive”, “negative” influence of vehicle lead to increase in amount of substance. And it, in turn, leads to increase in pavement entropy.

Vehicle positive influence on asphalt pavement condition is reflected in the second summand of Eq. (7). This summand plays a role in the recovery processes. Thus, the transport traffic has both positive and negative effects. Domination of negative effects, obviously, will lead to pavement degradation, and, on the contrary, domination of positive effects – to increase in pavement service life. It is possible to conclude that optimum transport traffic should exist (where pavement service life has the maximum value). Existence of such extreme dependence was shown in the seventies of the last century [25].

If to present Eq. (7) as a function of time, we get

$$\Delta S(t) = 3 \cdot \nu(t) \cdot R \cdot \ln\frac{T_2}{T_1} - \int_0^t \frac{\mathrm{d}A_{\text{ex}}}{T}, \tag{8}$$

where t – time passed from the initial moment of road startup.

There are two approaches will be applied to determine pavement lifetimes:

1) The analysis of changes in molar mass associated with the change in entropy and free energy;

2) A comparison of the free energy change to the amount of the internal energy.

A principal goal of this study is to develop a system of monitoring of asphalt pavement condition using the thermodynamic framework. The mechanism of the effect of specific heat on the pavement lifetime will be investigated by applying the thermodynamic approach and using the dependences of thermodynamic parameters from specific heat of asphalt concrete, in this paper. Thus, the specific objectives of this study are as follows:

- To derive the functional relationship of pavement lifetime on the basic parameter – specific heat;
- To determine the numerical values of pavement lifetimes suitable for exploitation under the Russian conditions (transportation and construction terms);
- To develop an approach that takes into account the variation of the free energy and its deficit;
- To substantiate the application of the statistical approach to pavement lifetime description of the dynamics properties of the pavement.

Methods

1) Molar mass application

We assume that asphalt concrete consists of two main substances: mineral aggregate and bitumen; with own molar masses M_1 and M_2 subsequently. Hence the molar mass of the asphalt concrete has the form

$$M = \frac{(1+k)M_1M_2}{kM_1+M_2}, \tag{9}$$

where $k=m_2/m_1$ – the relation of corresponding components of masses.

We also assume that the rate of decay of molecular links in the bitumen is proportional to their number; the molar mass of bitumen decreases under the exponential law:

$$M_2 = M_{20}e^{-\frac{t}{t^*}}, \tag{10}$$

where M_{20} – the initial molar mass of "young" bitumen; t^* – time constant (period of time when molar weight decreases by a factor of e times).

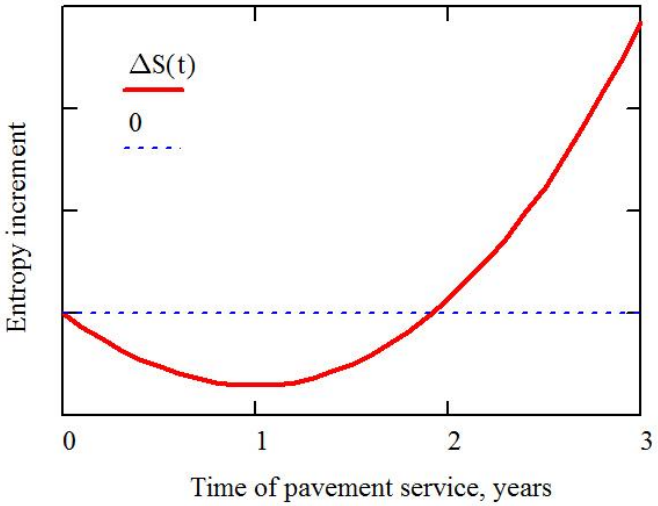

Figure 2. Qualitative entropy increment of asphalt pavement

Taking into account the reduction of molar mass of an asphalt concrete and constancy of daily work of external forces on pavement we get the following form for entropy increment:

$$\Delta S(t) = 3 \cdot \frac{m_1}{M_1} \cdot R \cdot \ln\frac{T_2}{T_1} \cdot \left(\frac{M_{20}e^{-\frac{t}{t^*}}+kM_1}{M_{20}e^{-\frac{t}{t^*}}} - \frac{M_{20}+kM_1}{M_{20}} \right) - \frac{b}{T} \cdot a \cdot t, \tag{11}$$

where a – the speed of work made by external forces; b – dimensionless coefficient considering material characteristics of asphalt concrete and technological aspects of pavement construction. Figure 2 shows the qualitative type of Eq. (11).

Material parameters of asphalt concrete, technological and climatic factors are integrally considered in time constant t^* and coefficient b.

We rewrite Eq. (9) as

$$M = \frac{(1+k)M_1M_{20}e^{-\frac{t}{t^*}}}{kM_1+M_{20}e^{-\frac{t}{t^*}}}, \tag{12}$$

The molar mass M is connected with specific heat of the asphalt concrete: $C = 3R/M$, thus Eq. (11) takes the form,

$$C(t) = 3R\frac{kM_1+M_{20}e^{-\frac{t}{t^*}}}{(1+k)M_1M_{20}e^{-\frac{t}{t^*}}}. \tag{13}$$

Zavyalov M.A., Kirillov A.M. Evaluation methods of asphalt pavement service life. *Magazine of Civil Engineering*. 2017. No. 2. Pp. 42–56. doi: 10.18720/MCE.70.5

It is enough to make one measurement of specific heat of the asphalt concrete in some time point for calculation of time constant t^* and, according to Eq. (13), to calculate value of this constant.

Using Eq. (13), we obtain

$$t^* = t \cdot \ln\left(\frac{C(t)\cdot(1+k)M_1M_{20}+3RM_{20}}{3RkM_1}\right). \quad (14)$$

For example, for M_1 = 100 g/mol, M_{20} = 500 g/mol, k = 0.1 and value of specific heat for fine-grained asphalt concrete of *A* type (traffic – 15–20 thousand vehicles per day) C = 1065 J/(kg·K), one year later after the initial road startup the value of time constant calculated by Eq. (14) is equal to 5.2 years.

It is possible to determine α with help of the equations derived in [26]. We can also calculate the coefficient b, using Eq. (8). If to take a small period of time during which the change of entropy can be neglected, Eq. (8) allows us to obtain system of two equations with two unknowns (ΔS and b). The solution of that system defines constant b as

$$b = 3 \cdot \frac{T}{a(t_2-t_1)} \cdot \frac{m_1}{M_1} R \cdot \ln\left(\frac{T_2}{T_1}\right) \cdot \left(\frac{M_{20}e^{-\frac{t_2}{t^*}}+kM_1}{M_{20}e^{-\frac{t_2}{t^*}}} - \frac{M_{20}e^{-\frac{t_1}{t^*}}+kM_1}{M_{20}e^{-\frac{t_1}{t^*}}}\right). \quad (15)$$

We are able to calculate constant b for the current values: t^* = 5.2 years, T_1 = 280 K, T_2 = 300 K, T = 290 K, m_1 = 20 kg. Using method from paper [25], we get $\alpha = 8.6\cdot10^7$ J/year. Calculation at the specified above values and $(t_2 - t_1) \to 0$ showed that $b \to 5.4\cdot10^{-6}$. Figure 2 models the entropy increment for asphalt concrete for above parameters. For example, Figure 3 shows the relationship of specific heat versus time (for stated above asphalt concrete and road category), this graph is constructed using the dependence: $C(t) = 7.82 \cdot (t - 0.9)^2 + 1065$. This dependence was proposed as a result of data approximation in paper [26].

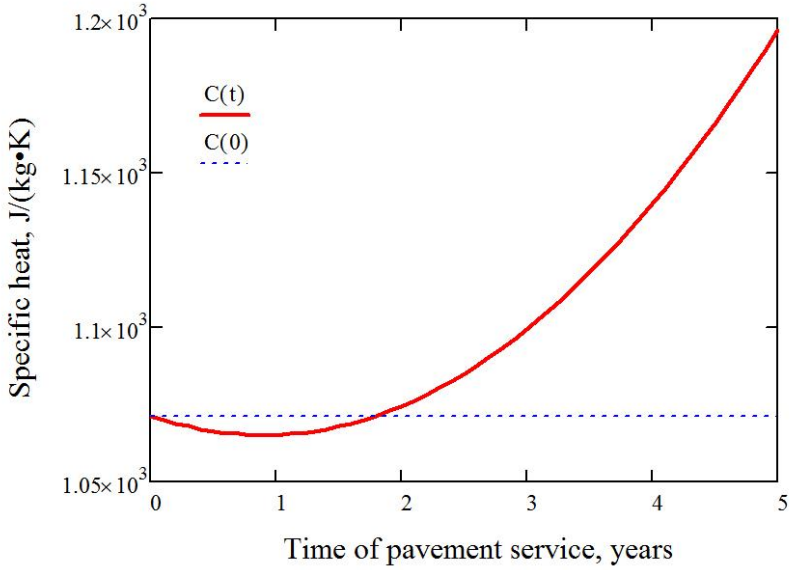

Figure 3. Dependence of the asphalt concrete specific heat versus time

Comparing Figure 2 to Figure 3, it is possible to conclude that the behavior of entropy and specific heat increments coincide qualitatively in time, it can be shown on Figure 4 by dependences of time derivatives of the above values.

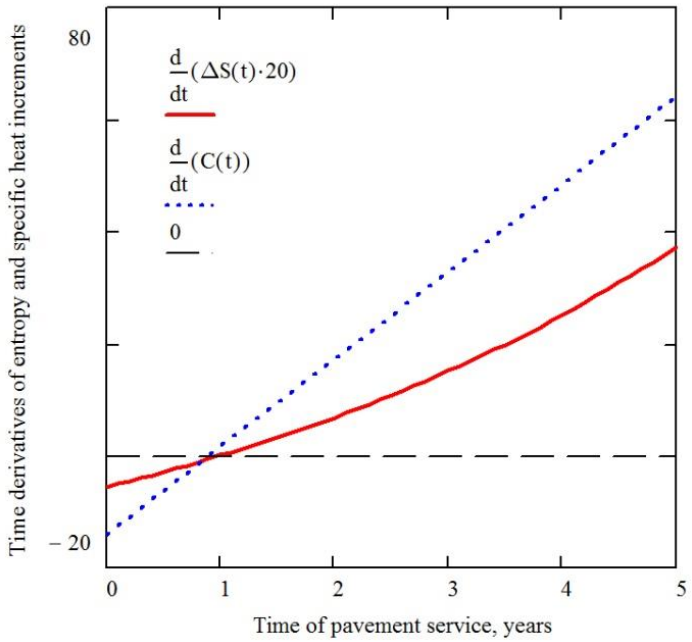

Figure 4. Time derivatives of entropy and specific heat increments

Figure 4 also shows that entropy and specific heat increments reach the minimum value approximately at the same time. Such "good" correlation between increment of entropy and specific heat serves as argument that specific heat, this thermophysical parameter, is possible to choose as basic parameter in the thermodynamic method of monitoring and predicting of a service life of asphalt pavements.

2) Free energy criteria

Using Eq. (5) and equation for internal energy of a solid state, and also considering correlation between entropy and specific heat of pavement material, it is possible to deduce the increment of free energy as follows:

$$\Delta F(t) = 3\nu RT\left(1 - \frac{C(t)}{C(0)}\right), \tag{16}$$

where $C(0)$ – value of specific heat in the initial time point.

Figure 5 models free energy increment versus time, it is constructed with use of experimental dependence of specific heat of the asphalt concrete.

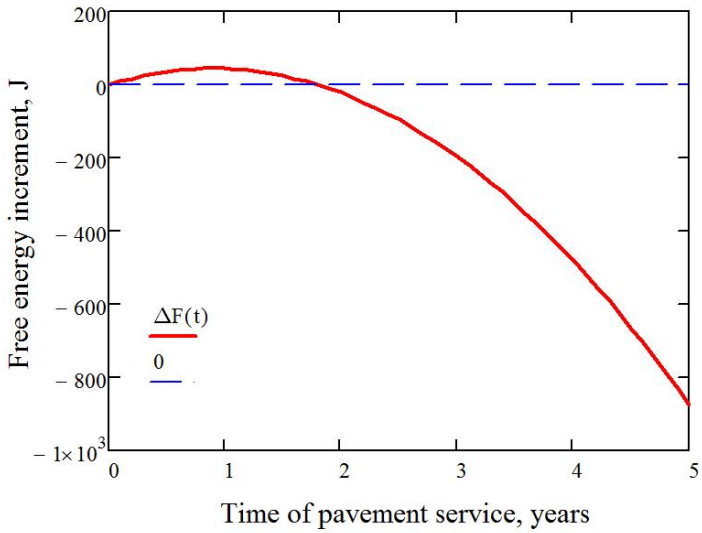

Figure 5. Free energy increment of asphalt pavement (for 1 mole of a substance and temperature 300 K)

Zavyalov M.A., Kirillov A.M. Evaluation methods of asphalt pavement service life. *Magazine of Civil Engineering*. 2017. No. 2. Pp. 42–56. doi: 10.18720/MCE.70.5

The analysis of Eq. (16) shows that at $C(t) = 2 \cdot C(0)$ decrease of free energy becomes equal to value of internal energy $U = 3\nu RT$. This time point can be considered critical for asphalt pavement. Figure 3 shows result of specific heat versus time that is constructed using the approximating dependence: $C(t) = 7.82 \cdot (t - 0.9)^2 + 1065$ $\left(\frac{\text{J}}{\text{kg·K}}\right)$. The critical time calculated for this case $t_{\text{cr}} = \sqrt{\frac{1065}{7.82}} + 0.9 = 12.6$ years. If we define this time period as pavement lifetime before reconstruction, then it is possible to offer time interval t_{r} equal to some part of critical time, i.e., t_{r}=0.5·t_{cr}, as pavement lifetime before rehabilitation, t_{r}=6.3 years.

We can suggest another option to estimate t_{r}, it can be accepted as boundary value of free energy decrease, for example, 70 percent of the level of internal energy. Then from Eq. (16) it follows that $t_{\text{r}} = \sqrt{\frac{0.7 \cdot 1065}{7.82}} + 0.9 = 10.7$ years.

Previous researches [26] show that specific heat for various asphalt pavements is approximated by dependences in the following form:

$$C(t) = k(t - t_0)^2 + C_0, \tag{17}$$

where k – the proportionality coefficient that defines speed of specific heat change, t_0 – time point of the beginning of specific heat increase, C_0 – value of specific heat in time point $t = t_0$ (the minimum value of specific heat).

Thus, the particular case considered above can be generalized as:

$$t_{\text{cr}} = \sqrt{\frac{C_0}{k}} + t_0 \tag{18}$$

and, respectively,

$$t_{\text{r}} = 0.5\left(\sqrt{\frac{C_0}{k}} + t_0\right) \tag{19.1}$$

or

$$t_{\text{r}} = \sqrt{\frac{0.7 \cdot C_0}{k}} + t_0. \tag{19.2}$$

Though Figure 5 was obtained by different method from paper [23] it shows coincidence with previous graphs. Figure 6 models coefficient of free energy deficiency as the relation of the module of an increment of free energy at present time to the maximum positive value of this increment for the entire period of pavement life.

$$K_{\text{def}} = \frac{|\delta F|}{\delta F_{\max}}. \tag{20}$$

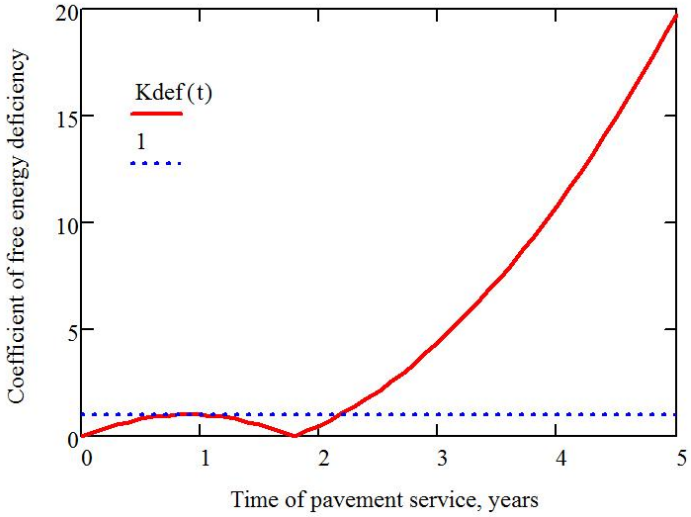

Figure 6. Coefficient of free energy deficiency

Schedule of dependence on the Figure 6 qualitatively and quantitatively identical to the same schedule in the paper [2], which is another argument in favor of the adequacy of the model.

The accepted value of coefficient of free energy deficiency can be considered as the standard criterion, determining the time of repair. In other words, a time point in which the current value of coefficient of free energy deficiency becomes more than its standard value. The question how to define the standard value of coefficient of free energy deficiency appears. Standard value of coefficient of free energy deficiency may be corresponded to the end of quasilinearity of specific heat dependences, from the point where dependences become nonlinear. Using this statement in paper [23] the standard value of coefficient of free energy deficiency was obtained within numerical values from 3 to 6, depending on pavement service conditions and type of asphalt concrete; for example, the coefficient of free energy deficiency for asphalt concrete of *A* type and the first category of road accepts value close to the left border, for porous asphalt concrete and the second category of road – to the right border. It is also necessary to note that after each repair we need to define the standard value of coefficient of free energy deficiency, because it tends to be reduced (in comparison with the previous one). Thus if we evaluate the standard value of coefficient of free energy deficiency, using Figure 6 we can define the service life of asphalt pavement.

3) Thermophysical uniformity as a condition criterion

Spatial uniformity of property of construction material can serve as an additional condition criterion. Using specific heat as the basic parameter in the thermodynamic approach, it is possible to input such criteria parameter as the index of thermophysical uniformity (*ITU*), that takes the form,

$$ITU = \frac{\Delta C_{\text{in}}}{\Delta C_{\text{pr}}}, \tag{21}$$

where ΔC_{in}, ΔC_{pr} – initial and present distribution of a specific heat, respectively.

We assume that the distribution of specific heat of asphalt concrete has normal character. This dependence reflects the specific heat deviation character of asphalt concrete of rather standard value that corresponds to the center of a curve. Figure 7 shows the distribution of specific heat during pavement lifetime. We can see that at initial stage of pavement service (curve 1) deviations from standard value are small, but then variation becomes more significant (curve 2). Values of ΔC_{in} and ΔC_{pr} also determine distribution width at the identical level concerning a maximum (in Fig. 7 it is level 0.7). From properties of normal distribution it follows that *ITU* has identical value on any level (i.e. it is not obligatory to consider a certain level), and also $\frac{\Delta C_{\text{in}}}{\Delta C_{\text{pr}}} = \frac{f_{\text{pr}}^{max}}{f_{\text{in}}^{max}}$.

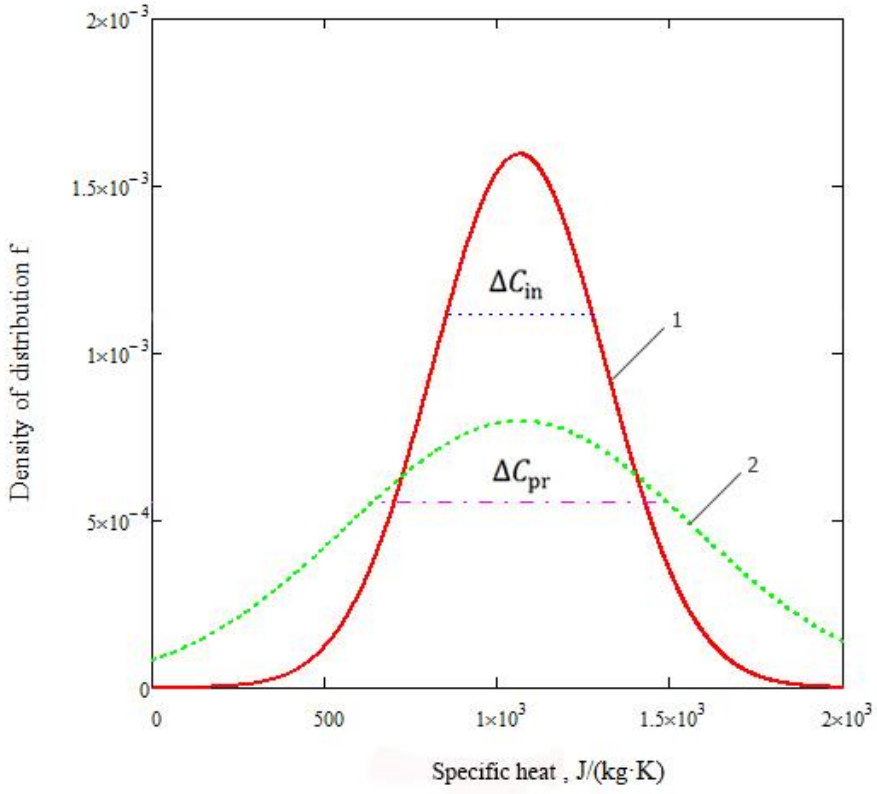

Figure 7. Normal distribution of specific heat C (density of distribution f):
1 – in initial stage of service;
2 – at present time of service of asphalt pavement

Properties of normal distribution allow us to derive more convenient equation for practical application:

$$ITU = \sqrt{\frac{\sum_{i=1}^{n}(\langle C_{\text{in}}\rangle - (C_{\text{in}})_i)^2}{\sum_{i=1}^{n}\left(\langle C_{\text{pr}}\rangle - (C_{\text{pr}})_i\right)^2}}. \quad (22)$$

The value of *ITU* is positive and does not surpass unit. In initial time point (t = 0) $\Delta C_{\text{in}} = \Delta C_{\text{pr}}$ and, therefore *ITU* = 1.

Practice shows that the higher the quality of asphalt pavement construction is, the higher and thermophysical uniformity is, that is *ITU* → 1. In process of aging and degradation the *ITU* index decreases. The analysis of experimental data allows us to conclude that change of *ITU* during pavement service can be described adequately as follows:

$$ITU = e^{-at^2}, \quad (23)$$

where a – the parameter depending on type and brand of asphalt concrete and service conditions, 0< a <1; t – time, years. The analysis of Eq. (23) shows that *ITU* sharply decreases before inflection point of function graph. Figure 8 shows that after the inflection point the speed of *ITU* reduction decreases. It is advisable to take this time point for time of the beginning of repair. This time point, from condition of equality of the second derivative of *ITU* to zero, is defined as

$$t_{\text{r}} = \sqrt{\frac{1}{2a}}. \quad (24)$$

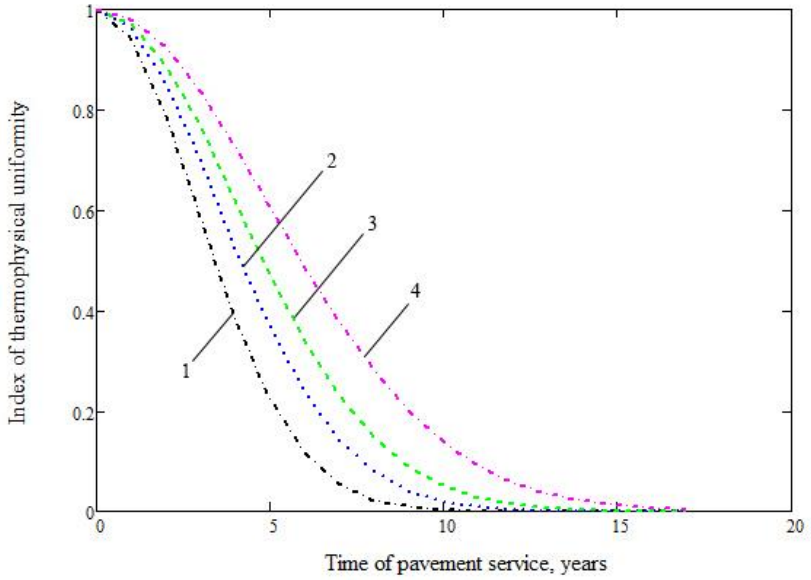

Figure 8. The character of the thermophysical uniformity index change in time: 1,2,3,4 lines are built for *a* = 0.06; 0.04; 0.03; 0.02 respectively

It is necessary to know a value of a, it can be defined at each pavement service interval, to define t_r, using equality of the right parts of Eqs. (21) and (23). Besides, ln(*ITU*) = $-at^2$ and using Figure 9, it is possible to calculate a as the relation of value increments of ln(*ITU*) and t^2.

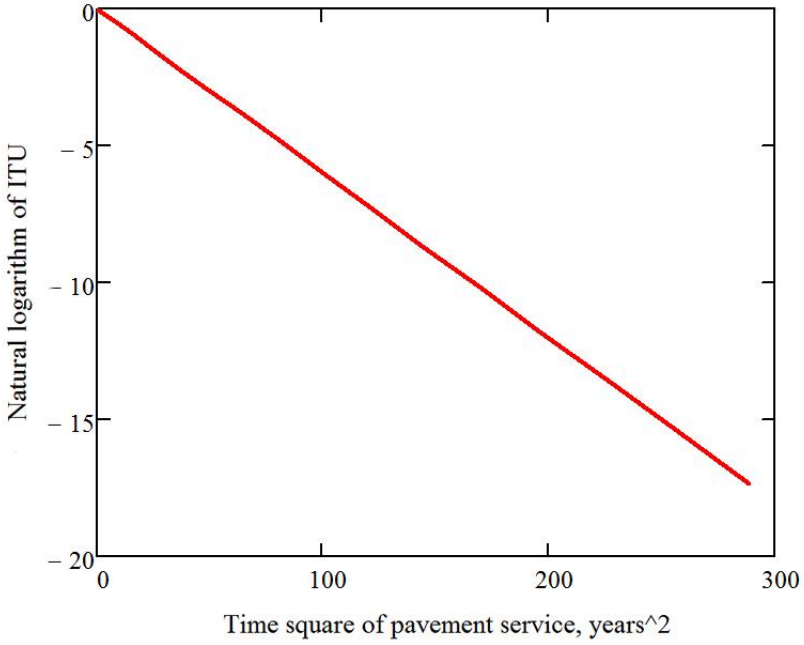

Figure 9. Linearized dependence of ITU on time square

Figure 9 also allows us to show visually the theses sounded above 1) the higher the quality of construction is, the closer the *ITU* to unit is, *ITU* → 1 (dependence in this case will be “sharper”); 2) *ITU* during service of asphalt pavement eventually aspires to zero, *ITU* → 0.

One more option of definition of repair time can be set by boundary value of *ITU*, for example, if *ITU*=0.5, then from Eq. (23) we get

$$t_r = \sqrt{\frac{\ln 2}{a}}. \qquad (25)$$

Or it is possible to find the time at which *ITU* is reduced to *e* times its initial value as follows:

$$t_r = \sqrt{\frac{1}{a}}. \quad (26)$$

At α = 0.04 year^{-2} using Eq. (24) we get $t_r = 3{,}5$ years; using Eq. (25) – $t_r = 4{,}2$ years; and finally using Eq. (26) – $t_r = 5$ years.

Results and Discussions

We used the experimental data of the previous study to calculate the values of pavement lifetime ([t] = 1 year). The results of calculation of pavement lifetime values and dependences of the specific heat are given in Table 1.

Table 1. Calculation of pavement lifetimes (years)

	1	**2**	**3**	**4**
Type of asphalt concrete / road category	Coarse porous asphalt, II grade / I-B	Fine dense asphalt, A type, I grade / I-B	Fine dense asphalt, B type, I grade / I-A	Fine dense asphalt, B type, I grade / II
Specific heat, J/(kg·K)	$C_1 = = 7.82(t-0.9)^2 + +1065$	$C_2 = = 7.91(t-1.35)^2 + +1033$	$C_3 = = 9.8(t-1.25)^2 + +965$	$C_4 = = 7.02(t-1.2)^2 + +1000$
Molar mass application, Eq. (14)				
*t**	4.7	7.0	6.4	6.2
Free energy criteria, Eq. (16) – (19)				
t_{cr} (Eq.18)	12.6	12.8	11.2	13.1
t_r (Eq.19.1)	6.3	6.4	5.6	6.5
t_r (Eq.19.2)	10.7	10.9	9.6	11.2

Despite the different approaches, pavement lifetime values calculated by Eqs. (14) and (19.1) are equivalent to results calculated previously by Eqs. (1)–(3).

Analyzing graphical representation of deterioration curves predicted by the different pavement deterioration models [27], we can conclude that if a boundary PCI (pavement condition index) value is chosen between “fair” and “poor” (= 55) as per ASTM D 6433-07, we obtain the age of the pavement equal to 6.5 - 7 years. These values are identical to the pavement lifetime values calculated by Eqs. (14) and (19.1).

According to the typical Maintenance and Rehabilitation (M&R) strategy the asphalt pavement with PCI value from 55 and below is in need of rehabilitation. Comparison of the calculated pavement lifetimes to the level of serviceability and determination of the required treatment values is a promising direction of future research.

Considering the correlation between the PCI value and the remaining service life of asphalt pavements [28], we calculate approximately 4.5 years of remaining useful lifetime for pavement with the PCI of about 90. Thus, for new pavements with age of 1–1.5 years, we also obtain rather close values of total age to the values calculated by Eqs. (14) and (19.1).

The analysis of change of PSI values (present serviceability index) as a function of time also allows us to define approximately 6–7 year cycles for application of the M&R operation [29].

Currently, experiments on the *ITU* are not available, so we cannot calculate the pavement lifetime using this method. However, we can solve the inverse problem – to determine the order of magnitude of the parameter a, Eq. (23).

Table 2 shows the results of calculations using the pavement lifetime, obtained by the Eqs. (14) and (18).

The values of parameter a calculated by Eqs. (14) and (18) differ by an order of magnitude. Since the Russian service conditions correspond to the pavement lifetimes calculated by Eq. (14), the most appropriate order of values a is the order of the values listed at the top of the Table 2. Figure 8 also models dependencies, using the value of a of the same order.

Table 2. Parameter α

The calculation formula of the parameter α	for C_1	for C_2	for C_3	for C_4
Parameter α calculated according to t^* Eq. (14)				
(24) $a = \frac{1}{2t_r^2}$	0.023	0.010	0.012	0.013
(25) $a = \frac{ln2}{t_r^2}$	0.031	0.014	0.017	0.018
(26) $a = \frac{1}{t_r^2}$	0.045	0.020	0.024	0.026
Parameter α calculated according to t_{cr} Eq. (18)				
(24) $a = \frac{1}{2t_r^2}$	0.0031	0.0031	0.0040	0.0029
(25) $a = \frac{ln2}{t_r^2}$	0.0044	0.0042	0.0055	0.0040
(26) $a = \frac{1}{t_r^2}$	0.0063	0.0061	0.0080	0.0058

Conclusion

Three alternative but complementary approaches are described to determine pavement service interval using either a molar weight, a change of free energy, or the uniformity of the basic parameter – specific heat based the index of thermophysical uniformity (a dimensionless coefficient).

The following conclusions can be drawn from this research:

- Pavement lifetime dependence is derived from the basic parameter – specific heat;
- Pavement lifetime values suitable for exploitation under the Russian service conditions (transportation and construction terms) are calculated analytically. Regardless of the approach used of the calculated pavement lifetimes are of the same order of magnitude.
- An approach of a variation of the free energy and its deficit has got a further development;
- The statistical approach (*ITU*) to determination of pavement lifetime, based on the analysis of the temporal changes in the spatial distribution of the basic parameter (specific heat) is proposed.

References

1. Kirillov A.M., Zavyalov M.A. Modelirovaniye protsessov energoobmena v sisteme dorozhnoe pokrytiye – transportnoe sredstvo [Modeling of energy dissipation processes in a pavement – vehicle system]. *Magazine of Civil Engineering.* 2015. No. 5(57). Pp. 34–44. (rus)
2. Zavyalov M.A. *Termodinamicheskaya teoriya zhiznennogo cickla dorojnogo asphaltobetonnogo pokritiya* [Thermodynamic theory of asphalt pavement life-circle]. Russia: Omsk, 2007. 283 p. (rus)
3. Chupin O., Piau J.M., Chabot A. Effect of bituminous pavement structures on the rolling resistance. *Proc. of 11th Int. Conf. on Asphalt Pavements.* 2010. Pp. 73–82.
4. Louhghalam A., Akbarian M., Ulm F.J. Flugge's conjecture: dissipation-versus deflection-induced pavement–vehicle interactions. *Journal of Engineering Mechanics.* 2013. Vol. 140. No. 8. Pp. 171–179.
5. Anupam K. et al. Influence of Temperature on tire-pavement friction. *Transportation Research Record: Journal of the Transportation Research Board.* 2013. Vol. 2369. No. 1. Pp. 114–124.
6. Lu T., Thom N.H., Parry T. Numerical simulation of the influence of pavement stiffness on energy dissipation. *Computing in Civil and Building Engineering, Proceedings of the International Conference.* 2010. Vol. 30. 483 p.
7. Pouget S. et al. Viscous energy dissipation in asphalt pavement structures and implication for vehicle fuel consumption. *Journal of Materials in Civil Engineering*.

Литература

1. Кириллов А.М., Завьялов М.А. Моделирование процессов энергообмена в системе дорожное покрытие – транспортное средство // Инженерно-строительный журнал. 2015. № 5(57). С. 34–44.
2. Завьялов М.А. Термодинамическая теория жизненного цикла дорожного асфальтобетонного покрытия. Омск, 2007. 283 с.
3. Chupin O., Piau J. M., Chabot A. Effect of bituminous pavement structures on the rolling resistance // Proc. of 11th Int. Conf. on Asphalt Pavements. 2010. Pp. 73–82.
4. Louhghalam A., Akbarian M., Ulm F. J. Flugge's conjecture: dissipation-versus deflection-induced pavement–vehicle interactions // Journal of Engineering Mechanics. 2013. Vol. 140. No. 8. Pp. 171–179.
5. Anupam K. et al. Influence of Temperature on tire-pavement friction // Transportation Research Record: Journal of the Transportation Research Board. 2013. Vol. 2369. No. 1. Pp. 114–124.
6. Lu T., Thom N.H., Parry T. Numerical simulation of the influence of pavement stiffness on energy dissipation // Computing in Civil and Building Engineering, Proceedings of the International Conference. 2010. Vol. 30. 483 p.
7. Pouget S. et al. Viscous energy dissipation in asphalt pavement structures and implication for vehicle fuel consumption // Journal of Materials in Civil Engineering. 2011. Vol. 24. No. 5. Pp. 568–576.
8. Gui J. et al. Impact of pavement thermophysical properties

Zavyalov M.A., Kirillov A.M. Evaluation methods of asphalt pavement service life. *Magazine of Civil Engineering*. 2017. No. 2. Pp. 42–56. doi: 10.18720/MCE.70.5

2011. Vol. 24. No. 5. Pp. 568–576.

8. Gui J. et al. Impact of pavement thermophysical properties on surface temperatures. *Journal of Materials in Civil Engineering.* 2007. Vol. 19. No. 8. Pp. 683–690.
9. Feng D. et al. Impact of asphalt pavement thermophysical property on temperature field and sensitivity analysis. *Journal of Highway and Transportation Research and Development*. 2011. Vol. 11. Pp. 12–19.
10. Hansson J., Lenngren C.A. Using deflection energy dissipation for predicting rutting. *10th International Conference on Asphalt Pavements.* Quebec City, Canada. 2006. Pp. 112–123.
11. Zhang Q., Lu Y., Jia X. The Deformation characteristics of asphalt mixture based on dissipation energy. *International Conference on Transportation Engineering 2009.* ASCE, 2009. Pp. 1250–1255.
12. Graczyk M. et al. Analytical solution for the heat propagation with infinite speed in the multilayer pavement system. *ARRB Conference.* Sydney, New South Wales, Australia. 2014. No. 6.1. Pp. 1-13.
13. Marc P., Belc F., Lucaci G. Modeling road pavements taking into consideration the thermo-physical characteristics of the layers. *Energy and Clean Technologies, Proceedings of the 13th International Multidisciplinary Scientific Geoconference, SGEM.* 2013. Pp. 709–716.
14. Hall M. R. et al. Influence of the thermophysical properties of pavement materials on the evolution of temperature depth profiles in different climatic regions. Journal of Materials in Civil Engineering. 2011. Vol. 24. No. 1. Pp. 32–47.
15. Chen B.L., Bhowmick S., Mallick R.B. A laboratory study on reduction of the heat island effect of asphalt pavements. *Journal of the Association of Asphalt Paving Technologists.* 2009. Vol. 78. Pp. 209–248.
16. Mallick R. B. et al. Capturing solar energy from asphalt pavements*. International symposium on asphalt pavements and environment, international society for asphalt pavements.* Zurich, Switzerland. 2008. Pp. 161–172.
17. Loomans M. et al. Design tool for the thermal energy potential of asphalt pavements. *8th International IBPSA Conference*. Eindhoven, Netherlands. 2003. Pp. 745–752.
18. Fu P., Jones D., Harvey J.T. Micromechanics of the effects of mixing moisture on foamed asphalt mix properties. *Journal of Materials in Civil Engineering.* 2010. Vol. 22. No. 10. Pp. 985–995.
19. Pradeep H. et al. Modelling constant displacement rate experiments of asphalt concrete using a thermodynamic framework. *The International Journal of Pavement Engineering. 2005.* Vol. 6. No. 4. Pp. 241–256.
20. Ravindran P. et al. Modelling sand–asphalt mixtures within a thermodynamic framework: theory and application to torsion experiments. *International Journal of Pavement Engineering.* 2009. Vol. 10. No. 2. Pp. 115–131.
21. Moghadas Nejad F., Hamedi G.H., Azarhoosh A.R. Use of surface free energy method to evaluate effect of hydrate lime on moisture damage in hot-mix asphalt. *Journal of Materials in Civil Engineering.* 2013. Vol. 25. No. 8. Pp. 1119–1126.
22. Murali Krishnan J., Rajagopal K.R. Thermodynamic framework for the constitutive modeling of asphalt concrete: Theory and applications. *Journal of Materials in Civil Engineering.* 2004. Vol. 16. No. 2. Pp. 155-166.
23. Chowdary V., Murali Krishnan J. A Thermodynamic Framework for Modelling Healing of Asphalt Mixtures. *International Journal of Pavement Research and Technology.* 2010. Vol. 3. No. 4. Pp. 186–198.
24. Houel A., Arnaud L., Dumont A.G. Thermomechanical characterisation of asphalt pavements in laboratory conditions. *International Journal of Pavement Engineering.*

on surface temperatures // Journal of Materials in Civil Engineering. – 2007. Vol. 19. No. 8. Pp. 683–690.

9. Feng D. et al. Impact of asphalt pavement thermophysical property on temperature field and sensitivity analysis // Journal of Highway and Transportation Research and Development. 2011. Vol. 11. Pp. 12–19.
10. Hansson J., Lenngren C. A. Using deflection energy dissipation for predicting rutting // 10th International Conference on Asphalt Pavements. Quebec City, Canada. 2006. Pp. 112–123.
11. Zhang Q., Lu Y., Jia X. The Deformation characteristics of asphalt mixture based on dissipation energy // International Conference on Transportation Engineering 2009. ASCE, 2009. Pp. 1250–1255.
12. Graczyk M. et al. Analytical solution for the heat propagation with infinite speed in the multilayer pavement system // ARRB Conference. Sydney, New South Wales, Australia. 2014. No. 6.1. Pp. 1–13.
13. Marc P., Belc F., Lucaci G. Modeling road pavements taking into consideration the thermo-physical characteristics of the layers // Energy and Clean Technologies, Proceedings of the 13th International Multidisciplinary Scientific Geoconference, SGEM. 2013. Pp. 709–716.
14. Hall M. R. et al. Influence of the thermophysical properties of pavement materials on the evolution of temperature depth profiles in different climatic regions // Journal of Materials in Civil Engineering. 2011. Vol. 24. No. 1. Pp. 32–47.
15. Chen B. L., Bhowmick S., Mallick R. B. A laboratory study on reduction of the heat island effect of asphalt pavements // Journal of the Association of Asphalt Paving Technologists. 2009. Vol. 78. Pp. 209–248.
16. Mallick R. B. et al. Capturing solar energy from asphalt pavements // International symposium on asphalt pavements and environment, international society for asphalt pavements, Zurich, Switzerland. 2008. Pp. 161–172.
17. Loomans M. et al. Design tool for the thermal energy potential of asphalt pavements // 8th International IBPSA Conference, Eindhoven, Netherlands. 2003. Pp. 745–752.
18. Fu P., Jones D., Harvey J.T. Micromechanics of the effects of mixing moisture on foamed asphalt mix properties // Journal of Materials in Civil Engineering. 2010. Vol. 22. No. 10. Pp. 985–995.
19. Pradeep H. et al. Modelling constant displacement rate experiments of asphalt concrete using a thermodynamic framework // The International Journal of Pavement Engineering. 2005. Vol. 6. No. 4. Pp. 241–256.
20. Ravindran P. et al. Modelling sand–asphalt mixtures within a thermodynamic framework: theory and application to torsion experiments // International Journal of Pavement Engineering. 2009. Vol. 10. No. 2. Pp. 115–131.
21. Moghadas Nejad F., Hamedi G.H., Azarhoosh A.R. Use of surface free energy method to evaluate effect of hydrate lime on moisture damage in hot-mix asphalt // Journal of Materials in Civil Engineering. 2013. Vol. 25. No. 8. Pp. 1119–1126.
22. Murali Krishnan J., Rajagopal K.R. Thermodynamic framework for the constitutive modeling of asphalt concrete: Theory and applications // Journal of Materials in Civil Engineering. 2004. Vol. 16. No. 2. Pp. 155–166.
23. Chowdary V., Murali Krishnan J. A Thermodynamic Framework for Modelling Healing of Asphalt Mixtures // International Journal of Pavement Research and Technology. 2010. Vol. 3. No. 4. Pp. 186–198.
24. Houel A., Arnaud L., Dumont A.G. Thermomechanical characterisation of asphalt pavements in laboratory conditions // International Journal of Pavement Engineering. 2010. Vol. 11. No. 6. Pp. 441–447.

Завьялов М.А., Кириллов А.М. Методы оценки срока службы асфальтобетонного покрытия // Инженерно-строительный журнал. 2017. № 2(70). С. 42–56.

2010. Vol. 11. No. 6. Pp. 441–447.

25. Slavutsky O.A. Sroki sluzhbi bitumomineral'nikh i asphaltobetonnikh pokritiy [Service terms of bitumen-mineral and asphalt-concrete pavements]. *Automobile roads.* 1972. No. 9. Pp. 19–21. (rus)
26. Zavyalov M.A., Zavyalov A.M. Teployemkost' asfaltobetona [Specific heat of asphalt concrete]. *Construction Materials.* 2009. No. 7. Pp. 6–9. (rus)
27. Kırbaş U., Karaşahin M. Performance models for hot mix asphalt pavements in urban roads. *Construction and Building Materials.* 2016. Vol. 116. Pp. 281–288.
28. Setyawan A., Nainggolan J., Budiarto A. Predicting the remaining service life of road using pavement condition index. *Procedia Engineering*. 2015. Vol. 125. Pp. 417–423.
29. Jorge D., Ferreira A. Road network pavement maintenance optimisation using the HDM-4 pavement performance prediction models. *International Journal of Pavement Engineering.* 2012. Vol. 13. No. 1. Pp. 39–51.

25. Славуцкий О.А. Сроки службы битумоминеральных и асфальтобетонных покрытий // Автомобильные дороги. 1972. № 9. С. 19–21.
26. Завьялов М.А., Завьялов А.М. Теплоемкость асфальтобетона // Строительные материалы. 2009. № 7. С. 6–9.
27. Kırbaş U., Karaşahin M. Performance models for hot mix asphalt pavements in urban roads // Construction and Building Materials. 2016. Vol. 116. Pp. 281–288.
28. Setyawan A., Nainggolan J., Budiarto A. Predicting the remaining service life of road using pavement condition index // Procedia Engineering. 2015. Vol. 125. Pp. 417–423.
29. Jorge D., Ferreira A. Road network pavement maintenance optimisation using the HDM-4 pavement performance prediction models // International Journal of Pavement Engineering. 2012. Vol. 13. No. 1. Pp. 39–51.

Mikhail Zavyalov,
+7(964)7744042; zavyalov.m.a@gmail.com

Andrey Kirillov,
+7(918)1302257; kirill806@gmail.com

Михаил Александрович Завьялов,
+7(964)7744042;
эл. почта: zavyalov.m.a@gmail.com

Андрей Михайлович Кириллов,
+7(918)1302257; эл. почта: kirill806@gmail.com

Zavyalov M.A., Kirillov A.M. Evaluation methods of asphalt pavement service life. *Magazine of Civil Engineering*. 2017. No. 2. Pp. 42–56. doi: 10.18720/MCE.70.5

doi: 10.18720/MCE.70.6

Engineering kinematic theory in application to the calculation of pile foundations

Инженерная кинематическая теория в приложении к расчету свайных фундаментов

V.S. Korovkin,
Peter the Great St. Petersburg Polytechnic University, St. Petersburg, Russia

д-р техн. наук, преподаватель
В.С. Коровкин,
Санкт-Петербургский политехнический университет Петра Великого, г. Санкт-Петербург, Россия

Key words: pile foundation; lateral pressure; vertical jet pressure; high and low pile grillage; the stiffness coefficient of the soil; dimensionless curve relation from the horizontal and vertical pressure

Ключевые слова: свайный фундамент; боковое давление; вертикальное реактивное давление; высокий и низкий свайный ростверки; коэффициент жесткости грунта; безразмерная кривая связи от горизонтального и вертикального давлений

Abstract. The author has proposed a variant of calculation of pile foundation with the use of the engineerin kinematic theory of ground contact pressure. This calculation uses two separate graph connection, the pressure – vertical or horizontal offset. The diagrams are dimensionless, so is not related to the scale of the building. The absolute values of the end points of the graphs are determined considering the plastic deformation modulus of the soil. Diagram enables the calculation of pile foundation for the entire load cycle. Practical implementation of calculations uses variable from of the depth and the load of the coefficient stiffness soil. The author considered the combined model the stiffness of the soil based on the structural surrounding the pile. The article presents fragments of the calculation of stresses and displacements of pile foundations.

Аннотация. Автор предложил вариант расчета свайного фундамента с применением инженерной кинематической теории контактного давления грунта. Приведено решение по определению сил трения на боковую поверхность сваи дополнительно зависящее от размеров поперечного сечения внедряемой в грунт сваи. Описано решение по определению реактивного давление грунта на острие сваи или условный фундамент для всего цикла нагрузки. Рассмотрено влияние расположения плиты ростверка в свайном основании на несущую способность конструкции. Учтено взаимное влияние свай на распределение усилий в свайном ростверке. Получено решение по определению горизонтального уплотнения и осадки свайного фундамента с использованием относительных кривых связи «давление-перемещение» и «давление-осадка» для всего цикла нагрузки. Приведена комбинированная модель коэффициента жесткости грунта с учетом структурного элемента. Показан прием определения коэффициента жесткости грунта у боковой и торцевой поверхностей сваи от нагрузки. Приведен порядок расчета и его практическая реализация применительно к низкому свайному ростверку городской набережной с использованием программы SCAD.

Introduction

Pile foundation is the most effective, but least studied type of foundation. This is facilitated by a variety of factors affecting its load-bearing capacity while construction and exploitation process. The use of software systems using the theory of continuous media has enabled more fully to describe the work of pile foundation in the ground. However, this theory is for the behavior of structural materials in relation to soils is of the approximate. This is due to different structures of the environments (continuous and discrete), which are more diverse in soil than in metals with larges the intercrystalline by contacts. To adjust the solutions of the theory as applied to soils used various artificial techniques. On the other hand, the use of solutions of the theory of continuous medium at this stage of development of soil mechanics is justified, as the discrete theory soils not quite developed.

Коровкин В.С. Инженерная кинематическая теория в приложении к расчету свайных фундаментов // Инженерно-строительный журнал. 2017. № 2(70). С. 57–71.

The interaction of piles with soil were considered by scientists: V.A. Barbashov [1], A.A. Bartolomey [2], B.V. Bakholdin [3], S.N. Bezvolen [4], V.S. Glukhov [5], A.V. Savinov [6], V.N. Paramonov [7], V.V. Znamenskiy [8], Y.K. Zaretsky [9], A.B. Fadeev [10], V.G. Fedorovsky [11], D.E. Razvodovsky [12], A.L. Gotman,. [13], K. Terzaghi [14], A. Kezdi, G.P. Chebotarev, B.N. Fellenius [15], D.A. Brown [16], Neil Taylor [17], D.J. White [18], S. Nakajima and others.

Extensive experimental and theoretical studies of the pile foundation works were conducted by A.A. Bartolomey [2]. He studied the propagation process of sealing areas soil, the deformation modulus of the soil, and the nature of the behavior in time of the pore pressure, etc. A.A. Bartolomey received a calculation expression to determine the limit loads and settlement of pile foundations based on the research.

Research in recent decades include both engineering methods of calculation [8], the model using the coefficient, [11], etc. and rigorous solutions using elastic-plastic and visco-plastic model of soil [9, 10], etc.

Researchers conducted numerous experimental investigations of the operation of piles in the estimation of spatial models of continuous soil medium [14–25].

Despite the progress made in the calculation of pile foundations, individual issues cannot be considered fully resolved. For example, the recommended Russian Constructions Normsand Regulations SNiP 2.02.03.85 [26] action of the load and the sediment on pile foundation are not linked together, and their results in some cases, differ substantially from full-scale.

The article aims at linking of the load on pile foundation up to the limit with his draught. Diagram lateral pressure – ground compaction allows defining a variable friction along the length of the pile from the value of the seal. Graph vertical pressure – soil settlement allows you to define a variable jet pressure on the end of the piles from the soil settlement. This allows you to more fully determine the nature of the work piles design in all load range. Recommendations SNiP 2.02.03.85 is a special case of the proposed solution, since they give the maksismum value of the effort.

The author offers a variant of the calculations on the basis of the Engineering kinematic theory of ground contact pressure, for a simplified evaluation of stress-strain state of pile foundations [27].

The main provisions of the engineering kinematic theory of ground contact pressure

The theory assumes that the behavior of soil under load does not depend on a constructive basis of buildings. It integrates and complements the existing special cases of engineering analysis of structures interacting with the soil in the elastic and limit states. This makes for a more clear overall picture of the interaction of soil with the structure [27].

In a soil environment, interacting with any engineering construction (retaining wall, strip foundation, pile) under load is formed by a variable active area. She crosses to the region of shear of the soil at extreme loads (Fig.1). This area is divided into arbitrary strips with the trajectories of moving soil particles. The resistance to compression of the stripes is determined of the stiffness of the soil, the value of which depends on its length and the magnitude of the load.

Load is forming the active region associated with the diagram of compression of the ground in horizontal or vertical directions. The relative nature of the diagram makes it common to describe the behaviour under load of all the strips of ground.

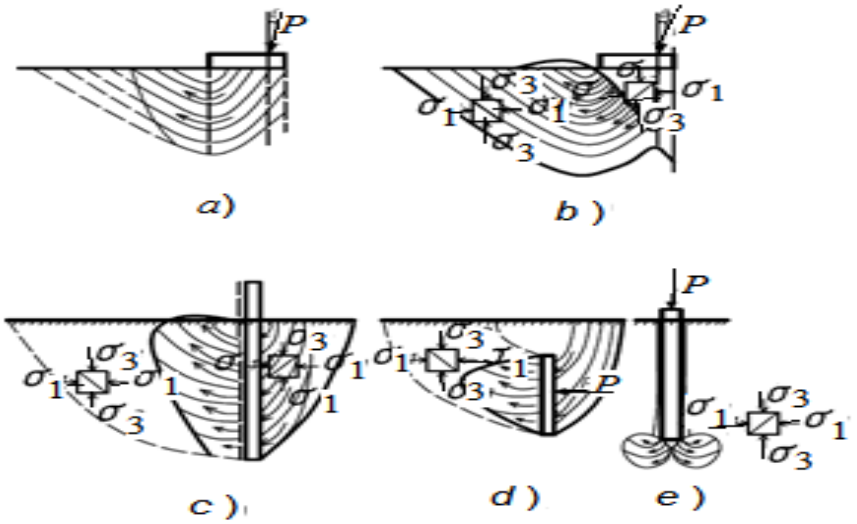

Figure 1. The influence of the degree of the impact of design on the shape of the active zone of the soil

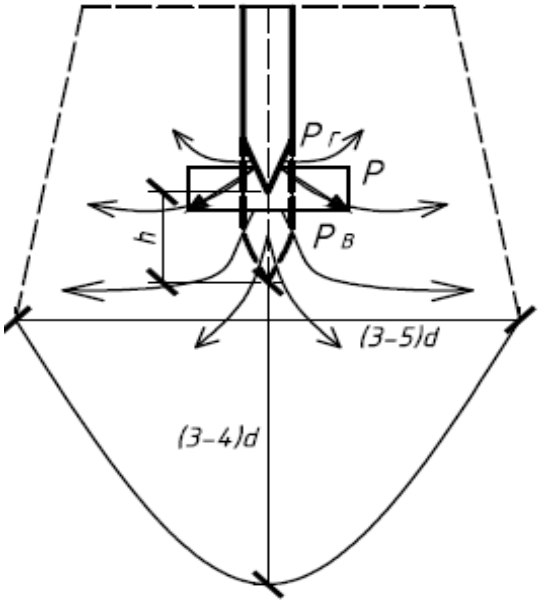

Figure 2. The active area and the trajectory displacement at the pile toe

The soil area in the foundation is active when small loads more or less of the vertical (Fig. 1a). Ground wedge below the foundation from extreme load, similarly, to inclined surface wall pushes ground in the adjacent region (Fig. 1b). Horizontal active area moves at extreme loads in the prism of the shift in the retaining walls, anchor slab (Fig. 1g). In the pile foundation composite region of the ground comprises two of the above areas, acting on the lateral part and the end portion of the piles (Fig. 1d). Earth pressure on the lateral part of the piles is determined by the displacement of soil from the lateral introduction of piles [28], and by the pressure of the soil on the edge of the piles respectively under the sediment the buried piles (Fig. 1e) [29].

The mechanism of the phenomena occurring in the soil when submerged piles

The active region of the soil deformation are formed in the side and in the edge surfaces of the pile [2]. The side seal area of soil to pile is (3÷5)diameter (d), in the strip foundation respectively – (10÷11)d. Vertical active area at the edge of a single pile is (3–4)d and under by number piles, respectively – (4–5)d, Figure 2 [2].

Коровкин В.С. Инженерная кинематическая теория в приложении к расчету свайных фундаментов // Инженерно-строительный журнал. 2017. № 2(70). С. 57–71.

In the pile, submerged in the soil, emerge in the field the tip lateral (Pl) and vertical (PV) components of the forces acting on the foundation soil (Fig. 2). The process of immersion is provided by the excess forces on the components of the reactive resistance of the soil in horizontal and vertical directions. The one concrete rectangular pile, immersed to a depth h, displaces a volume of soil:

$$V =\cdot \int_0^h F_p \cdot dh =\cdot F_p \cdot h,$$

This volume of soil contains the offset in the vertical and horizontal directions. The resistance of the soil in the vertical direction is 3–4 times higher than in the horizontal. Therefore, coefficient the ratio of the horizontal seal equal K_l=0.7–0.8, which takes into account part of the amount of compacted soil in a lateral direction. Therefore, the horizontal lateral displacement of the soil medium per unit height Δ_h = 1.0 m, K_l =0.8 will be:

$$\Delta_l \cdot= 0.25 \cdot K_l \cdot d = 0.2d,$$

where *d* is the side or the diameter of the piles.

Thus, at the piles size 35 × 35 cm each face compresses the soil to 7 cm horizontally and respectively vertically $\Delta_v = 0.05 \cdot d = 1.75$ cm, with K_V= 0.2.

Piles in case dive cause constant horizontal soil compaction. But the calculated value of the maximum horizontal compaction with the depth increases. Hence the magnitude of lateral pressure and thus the friction force on the pile will decrease under the depth. The magnitude of the vertical soil compaction under the pile is significantly less than horizontal. However, the reactive pressure on the end faces piles increases with depth, due to the increase of the higher resistance of the soil. Dive into the soil piles causes arising in the active region does to the change of physico-mechanical characteristics of the soil. These characteristics increase to an average of 30–35 %, and the adhesion and modulus of deformation, respectively several times. This happens is in non-cohesive and a little moist clay soils. [2]. However, during "rest" piles in non-cohesive soils is the dissipation (relaxation) voltage and the resistance of the soil is reduced. In very wet clayey soils the pressure perceives the pore fluid [2]. The unstable condition of the soil gradually approaches to natural stable. In water saturated silty-clay soils during this period, there is dissipation of pore pressure. This leads to an increase of pressure of the solid phase of soil and its strength around the piles to a considerable extent restored. The necessary duration of the "rest" of the pile depends on the type of soil. For sandy loams and sands it is one week. Loam – to clay – at least three weeks.

Earth pressure on the pile

The lateral surface of the pile. The Russian Set of Rules SP 24.13330.2011 contains the empirical table limit friction forces on the lateral surface of the pile (ff) [26].The value ff depends on the type of ground and depth of piles. However, friction forces at a certain depth are not permanent, according to the experiments unlike SNIP [26]. They are associated with the value of the jet lateral pressure of compacted soil to the piles. This value will be depending on the shape of the cross section of the pile. The cross-section two piles are shown in Figure 3. The cross-section have the same perimeter: a square cross-section 40x40 cm (fig. 3*a*) and rectangular cross-section 30 x 50 cm (Fig. 3*b*).

The Russian Set of Rules SP 24.13330.2011 contains equal the value of the specific lateral pressure ff on piles with cross-sections *a* and *b* (Fig. 3). In fact, equality the friction force acts only on the square piles, equally compacted the soil in two directions to the cross-sections *a*. The friction force on the sides of reinforced concrete pile will be different due to different values of the compaction parties the cross-sections *b*. This value will depend on the values of the horizontal displacement of the soil. Therefore, the friction force on the lateral the surface cross-section of the piles will be greater than on its front surface (Fig. 3*b*).

In accordance with the article [27] the value of 1rm lateral earth pressure on the pile is equal to:

$$\sigma_{x,\ y} = K_{l\,p} \cdot K_s \cdot u \left(\gamma \cdot h \cdot \lambda(\delta) + c \cdot \lambda_{pc}(\delta)\right) \le \sigma *_{x,\ y,} \quad (1)$$

where $\sigma_{x,\ y}$, $\sigma^*_{x,\ y}$ – up to of passive and passive lateral pressure 1rm ground on the pile on depth *y*; *K(l p)*– coefficient of lateral pressure; *Ks* = 0.8–1.2 – coefficient taking into account the way of immersion and the perimeter of the pile; *u* – perimeter pile γ – density of soil; λ (δ), λ_{pc} (δ) – power functions-pressure lateral (FLP) and the grip of the clay that describes the relationship diagram "pressure displacement" [28]. The limit value of the seal of the ground along the piles creates a passive

pressure and is described by equation (1) with three-dimensional effect. Accordingly, the magnitude of the frictional force on the lateral surface of the pile is equal to:

$$\tau_{x,y} = \sigma_{x,y} tg\varphi \quad (2)$$

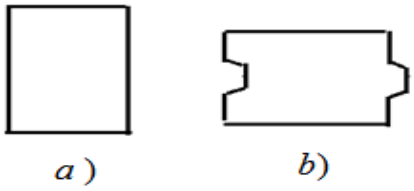

Figure 3. Cross section 2 piles with different cross-sections with the same perimeter

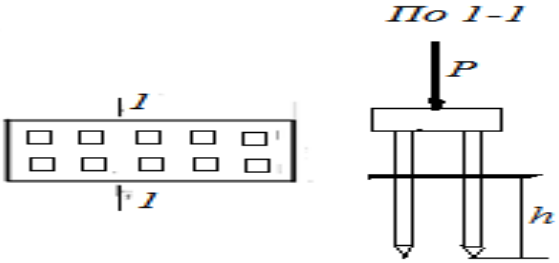

Figure 4. To the determination of the bearing capacity of pile foundation

Example 1. To determine the friction forces on the lateral surface of the single reinforced concrete piles section 30x30 cm, immersed to a depth of 5 m in loamy soils. $I_L = 0.5$, $\varepsilon = 0.7$, $\varphi = 20^0$, C = 0.02 MPa; E = 8.5 MPa; γ = 16 kN/m³; λ_p= 2.04, $\delta = \varphi = 0$; λ_0= 1.0 – coefficient of household pressure soil; λ_{pc}= 2.3, $\delta = \varphi$; K_s = 0.8; u =1.2 m is the perimeter of the pile; K_a = 0.7 is a coefficient of anisotropy of the soil horizontally; Δ_l = 0.2 d = 0.06 m.

Table 1 Comparative data of the calculated and experimental values of shear stress, kPa

Deep	Δ	Δ_i^*,	$\delta = (\Delta_i/\Delta_i^*)^n$ *n =1*	$\sigma_{x,y}$ (1)	$\tau_{x,y} = \sigma_{x,y} tg\varphi$ (2)	Experience [2]	SNIP [26]
1	2	3	4	5	6	7	8
1	0.06	0.0067	1	37.3	13.5	18.0	14.4
2	0.06	0.027	1	55.76	19.5	18.7	20.4
3	0.06	0.06	1	69.0	25.1	19.1	24.0
4	0.06	0.11	0.55	56.3	20.6	19.9	26.4
5	0.06	0.17	0.35	48.46.	18.9	20.0	28.9

Note: If relative offset is more than the limit of δ>1 take δ=1, since lateral pressure is not to exceed of the passive.

In the table 2 the second column shows the horizontal displacement of soil from pile at a value of 0.2*d*, and the third column is accordingly of the limit lateral displacement of soil at depth h, which equal [27]:

$$\Delta^* = K_{h\,d} \cdot \gamma \cdot h^2 \cdot B;$$
$$B = (\lambda_p - \lambda_0) tg\left(45^0 + \frac{\varphi}{2}\right) / K_a E_{PL} (h/h_\delta)^m, \quad (3)$$

where $K_{h\,d} = -0.5 \div 1.5$ coefficient of lateral movement, depending on the type of soil: E_{PL} – plastic soil deformation modulus equal to $E_{PL} = 0.6\,E_Y = 0.6\,E(h/h_\delta)^m$, $m = 0-2$ is the exponent; $h_b = (200 - \lambda_{pc}) / \gamma \cdot \lambda_p = 4.7\,m$ base depth, which corresponds to the regulatory module of deformation, from the load 200 kPa; the remaining dimensions are given in [27].

The fifth and sixth columns are the estimated lateral and shear stress on the piles.

The analysis table 1 shows that the horizontal limit displacement of soil from pile and corresponding friction force occur to a depth of 3 M (3rd column). Less the value of stress occurs when a further increase in depth.

Calculations show that in the table the SP 24.13330.2011 consists into a single column of values of ground resistance at the side surfaces are of the sand and clay soils is not correct. The large difference in the behavior of these soils under load, especially if the soils are with water.

For example, physico-mechanical characteristics of soil silty sand and clay at the rate of $I_L = 0.4$. In the Russian Constructions Norms and Regulations SNiP 2.02.03.85: silty sands have φ = 26^0– 36^0 depending on the porosity ratio $E = 11–39$ MPa and clay (loam absent), respectively φ =11^0–18^0, clutch 32–57 kPa, the soil deformation modulus *E* = 9–21 MPa.

Value $\tau_{x,y}$ obtained by the proposed solution, for these soils will be different, which is confirmed by the data of natural experiments [2].

Therefore, the table of the limiting values of friction forces on the lateral surface of the pile in the SP 24.13330.2011 are a particular case of solutions of the maximum the horizontal shift of the soil. Limit values of the friction forces recommended by the SP, if significant depths of immersion, as a rule, do not spring up [2].

The edge of the piles. After mobilization of the friction forces begin towork more actively the force the resistance of the soil under the tip piles. For disclosure of the behavior of the soil under the pile tip is used dimensionless chart vertical compression of the soil, presented in the form of nonlinear function [27]. The relative nature of this chart is not associated with a scale factor, allowing use of a single curve.

The values of vertical earth pressure on 1rm to the axis of symmetry of the piles on the entire range of action of the load is equal to [27]:

$$\sigma_{y,x} = K_{v\,p} \cdot K_s \cdot a[q_{br} + q_{1br} + \gamma \cdot x/tg(45^o - 0.5\varphi)]\lambda_v(\delta) \le \sigma^*_{y,x}, \quad (4)$$

where $\sigma_{y,x}$, $\sigma^*_{y,x}$ – vertical and the limit vertical pressure of the soil on the edge of the pile to the axis of symmetry (the first index "*y*" indicates the direction of stresses, the second "*x*" coordinate by the width of the piles; $K_{V\,p} = 4 \div 6$ – coefficient of the vertical pressure, the larger value refers to dense soils; $K_s = 0.8 - 1.2$ – coefficient taking into account the immersing of piles, and is the largest dimension of the pile section, q_{br} , q_{1br} – additional weight of the overlying soil and at the expense of the adhesion forces; γ – specific weight of soil; x is the horizontal coordinate of the considered point, counting from the face of the piles in the range $0 \le x \le 0.5b$ (b is the smallest dimension of the pile section; $\lambda_v(\delta) = \lambda_{pa}/\lambda_{aa}$ – function diagram of the vertical deformation [27].

Taking in the expression (4) $\lambda_v(\delta) = \lambda_v$ (where λ_v – limit value) get the limit value of the vertical pressure on the tip of the pile to the axis of symmetry.

Due to the small width of the piles, it is possible to take a rectangular plot of reactive ground pressure. Then taking into account (4) limiting of the resultant vertical pressure on the end piles is equal:

$$N = K_{v\,p} \cdot K_s \cdot a \cdot b[q_{br} + q_{1br} + 0.5\gamma \cdot b/tg(45° - 0.5\varphi)]\lambda_v \quad (5)$$

Example 2. To determine the ultimate bearing capacity of high pile grillage of reinforced concrete piles sunk 6m, section 30 x 30 cm. Soil base: φ = 20°; C = 0.022 MPa; γ = 19.7 kN/m3; λ_{pa} = 4.05, δ = φ; λ_{aa} =0.59; λ_v =6.86, $K_{v\,p}$ = 5, K_s = 1.0. Using the expression (5), with of the calculation friction forces on the lateral surface of the piles F_{fr} obtains (Fig. 4):

$$N = \cdot K_{v\,p} \cdot K_s \cdot n \cdot a \cdot b[q_{br} + q_{1br} + 0.5\gamma \cdot b/tg(45° - 0.5\varphi)] \cdot \lambda_v + n \cdot F_{fr} = 5 \cdot 1.0 \cdot 10 \cdot 0.09 =$$
$$= [118.4 + 60.43 + 0.5 \cdot 19.7 \cdot 0.3/0.7] \cdot 6.86 + \cdot 1145.6 = 6796.4 \text{ кН}$$

The experimental ultimate bearing capacity the high pile grillage was not achieved [2]. At sediment equal 70 mm the bearing capacity was of the order of 5100 KN. The bearing capacity on SNIP amounted to 4500 KN. On the experimental curve the sediment-load this corresponds of the sediment order of 55 mm .

The effect of construction of pile foundation at its carrying capacity

Low pile grillage (combined pile-slab foundation – PCB) increases the load carrying capacity due to the additional reactance of the ground from his slab. This is confirmed by experimental data [2]. This foundation is recommended to count as plate on elastic foundation with a variable in terms of the coefficient of elastic resistance of the soil in the SP 24.13330.2011. Depending on the position plate design relative to the surface of the soil it load-bearing capacity will be different (Fig. 5).

On the Figure 5, a and b bearing capacity of single pile or high pile grillage related to heaving soil from under the end of the pile and with by friction of soil on its side surface

Work low pile cap occurs in two stages. At the first stage it works similar to high pile grillage taking into account the additional resistance of the soil on the slab of the raft foundation (Fig. 5c). The second stage begins, when the proportion of pile cap to bearing capacity of pile foundation is about 30 – 35 %. Then the work included the compacted soil mass between the piles. (Fig. 5*d*). The author proposes determine the bearing capacity of low raft foundation with piles step ≤ 3*d* in the form of a conditional soil mass with the piles. The nature of its work is confirmed by the experiments of A. A. Bartolomey at extreme loads [2].

The expression of the resultant ultimate bearing capacity of the soil:

$$N = K_m \cdot a \cdot b[q_{br} + q_{1br} + 0.5\gamma \cdot b/tg(45° - 0.5\varphi)]\lambda_v + K_n \cdot E_b \cdot tg\varphi - \gamma \cdot V, \quad (6)$$

where K_m= 1.0–1.2 – generalized coefficient array; q_{br}, q_{1br}, λ_v – conventional sign is given in equation (4); K_N=1.0–1.2 – coefficient of uneven friction forces, depending on the step of the piles; E_b – resultant pressure on the side of the pile foundation, *V* – volume of the conditional foundation.

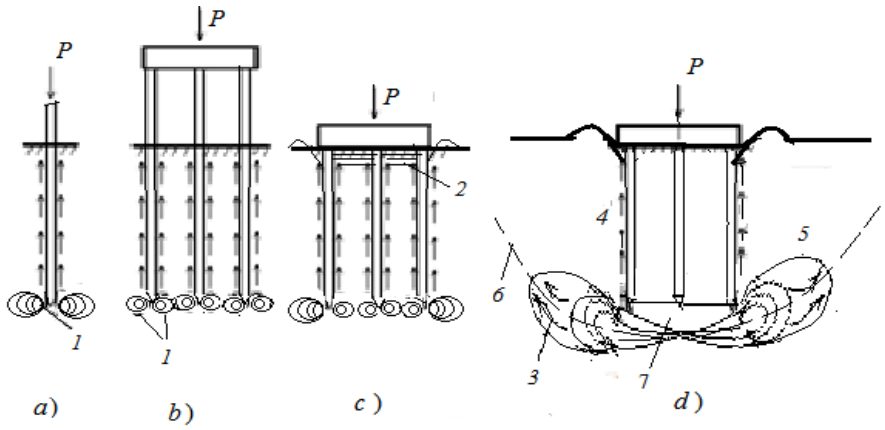

Figure 5. The active region constrained deformation of soil from variable loads: *a*) single pile; *b*) high pile grillage; *c*, *d*) low-pile grillage

Legend: 1 – boundary of the const-rained deformation of a bottom single and group of piles from the variable load; 2 – boundary of the zone of compaction of soil under the slab of the raft foundation. 3 – trajectories of movement of particles; 4 – the friction forces on the lateral surface; 5 – the boundary of the constrained deformation of conditional array; 6 – origin curve move; 7 – lower boundary soil of the wedge sealing.

Example. 3. The constructions from example 2 to determine the bearing capacity of low pile grillage . The slab of the size in terms of *a* = 4.0 m; *b*= 1.3 m. The Length of pile 6 m. the foundation. Soil: K_m =1,1; φ = 20°; C = 0.022 MPa; γ = 19.7 kN/m^3; α = 35^0; λ_{pa}=4.05, δ=φ; λ_{aa}=0.59, δ=0.5 to φ; λ_v=6.86; K_n =1.2.

Lateral pressure on a conditional array have of the hydrostatic law. Limit load including self weight of the array, and the structures (6):

$$N = K_m \cdot a \cdot b[q_{br} + q_{1br} + 0.5\gamma \cdot b/tg(45° - 0.5\varphi)]\lambda_v + K_n \cdot E_b \cdot tg\varphi - \Sigma\gamma_i \cdot V_i,$$
$$= 1.1 \cdot 4{,}0 \cdot 1.3[19.7 \cdot 6 + 22/0.364 + 0.5 \cdot 19.7 \cdot 1.3/0.364]6.86 + \cdot 1641.8$$
$$- 668{,}4 = 9364.3\ кН$$

Коровкин В.С. Инженерная кинематическая теория в приложении к расчету свайных фундаментов // Инженерно-строительный журнал. 2017. № 2(70). С. 57–71.

Experienced the load on the foundation is not reaches carrying capacity and reaches 6000 KN. This load corresponds to the draught of the order of 70 mm [2]. Limit load on the Russian Constructions Normsand Regulations SNiP 2.02.03.85 is about 7000 KN. The comparison examples no. 2 and no. 3 shows that in the lower pile grillage plate increases the bearing capacity of pile foundation up to 30 %. In fact, this effect will be more, but there are restrictions on the offset.

The influence of the location of piles on effort into them

Load on pile grillage causes shear stresses in the area along the height of the piles. Intermediate lateral resistance of the pile decreases from the overlay plots of the shear stresses of the neighbouring piles (Fig. 6).The other thing is the voltage under the tip of the piles. On the one hand, the seal space during pile driving, have increases of the bearing capacity. On the other hand, the overlay plots of the voltages from the intermediate piles increases the reactive presure under its. This creates conditions of greater precipitation and thus a reduction of effort due to redistribution to other piles.

Experience shows, that in clay ground and silty and fine sands, bearing capacity of piles in the bush, generally reduced in comparison with the bearing capacity of single piles. The sands with medium-sized and large have it increases. The use of method of angular points in the determination of additional stresses within the edge of the piles, shows that the influence of adjacent piles leads to redistribution of effort of approximately 30 % [30]. Data full-scale have bearing capacity of the intermediate piles are lower than from the outside of the piles in from 20 to 40 % [2].

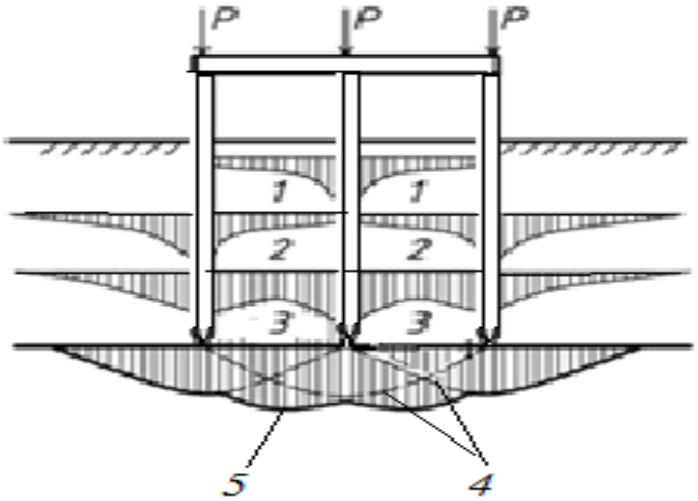

Figure 6. Summary plots of the tangential (1+2=3) and vertical stress (4+4=5).
Legend: 1, 2 – a plot of the tangential stresses in the cross-section for the central and outer piles;
4 – plot of the normal stress beneath the central and outer piles;
3, 5 – plot the resulting shear and normal stresses

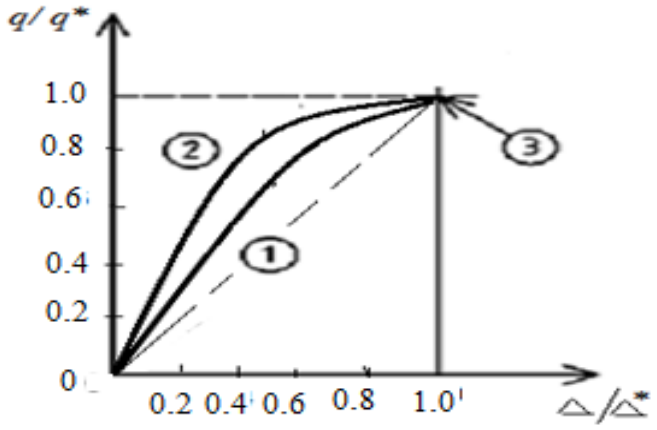

Figure 7. Schedule dimensionless relationship diagram precipitation subgrade from t he load depending on soil density of the base in dimensionless terms.
Legend 1 – loose soil; 2 – dense soil; 3 – coordinate of the point limit load

Korovkin V.S. Engineering kinematic theory in application to the calculation of pile foundations. *Magazine of Civil Engineering*. 2017. No. 2. Pp. 57–70. doi: 10.18720/MCE.70.6

The sediment pile foundation

Sediment, wich implements the friction forces on the lateral surface. The force Friction in pile foundations involves in the work in two stages [2]. In the first stage, consolidation soil mass with the piles is of 10–15 mm. However, the load of perceived by the end face of the pile increases slightly to full mobilization of the friction forces on the lateral surface of the pile.

The second phase of the work from the lateral surface observed from the draught from 10–15 mm to 30–35 mm. At this stage, is as if "failure" of the piles foundation. It leads to an increase of the friction forces. Therefore, of the external load exerted on the pile at the beginning perceive the friction force of the side surface. To them requires a smaller offset than for the mobilization of reactive pressure on the tip of the piles. Maximum draught of a soil mass or a single pile, which implements the friction forces on the lateral surface are equal [27].

$$\Delta^*_{\text{f}} = E_l \cdot tg\,\varphi\,/U \cdot \Sigma L_{\text{i}} \cdot K_{b\,d\,\text{i}},$$

where E_l is the resultant lateral pressure on the pile; U is the perimeter and L_{i} is the areas of the conventional length of an array or piles to the ground, $K_{b\ d\,\text{i}} = 0.7 \bullet K_{\text{a}} \bullet K_{\text{pl}} \bullet K \bullet y$ – variable in depth coefficient of bed shear (K_{a} – anisotropy factor, K_{pl} is the factor of the plastic properties shear, K – coefficient of proportionality, y – the depth of the considered layer).

The vertical sediment that implements the force on an end face of the piles or piles of the array soil. After the exhaustion of the forces of friction, holds the load, the edge of the piles. Vertical pressure begins to rapidly increase until a complete loss of bearing capacity.

In the conventional array of draught of the basement increases gradually and it is impossible to distinguish clearly the ultimate load [2]. In connection with sediment limit necessary to limit the load for the maximum allowable precipitation. Analysis of pile foundation shows that whatever the design of single pile or pile grillage, the nature of their work is similar**.**

In the both of the application cases there is restricted from the subsidence of soil.

The relative diagram connection (8) based (4), (7) and (8) allows to determine direct and inverse problem using the maximum allowable draught of pile foundation (Fig. 7).

The marginal precipitation conditional massif (piles), (Fig. 5).

The marginal precipitation piles or conditional array to the width 1пог m, (Fig. 5, point 3) equals [27]:

$$\Delta^* = \text{K}_g \cdot \gamma \cdot b^2 B;$$
$$B = \left(\lambda_{pa} - \lambda_{aa}\right) tg^2(45^0 + 0.5\varphi)/K_a \cdot E_{pl}[1 + \left(\frac{y}{y_1}\right)^m] tg^2\,(45^0 + 0.5\varphi), \quad (7)$$

where $K_{\text{g}} = 0.4\text{–}0.8$ – generalized coefficient taking into account the closeness of the calculated scheme; b is the width (smallest dimension) of a conditional pattern (piles); λ_{pa}, λ_{aa} – pressure coefficients of passive and active pressure of the compacted soil wedge inclined at an angle (45^0 – 0.5φ) to the vertical; $E_{pl,y} = 0.8E[1 + \left(\frac{y}{y_1}\right)^m$ – the plastic deformation modulus of soil at depth y; y and y_1 – considered and adopted a single depth; m is the exponent, $0 \le m \le 1$. The rest of the notation is given in equation (3).

The author believes that the sediment pile foundation (piles) includes the of sediment that implements the friction force at the lateral surface. The marginal precipitation (7) and the load (4) (point 3 on the chart Fig. 7) allow to determine the values of precipitation throughout the load range.

$$\Delta_{pl} = \Delta^* \left(\frac{q}{q^*}\right)^n \quad (8)$$

where n is the exponent (n =1–3). When $n = 1$ is a linear dependence (dotted line, Fig.7), the weaker the soil has a smaller curvature (curve 1, for $n = 3$).

Example 4: Determine the limit for sediment in pile foundation shown in example 3. The value of modulus of deformation with depth is $E_{\text{pl.y}} = 36.7$ MPa.

$$\Delta^{*}= К_{g}\cdot\gamma \cdot b^{2}B = 0.4 \cdot 19.7 \cdot 1.3^{2} \cdot 0.007 = 0.093\ m,$$

The value of precipitation of the pile cap at 40% load limit 9364.3 KN is equal to:

$$\Delta_{pl} = \Delta^{*}\left(\frac{q}{q^{*}}\right)^{1.5} = 0.093 \cdot 0.25 = 0.023\ m$$

The sediment of the low pile grillage with this load amounted to 0.025 m [2]. Specifying the maximum permissible amount of displacement of the foundation structures from equation (8) we get the desired maximum load.

Model the combined stiffness coefficient of the soil

Each strip in Figure 1 due to the variable length has a different degree of resistance to compression of the soil. In design scheme that corresponds to the different stiffness of the soil (variable coefficient).Variable coefficient better reflects the work of the foundation. Picking up the variation of the ratio bed, we provide the right character of precipitation.

Using the program CROSS procedure of successive approximations as applied to foundations can more accurately determine the stiffness coefficient of the soil [31]. The program CROSS is part of the package SCAD Office and provides both stand-alone operation and communication with integrated system of strength analysis of structures Structure CAD (SCAD) [32]. This procedure of successive approximations, according to the author, it is permissible for light loads on the foundation. Because there is no law of variation of stiffness of soil from the full load cycle and is not considered redistribution of the contact pressure of the marginal plastic areas.

The author proposes a mechanical model of the soil with a structural element acting on the lateral surface (Fig. 8 a) and of the low end the piles (figure 8 b). In the model, except of elastic Hooke body (H) and of plastic body of the Saint Venant (SV) , also have a structural element (S).

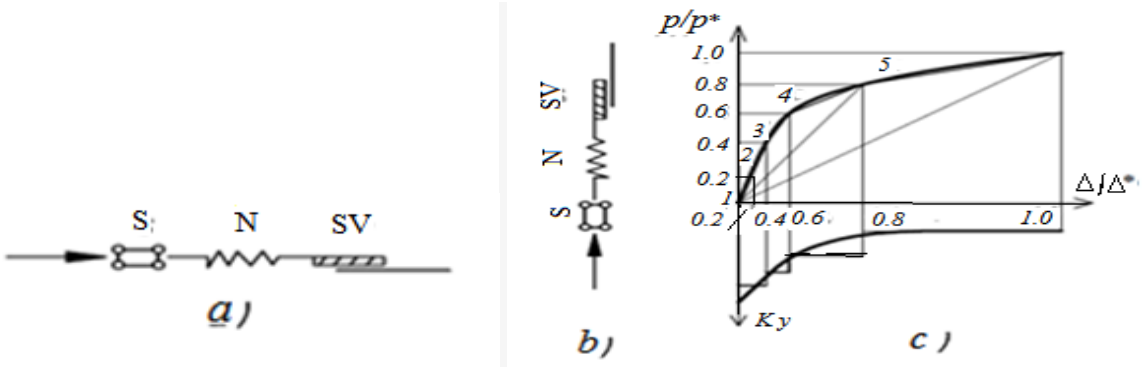

Figure 8. Mechanical model of compression of the soil taking into account the structural element in the side (*a*) end (*b*) surfaces of the piles. Dimensionless curve pressure – lateral displacement (pressure – vertical offset) and a variable coefficient of stiffness of the soil correspond to the model (*c*).

This element functionally connects of the curve pressure-displacement according the type of connection (Fig. 8). This model is similar to the adopted model for the aoundation [29].

The springs located both on the lateral surface of the pile (Fig. 8, *a*) and on its end face (Fig.8, *b*). The number of turns of the spring depends on the depth of the active zone of the soil. The springs resist compression more or less elastically under small external loads. The load increases to the limit value changes the value of resistance to compression of the springs due to the structural element (S). This leads to a nonlinear dependence of the "pressure-displacement".

Dimensionless curve "pressure-displacement (pressure-draught") is shown in Figure 8, in the upper part. Schedule of changes in relative stiffness between the level of load shown in Figure 8*b*, the lower part. The dimensionless character of the two curves is similar, but the degree of curvature is different. The dimensionless nature of the relationship allows you to use the curve to describe the interaction of the side or end portions of the pile with the soil from the load irrespective of the scale of the building. The conditional transfer of the stiffness coefficient of the soil in absolute value sets the regularity of this change on the side or lower surfaces of the piles. For example, each length segment of the lateral

surface of the pile or the width of its edge, depending on the load will correspond to a specific area of the connection curve of the contact and hence of the curve the stiffness of the soil (Fig. 8, *c*).

Expressions (1–7), in addition to independent values, according to Figure 8 allow us to determine the coefficients of stiffness of the soil elements to pile foundation. These coefficients are used as source data in the proposed calculation of pile foundation using the software complex "SCAD". For this of the purpose, calculated ultimate horizontal and vertical loads and the corresponding ultimate displacements.

The author believes that the coefficient of stiffness is in some respects is the type of the discrete model of the environment. So reducing the length of the element to the minimum size allows to obtain a family of discrete independent coefficients, whose values can be described the necessary desired function or set numerically.

In relation to the design scheme of pile grillage is used of the frame rack with different stiffness of the rigel and racks. The nature of the work structures in the soil is determined by its stiffness characteristics of the system elements: beams, uprights and ground.

Example 5. To calculate the reconstructed embankment on the canal Griboedova in St Petersburg. Original data: The old quay was built in the beginning of the last century (Fig. 9). In front of the old embankment to the form of rigid raft foundation of rubble concrete which masonry is based on three rows of wooden piles, and erected a new hard grillage. It has a crossbar of variable cross section of reinforced concrete on pile foundation of two rows of bored piles, 16 m long, with a diameter of 0.6 m. Step piles across the cordon line is 2.35 m, and respectively along the line of the cordon 1.4 m. Characteristics of the soil include four layers of the loam from the fluid (Kb = 350÷1750 kN/m^3) up plastic (Kb = 21300÷39700 kN/m^3), layer of sandy loam (Kb = 58000÷70000 kN/m^3), sand (Kb = 73000÷75000 kN/m^3), the coefficient on the tip of the piles, Kb v= 14792 MP/m3. The calculation with using the program SCAD performed by student of A. Melentiev. Results of the comparison of calculations are given in table 2.

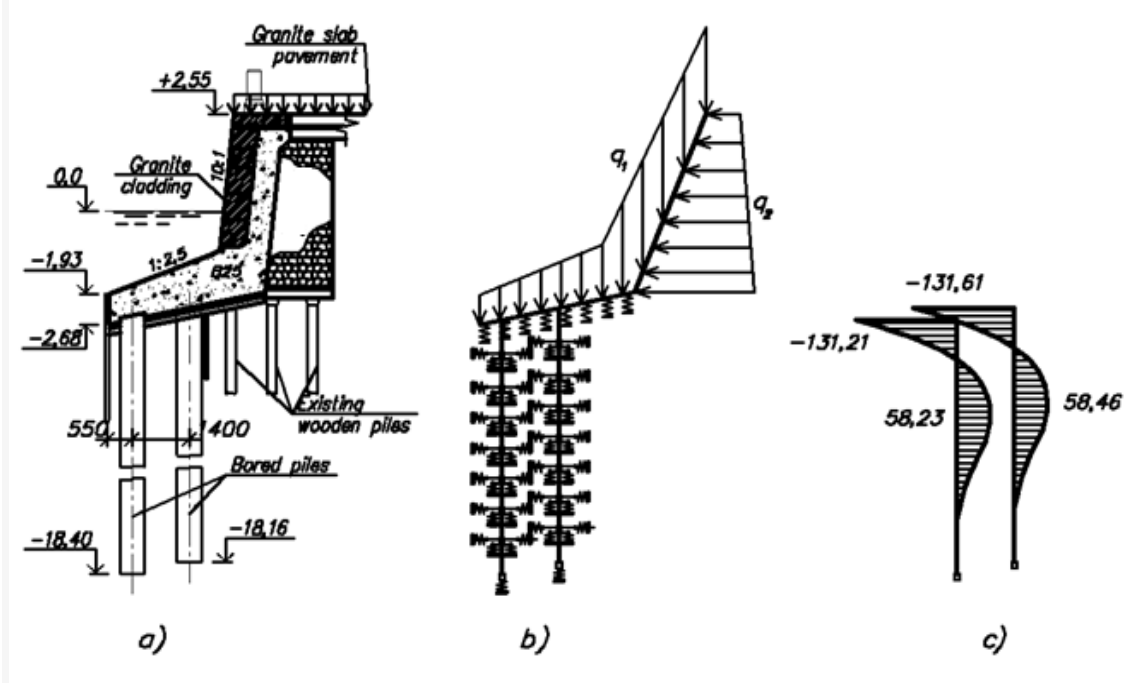

Figure 9. To the calculation of the city's waterfront. a) Cross section. b) design scheme. b) Plot bending moment in the piles

Table 2. Results of calculations

Name	Calculati for a SNP [26]	The calculation for a generic method
Moment in the topic sealing of the first pile, kNm	-135.23	-131.21
Moment at the topic sealing of the second pile, kNm	-135.23	-131.61
Moment in the span of the first pile, kNm	-	58.23
Moment in the span of the second pile, kNm	-	58,46
The effort in the first pile, kN	-470.0	-417.92
The effort in the second pile, kN	64.16	12.02
Horizontal displacement of the top, mm	-	4.87

Results and Discussion

Pile when submerged in the soil condenses it in the transverse and longitudinal directions. Seal give the effect on the piles lateral and vertical pressure of soil. The friction force along the length the piles depends on the value of lateral pressure. Analysis of example 1 shows that the maximum friction force occurs at a depth up 3 the meters. Further increase in depth does not implements the maximum force of the lateral pressure of soil. This leads to a decrease in the values of the tangential stresses along the length of the pile. The Russian Building Regulations SNIP [26] recommends a limiting value of the friction forces along the length of the piles, which usually is not confirmed by experimental data.

The work of pile foundation depends on the load, position of the grillage and the distance between the piles. The author gives of the engineering solution, in which the limit load and the sediment pile foundation, depending on conditions, determined by the number piles or by the ground massive. The analysis of examples No. 2 and No. 3 shows that the calculated values are comparable with experimental data A. A. Bartholomew [2]

Bearing capacity of pile foundation in the Russian Set of Rules SP 24.13330.2011 is below the limit load, so as by the limited by it sediment. However, in the proposed method of taking into account the allowable residue it is 15–25 % higher than in the SP 24.13330.2011.

Analysis of example No. 4 showed that the efforts in the pillars of the city's waterfront in the form of lower pile grillage in the proposed method, and SNIP [26] practically coincide.

Chart of the load-displacement allows solving in the proposed method direct and inverse problems for the entire load range.

Conclusions

1. The author proposed the variant of calculation of pile foundation using of the engineering theory of ground contact pressure.

2. This variant uses the mechanism of influence of piles in the ground on the magnitude of lateral and vertical seals.

3. The friction force on the lateral surface of the pile is variable and depends on the magnitude of lateral soil pressure on it. The normative document Russian Set of Rules SP 24.13330. 2011 gives the maximum value of the friction force. The maximum value, trenie can not occur at depths greater than 3–4 mm. In addition, SP 24.13330.2011 gives the joint values the calculated resistance of sands and clayey soils. This are the basis for criticism, as each type of soil has its own physical and mechanical characteristics associated with the friction forces.

4. The proposed option determines the jet pressure of the soil on the edge of the piles or on a conditional piler foundation for the entire load cycle.

5. Bearing capacity of pile Foundation additionally depends on the location of the plate grillage. The influence of the plate begins to emerge, usually with a load more friction forces on piles.

6. In the proposed calculation takes into account the mutual influence of piles on the distribution of forces in pile grillage.

7. The value of the precipitation of pile foundation gets from a dimensionless curve the "pressure-settlement" for the entire load cycle.

8. The author proposed a mechanical model of the ratio of stiffness of soil with the influence of the structural element. The stiffness coefficient of the soil load is determined based on a curve of deformation.

9. Analysis of sample data showed that the efforts in the pillars of the city's waterfront in the form of lower pile grillage in the proposed method, and SNIP [26] practically coincide.

10. In the calculation of structures using the model of the stiffness of the soil, special attention must be paid to the reliability of this characteristic, which substantially depends on the efforts and peremescheniya structural members. Each of those values recommended in the standards, have a broad range of values and require adjustment.

References

1. Barvashov V.A., Boldyrev G.G. Yeksperimental'no-teoreticheskie issledovanija svaino-plitnyh fundamentov [Experimental and theoretical investigations of pile-slab fundamentoweringy]. *Trudy mezhdunarodnoi konferencii po geotehnike "Geotehnicheskie problemy megapolisov".* Moscow, 2010. Vol. 4. Pp. 1209–1212. (rus)
2. Bartolomey A.A. *Prognoz osadok svainyh fundamentov* [Forecast sediment pile foundations]. Moskva: Stroiizdat, 1994. 390 p. (rus)
3. Baholdin B.V., Trufanova E.V. Soprotivlenie svai gorizontal'nym nagruzkam [Adjustment of current methods of evaluating the resistance of piles to horizontal loads] *Soil Mechanics and Foundation Engineering.* 2010. No. 6. Pp. 8–13. (rus)
4. Bezvolev S.G. Proektirovanie i raschety osnovanii i fundamentov vysotnyh zdanii v slozhnyh inzhenerno-geologicheskih uslovijah [Design and calculations of foundations and bases of tall buildings in complex geological engineering conditions]. *Razvitie gorodov i geotehnicheskoe stroitel'stvo.* 2007. № 11. Pp. 98–118. (rus)
5. Krutov V.I., Kogai V.K., Gluhov V.S. Uchet uplotnenija gruntov pri raschete svainyh fundamentov [Account of compaction in the calculation of pile foundations]. *Trudy mezhdunarodnoi konferencii po geotehnike "Geotehnicheskie problemy megapolisov"*. Moscow, 2010. Vol. 4. (rus)
6. Savinov A.V. *Primenenie svaj, pogruzhaemyh vdavlivaniem, pri rekonstrukcii istoricheskoj zastrojki gorodov. Avtoreferat doktora tekhnicheskih nauk* [The use of piles, submerged pressed in, during the reconstruction of the historical development of cities]. Volgograd, 2008. 34 p. (rus)
7. Ulickij V.M., Shashkin A.G., Paramonov V. N Opredelenie nesushchej sposobnosti buronabivnyh svaj [Determination of the bearing capacity of bored piles]. *Soil Mechanics and Foundation Engineering.* 2001. № 2. Pp. 13–16. (rus)
8. Znamenskii V.V., Ruzaev A.M. Vlijanie parametrov svainogo fundamenta na rabotu nizkogo rostverka [Influence of parameters of pile foundation to work low class]. Yeksperimental'no-teoreticheskie issledovanija svaino-plitnyh fundamentov. *Trudy mezhdunarodnoi konferencii po geotehnike "Geotehnicheskie problemy megapolisov"*. Moscow, 2010. Pp. 1250–1251. (rus)
9. Zareckii Y.K. *Vjazkoplastichnost' gruntov i raschety sooruzhenij* [Visco-plasticity of soils and calculation of structures]. Moscow: Stroiizdat, 1988. 350 p. (rus)
10. Matveenko G.A., Lukin V.A, Fadeev A.B. Opyt proektirovanija i stroitel'stva svaino-plitnogo fundamenta gruppy zdanii [Experience in the design and construction of pile-slab Foundation is a group of buildings. Experimental and theoretical investigations of pile-slab foundations]. Yeksperimental'no-teoreticheskie issledovanija svaino-plitnyh fun-damentov. *Trudy mezhdunarodnoi konferencii po geotehnike "Geotehnicheskie problemy megapolisov",* Moscow, 2010. Pp. 1513–1516. (rus)
11. Fedorovskii V.G. *K raschetu kombinirovannyh plitno-svainyh fundamentov* [The calculation of combined piled

Литература

1. Барвашов В.А., Болдырев Г.Г. Экспериментально-теоретические исследования свайно-плитных фундаментов // Труды международной конференции по геотехнике «Геотехнические проблемы мегаполисов». Москва, 2010. Т. 4.
2. Бартоломей А.А. Прогноз осадок свайных фундаментов. М: Стройиздат, 1994. 390 с.
3. Бахолдин Б.В., Труфанова Е.В. Корректировка существующих методик оценки сопротивления свай горизонтальным нагрузкам // Труды международной конференции по геотехнике "Геотехнические проблемы мегаполисов". Москва. 2010 г. Том 4.
4. Безволев С.Г. Проектирование и расчеты оснований и фундаментов высотных зданий в сложных инженерно-геологических условиях // Развитие городов и геотехническое строительство. 2007. № 11. С. 98–118.
5. Крутов В.И., Когай В.К., Глухов В.С. Учет уплотнения грунтов при расчете свайных фундаментов // Труды международной конференции по геотехнике Геотехнические проблемы мегаполисов. Москва, 2010. Т. 4.
6. Савинов А.В. Применение свай, погружаемых вдавливанием, при реконструкции исторической застройки городов. Автореферат дисс. на соиск. учен. степ. д.т.н.: Спец. 05.23.02. Волгоград, 2008. 34 с.
7. Улицкий В.М., Шашкин А.Г., Парамонов В.Н Определение несущей способности буронабивных свай // Основания фундаменты и механика грунтов. 2001. № 2 С. 13–16.
8. Знаменский В.В., Рузаев А.М. Влияние параметров свайного фундамента на работу низкого ростверка. Экспериментально-теоретические исследования свайно-плитных фундаментов // Труды международной конференции по геотехнике "Геотехнические проблемы мегаполисов". Москва, 2010 г.
9. Зарецкий Ю.К. Вязкопластичность грунтов и расчеты оснований. М: Стройиздат, 1988. 350 с.
10. Матвеенко Г.А., Лукин В.А, Фадеев А.Б. Опыт проектирования и строительства свайно-плитного фундамента группы зданий. Экспериментально-теоретические исследования свайно-плитных фундаментов // Труды международной конференции по геотехнике "Геотехнические проблемы мегаполисов". Москва, 2010 г.
11. Федоровский В.Г. и др. К расчету комбинированных плитно-свайных фундаментов // Расчет и проектирование конструкций в среде SCAD Office. Киев, 2006 [Электронный ресурс]. Сист.требования: MifrosoftPowerPoint. URL: http:://scadsoft.ru/download/KPSF.ppt (дата обращения: 21.01.2017).
12. Дзагов А.М., Разводовский Д.Е. О несущей способности забивных свай, опирающихся на малосжимаемые грунт // Основания фундаменты и механика грунтов. 2013. № 5. С. 7–12.
13. Готман А.Л. Анализ комбинированных свайных фундаментов, подвергающихся воздействию

Коровкин В.С. Инженерная кинематическая теория в приложении к расчету свайных фундаментов // Инженерно-строительный журнал. 2017. № 2(70). С. 57–71.

raft foundations] // Rascheti proektirovanie konstrukcii v srede SCAD Office. Kiev, 2006. [Electronic resourse]. Syst.requirements: MifrosoftPowerPoint. URL:http: //scadsoft.ru /download/KPSF.ppt. (date of application: 21.01.2017). (rus)

12. Dzagov A.M., Razvodovskii D.E. O nesushei sposobnosti zabivnyh svai, opirayushihsja na maloszhimaemye grunt [About the bearing capacity of driven piles based on a low-compression ground]. *Soil Mechanics and Foundation Engineering.* 2013. No. 5. Pp. 7–12.(rus)
13. Gotman A.L Analiz kombinirovannyx svajnyx fundamentov, podvergayushhixsya vozdejstviyu gorizontalnoj nagruzki i izgibayushhego momenta [Analysis of sombined pile foundations exposed to horizontal load and bending moment]. *Mehanika gruntov i fundamentostroenie.* 2015. No. 52(4). 225 p. (rus).
14. Terzaghi K. *Theoretical soil mechanics.* Wiley. New York, 1943. 507 p.
15. Fellenius B.H. *Basics of foundation design* [Electronic resource]. URL: www.Fellenius.net. 346 p.
16. Fellenius B.H. Discussion of "load and resistance factor design of drilled shafts in sand" by d. Basu and Rodrigo Salgado. *Journal of Geotechnical and Geoenvironmental Engineering.* 2014. No. 140(3).
17. Taylor R.N., Rose A.V., Gorasia, R.J. Pile and pile group capacity: some findings from centrifuge tests. *International Journal of Geo-Engineering.* 2013. No. 5(2). Pp. 5–15.
18. Boukpeti N., White D.J. Interface shear box tests for assessing axial pipe-soil resistance. *Geotechnique*. 2016. No. 67(1). Pp. 1–13.
19. Mandolini A., Russo G., Viggiani C. Pile foundations: Experimental investigations, analysis and design. *Proceedings of the 16th International Conference on Soil Mechanics and Geotechnical Engineering: Geotechnology in Harmony with the Global Environment.* 2005. No. 1. Pp. 177.
20. Viggiani C; Mandolini A. *Piles and Pile Foundations*. Taylor and Francis, 2011. 278 p.
21. Manandhar S., Yasufuku N. Vertical bearing capacity of tapered piles in sands using cavity expansion theory. *Soils and Foundations.* 2013. No. 6(53). Pp. 853–867.
22. Zhao C.F., Wang W.Z., Qiu Z.X. Field test study on bearing capacity of single pile under combined loads. *China Journal of Highway and Transport.* 2013. No. 26(6). Pp. 59–64.
23. Gandhi S.R. Observations on pile design and construction practices in India. *Indian Geotechnical Journal.* 2016. No. 46(1).
24. Shooshpashaa I., Mola-Abasia H., Amirib I. Evaluation of static and dynamic methods for determining the bearing capacity of the driven pipe piles. *International Journal of Engineering.* 2014. No. 2(27). Pp. 307–314.
25. Du J.Q., Du S.J., Zhao D.-L., Tang W.-Y. Numerical analysis of interaction of pile group-soil-raft under vertical load. *Rock and Soil Mechanics.* 2013. No. 8(34). Pp. 2414–2420.
26. *SP 24.13330.2011.* Svainye fundamenty. [Russian Set of Rules SP 24.13330.2011.Pile foundations]. 88 p.
27. Korovkin V.S. *Gidrotehnicheskie sooruzhenija morskih portov* [Hydrotechnical constructions of sea ports]. St.Petersburg: Lan', 2014. 427 p. (rus)
28. Korovkin V.S. Inzhenernaja kinematicheskaja teorija kontaktnogo davlenija grunta i ee prilozhenie k staticheskomu raschetu prichal'nyh stenok [Engineering kinematic theory of ground contact pressure in application to calculation of certain types of foundations]. *Magazine of Civil Engineering.* 2013. No. 6. Pp. 39–49.
29. Korovkin V.S. Inzhenernaja kinematicheskaja teorija kontaktnogo davlenija grunta v prilozhenii k raschetu nekotoryh tipov fundamentov [Engineering kinematic theory of ground contact pressure in the Annex to the calculation

горизонтальной нагрузки и изгибающего момента // Механика грунтов и фундаментостроение. 2015. № 4(52). 225 с.

14. Terzaghi K. Theoretical soil mechanics. Wiley, New York, 1943. 526 p.
15. Fellenius B.H. Basics of foundation design [Электронный ресурс]. URL: www.fellenius.net. 346 p.
16. Fellenius B.H. Discussion of "load and resistance factor design of drilled shafts in sand" by d. Basu and Rodrigo Salgado // Journal of Geotechnical and Geoenvironmental Engineering. 2014. № 140(3).
17. Taylor R.N., Rose A.V., Gorasia, R.J. Pile and pile group capacity: some findings from centrifuge tests // International Journal of Geo-Engineering. 2013. № 5(2). Pp. 5–15.
18. Boukpeti N., White D.J. Interface shear box tests for assessing axial pipe-soil resistance // Geotechnique. 2016. № 67(1). Pp. 1–13.
19. Mandolini A., Russo G., Viggiani C. Pile foundations: Experimental investigations, analysis and design // Proceedings of the 16th International Conference on Soil Mechanics and Geotechnical Engineering: Geotechnology in Harmony with the Global Environment. 2005. № 1. Pp. 177.
20. Viggiani C; Mandolini A. Piles and Pile Foundations. Taylor and Francis, 2011. 278 p.
21. Manandhar S., Yasufuku N. Vertical bearing capacity of tapered piles in sands using cavity expansion theory // Soils and Foundations. 2013. № 6(53). Pp. 853–867.
22. Zhao C.F., Wang W.Z., Qiu Z.X. Field test study on bearing capacity of single pile under combined loads // China Journal of Highway and Transport. 2013. № 26(6). Pp. 59–64.
23. Gandhi S.R. Observations on pile design and construction practices in India // Indian Geotechnical Journal. 2016. № 46(1).
24. Shooshpashaa I., Mola-Abasia H., Amirib I. Evaluation of static and dynamic methods for determining the bearing capacity of the driven pipe piles // International Journal of Engineering. 2014. № 2(27). Pp. 307–314.
25. Du J.Q., Du S.J., Zhao D.-L., Tang W.-Y. Numerical analysis of interaction of pile group-soil-raft under vertical load // Rock and Soil Mechanics. 2013. № 8(34). Pp. 2414–2420.
26. СП 24-13330.2011. Свайные фундаменты. Актуализированная редакция СНиП 2.02.03-85.
27. Коровкин В.С Гидротехнические сооружения морских портов. СПб: Лань, 2014. 427с.
28. Коровкин В.С. Инженерная кинематическая теория контактного давления грунта и ее приложение к статическому расчету причальных стенок.// Инженерно-строительный журнал. 2013. № 6. С. 39–49.
29. Коровкин В.С. Инженерная кинематическая теория контактного давления грунта в приложении к расчету некоторых типов фундаментов // Инженерно-строительный журнал. 2014. № 6. С. 40–52
30. Пособие по проектированию зданий и сооружений. (К СНиП 2.02.01.83). М.: НИИОСП им. Герсеванова, 1986. 415 с.
31. Крискунов Э.З., Перельмутер А.В., Перельмутер М.А., Семенцов А.И., Федоровский В.Г., КРОСС-программа для определения коэффициентов постели // Основания, фундаменты и механика грунтов. 2002. № 1.
32. Ватин Н.И., Мойся А.А. Совместный расчет здания и фундамента мелкого заложения в SCAD // Методические указания. Санкт-Петербург. 2007.

Korovkin V.S. Engineering kinematic theory in application to the calculation of pile foundations. *Magazine of Civil Engineering*. 2017. No. 2. Pp. 57–70. doi: 10.18720/MCE.70.6

of certain types of foundations]. *Magazine of Civil Engineering. 2014. No.* 6. Pp. 40–52. (rus)

30. *Posobie po proektirovaniyu zdanii i sooruzhenii* [A manual for design of buildings and structures]. Moscow: NIIOSP im Gersevanova, 1986. 415 p.
31. Kriskunov Y.Z., Perel'muter A.V., Perel'muter M.A., Semencov A.I., Fedorovskii V.G., KROSS-programma dlja opredelenija koyefficientov posteli [CROSS-program to determine the coefficients of bed]. *Soil Mechanics and Foundation Engineering.* 2002. No. 1.
32. Vatin, N.I. Moisja A.A. Sovmestnyi raschet zdanija i fundamenta melkogo zalozhenija v SCAD [Joint the structural design of shallow Foundation in SCAD]. *Metodicheskie ukazanija*. St.Petersburg. 2007. Pp. 1–7. (rus)

Vladimir Korovkin,
+7(911)1905172; korovkin40@yandex.ru

Владимир Сергеевич Коровкин,
+7(911)1905172;
эл. почта: korovkin40@yandex.ru

Коровкин В.С. Инженерная кинематическая теория в приложении к расчету свайных фундаментов // Инженерно-строительный журнал. 2017. № 2(70). С. 57–71.

doi: 10.18720/MCE.70.7

The method of calculation for the period of checking utility systems

Метод расчета периода контроля оборудования инженерно-технических систем

V.S. Soldatenko,
V.A. Smagin,
Y.N. Gusenitsa,
V.I. Gera,
Military Space Academy named after A.F. Mozhaysky, St. Petersburg, Russia
T.N. Soldatenko,
Peter the Great St. Petersburg Polytechnic University, St. Petersburg, Russia

Канд. техн. наук, доцент В.С. Солдатенко,
д-р техн. наук, профессор В.А. Смагин,
канд. техн. наук, преподаватель кафедры Я.Н. Гусеница,
канд. техн. наук, начальник факультета В.И. Гера,
Военно-космическая академия имени А.Ф. Можайского, г. Санкт-Петербург, Россия
старший преподаватель Т.Н. Солдатенко,
Санкт-Петербургский политехнический университет Петра Великого, г. Санкт-Петербург, Россия

Key words: equipment engineering and technical systems; optimal control period; technical condition; failure

Ключевые слова: инженерно-технические системы, оптимальная периодичность контроля; техническое состояние; отказ

Abstract. The model and the procedure of optimization of the periods of control and scheduled maintenance in relation to the equipment of technical systems are considered. This approach is implemented on the basis of performance of a condition of a minimum of average losses of target use of the equipment. The specified losses are possible because of non-optimal frequency of control and prophylaxis of objects of technical networks. In article the approach used in the theory of information for minimization of decrease in informative value because of breaks by its transfer is considered. Feature of the offered approach is use of integer quantization of intercontrol intervals and the accounting of casual duration of operation of the equipment. Theoretical conclusions are illustrated by settlement examples.

Аннотация. Рассматривается модель и процедура оптимизации периодов контроля и профилактических мероприятий применительно к оборудованию инженерно-технических систем. Данный подход реализуется на основе выполнения условия минимума средних потерь целевого использования оборудования. Указанные потери возможны из-за неоптимальной периодичности контроля и профилактики элементов инженерно-технических систем. В статье рассматривается подход, используемый в теории информации для минимизации снижения ценности информации по причине перерывов при ее передаче. Особенностью предложенной подхода является использование целочисленного квантования межконтрольных интервалов и учет случайной продолжительности периодов эксплуатации оборудования. Теоретические выводы иллюстрируются расчетными примерами.

Introduction

Utility systems have a sufficient weight considering the efficient application of technological equipment as well as the use of buildings and constructions [1–3]. Therefore the necessity to provide their faultless operation takes a lot of attention. The requirements to operational systems are implemented at the early stages of designing buildings and constructions [4–8]. One of the most efficient means to provide the necessary level of reliability of the utility systems is the prevention of failures based

Soldatenko V.S., Smagin V.A., Gusenitsa Y.N., Gera V.I., Soldatenko T.N. The method of calculation for the period of checking utility systems. *Magazine of Civil Engineering*. 2017. No. 2. Pp. 72–83. doi: 10.18720/MCE.70.7

on periodical check of their engineering status and carrying out the appropriate preventive maintenance during the operational period [9–11]. Hence the important part of operational security belongs to the matters considering the reasoning and construction of systems for checking the engineering status of utility systems [12–15]. At the same time the applied approaches are used in the most innovative fields of science and engineering [16–23].

A separate and rather complicated matter of introducing the monitoring of utility systems for buildings and constructions is the reasoning for the period of checking their elements and the following preventive maintenance. There are a number of approaches to solve the matter in question [24–35]. However, in the specified works reasoning of the required criteria for checks and preventive maintenance does not fully take account of the following peculiarities of utility systems: their ambiguous operational condition between the checks; discontinuity of the periods of checks and preventive maintenance, random periods of their operation between the prearranged repairs. In the present article these important assumptions are considered. It allows receiving results, more adequate for practice. Let us consider the physical representation of the given problem.

Methods

Physical interpretation of the model

Some considerably prolonged period of operation is considered. Such a period may be a regulatory period before the prearranged overhaul maintenance. Some divergence between the real and prescriptive periods of operation is expected to be possible. That happens due to a number of random factors and is consistent with the actual operation of facilities.

Let us suppose that during the operation of utility systems their operational condition can be determined only by means of checks. In a disabled state the facility cannot fulfill its main function. After receiving the relevant information about its condition, appropriate preventive maintenance is carried out. It includes the reconstruction of operational capability of the facility, if necessary. It is for that reason that regular checking of operational condition of the utility systems is introduced and put in practice. It is supposed that the facility has a limited reliability and can fail between two consecutive check measures. Therefore, two cases are possible. Firstly, the checking period may be determined too large, and the facility stays in a disabled condition for some time before it would be found out during the check. In this case there is a loss due to the utility system not performing its functions. Secondly, the checks may be carried out too often; therefore the facility would be operational before the checks. The operational loss stems from time loss for the excessive maintenance, as during this period the facility is also disabled. Hence it is essential to calculate such a value for the check and maintenance period, which would provide minimal average losses for the operational maintenance of utility systems in the given period of using the building (construction).

It is practical to consider the inter-check period as an integer value, divisible by some unit of time. Such a unit may be a workday or a work shift. This is more consistent with the reality of workload management for the staff of utility system's operational system, than the speculation about the continuity of this period. Let us now examine the mathematical interpretation of the given problem and the means to solve it.

Mathematical model 1 (basic model)

Suppose T is the operational time of a facility with a utility system. At the same time T is a random value and follows the distribution law $F(t)$. During the usage the operational condition of the facility is being checked. The period between consecutive check measures equals x. According to the abovementioned hypothesis x is an integer value of time units. The duration of checks and the following preventive maintenance equals c given units of time. Let us set p as the probability of faultless performance of the facility in a given time unit. Hence the random period of operation T has at the average K checks (and preventive maintenance). The chart in figure 1 shows the operational process in the graphical form.

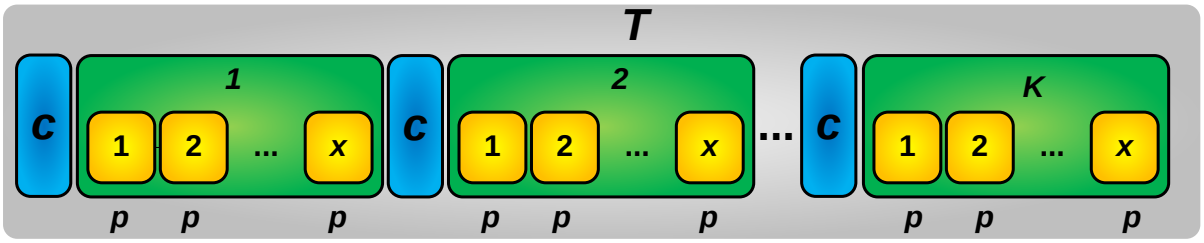

Figure 1. Graphical representation of operational process of a facility with a utility system

Let us use a well-known in information theory [36, 37] ratio for average losses $\Psi(x)$ of information in value x, determined by quantization of random period of time T. Under quantization we mean the choice of an integer value for x. For $\Psi(x)$ the expression takes the following form:

$$\Psi(x) = (x + c)\int_0^{\infty} \left(\left\lfloor \frac{z}{x} \right\rfloor + 1 \right) dF(z), \tag{1}$$

where z – an integration variable, characterizes operation interval size; record $\lfloor A \rfloor$ is Antje of number A.

However, the equation (1) does not take into account the possible failure of a facility during any time unit, as well as during the whole inter-check period (quantum). Let us introduce this clause in the following way. As the value p as the probability of faultless performance of a facility in a given time unit is known, then the probability $P(x)$ of its faultless performance in the period x is determined by the equation:

$$P(x) = \prod_{i=1}^{x} p = p^x \tag{2}$$

Clearly, considering equation (2), the mathematical expectancy $\overline{x}$ of duration of the period, when the facility works without fault in scope of the inter-check period x, is determined by the equation

$$\overline{x} = x \cdot p^x \tag{3}$$

Now let us insert equation (3) into formula (1). Besides, the value of average losses during the application of the check system is denoted as $M(x, p)$. As a result, the formula is written as following:

$$M(x, p) = (xp^x + c)\int_0^{\infty} \left(\left\lfloor \frac{z}{xp^x} \right\rfloor + 1 \right) dF(z). \tag{4}$$

Now it is necessary to find such a value of x, which allows the minimal overall loss $M(x, p)$ at the checks and maintenance of the facility with the utility system in the operational period T. At the same time one should take into consideration that x is a discrete value. The problem in question is solved comparatively easily via the method of computational analysis by means of the contemporary mathematical packages.

Mathematical model 2 (model for two check systems)

The base model, determined by the equation (4), does not account for a reliability index of checking the operational condition of utility systems. In practice, different ways of checking are applied with different probability of accurate determination of the operational condition of the facility. To take this peculiarity into consideration, let us analyze the following example.

Soldatenko V.S., Smagin V.A., Gusenitsa Y.N., Gera V.I., Soldatenko T.N. The method of calculation for the period of checking utility systems. *Magazine of Civil Engineering*. 2017. No. 2. Pp. 72–83. doi: 10.18720/MCE.70.7

Two independent check systems simultaneously determine the operational condition of a facility in a time period x. The reliability p_k of checks for each of the given systems will be determined via the probability of finding a failure. Therefore the reliability p_{s2} of estimating the operational condition of the facility by both check systems is defined as p_k^2. Time, spent on checking the operational capacity of the facility, is constant and equals c. Time for reconstructing a disabled facility is constant and equals c_B.

It is required to find the value of check period x^*, which allows the minimal mathematical expectancy of time losses during the operation, provided that the value of probability p_{s2} of faultless performance of the checked facility is not less than the given one.

The formula for the value $M(x, p, p_{s2})$ of the average losses in the operational period T considering the condition in question is written as following:

$$M(x, p, p_{s2}) = \left(xp^x + c\,p_{s2} + c_B(1 - p_{s2})\right) \int_0^\infty \left(\left\lfloor \frac{z}{xp^x} \right\rfloor + 1 \right) dF(z), \quad (5)$$

where $p_{s2} = p_k^2$.

Minimal value for $M(x, p, p_{s2})$ from the formula (4) is calculated by solving the given nonlinear problem.

Mathematical model 3 (model for three check systems)

Let us now introduce the following condition. The check of operational condition of a utility system is performed by three independent check systems. In addition, the results provided by these systems are combined in a majoritary way. Thus the reliability p_{s3} of the right estimation of the operational condition of the facility is determined by concurrence either of all three check systems or of two out of three. In such a case the probability p_{s3} to accurately estimate the performance of the equipment can be calculated with the following formula:

$$p_{s3} = 3p_k^2 - 2p_k^3. \quad (6)$$

The equation for the value $M(x, p, p_{s3})$ of average losses in operational period T considering the given condition is written as following:

$$M(x, p, p_{s3}) = \left(xp^x + c\,p_{s3} + c_B(1 - p_{s3})\right) \int_0^\infty \left(\left\lfloor \frac{z}{xp^x} \right\rfloor + 1 \right) dF(z). \quad (7)$$

The minimal value for $M(x, p, p_{mc})$ from the formula (7) can be calculated.

Results and Discussion

Let us explain the proposed approach to the optimization of the period of checking the utility systems with a theoretical examples.

Theoretical example 1 for mathematical model 1.

Given data.

Time c, necessary for performing the checks and preventive maintenance at the facility with the utility system, is 5 time units. Random period T of the anticipated time of facility operation is determined by the normal probability law with the expectancy m = 100 time units and the average squared displacement σ = 20 time units.

Required:

Find the value of check period x^*, which achieves the minimal value of average overall losses $M(x)$ at the check of the utility system in operational period T for the following values of probability p of faultless performance of the facility in a time unit: 0.999; 0.95 and 0.90.

Solution:

To solve the problem let us use the equation (4). For this purpose for each value of p probability it is necessary to calculate $M(x)$ for an allowed value area of x

The results of calculations, carried out by means of MathCad package, are shown in the graphs in Figure 2. In this case the graph $M_0(x)$ is corresponding to the calculated dependence of $M(x)$ at p = 0.999; and the graphs $M_1(x)$ and $M_2(x)$ at p, that equals 0.95 и 0.90 accordingly.

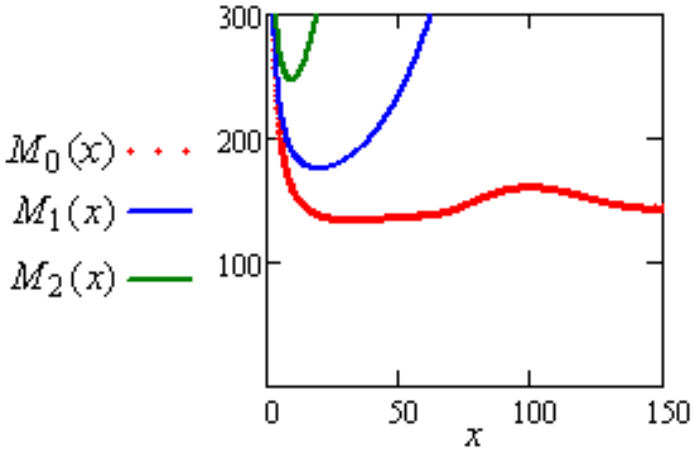

Figure 2. Graphs of functions $M_0(x)$, $M_1(x)$ and $M_2(x)$

Optimal values x^* of the time period x between consecutive checks and preventive maintenance of the utility system for the functions $M_0(x)$, $M_1(x)$ and $M_2(x)$ are 34, 20 and 9 time units accordingly. The corresponding minimal values of $M(x)$ expectancy for the probability p, which equals 0.999; 0.95 and 0.90 (functions $M_0(x)$, $M_1(x)$ и $M_2(x)$) are therefore equal to 134, 176 and 248 time units.

Graph analysis in picture 2 allows the following conclusions:

1) The more reliable is the facility of a utility system (higher probability p of faultless performance), the longer should be the period of checking its operation;

2) Improving the reliability of equipment significantly lowers the overall losses at its operation.

The abovementioned conclusions comply with the intuitive properties of the correlations in question. That also allows the inference that the model represented is conforming to the processes under examination.

Figures 3–6 present the calculated results of auxiliary parameters of the given mathematical model. On the abscissa axis of the first three pictures is plotted the value of the mathematical model. Figure 3 shows the graphs of variations for minimal $M(x, p)$ and optimal periods x^* of checking the operational condition of the utility system. Figure 4 describes the dependence of the second initial moment of check period $\alpha(p)$ on the probability p. Figure 5 presents the graphs of standard deviation of $\Xi(p)$, variability index $\eta(p)$ (magnified by 200 for descriptive purposes) and optimal value $K(p)$ of checks in operational period T depending on the value of p. Figure 6 shows the probability density

Soldatenko V.S., Smagin V.A., Gusenitsa Y.N., Gera V.I., Soldatenko T.N. The method of calculation for the period of checking utility systems. *Magazine of Civil Engineering*. 2017. No. 2. Pp. 72–83. doi: 10.18720/MCE.70.7

$g_i(u)$ for random values u of operational period of a utility system, i = 0, 1, 2 for the base values of probability p of faultless performance of the facility in a time unit.

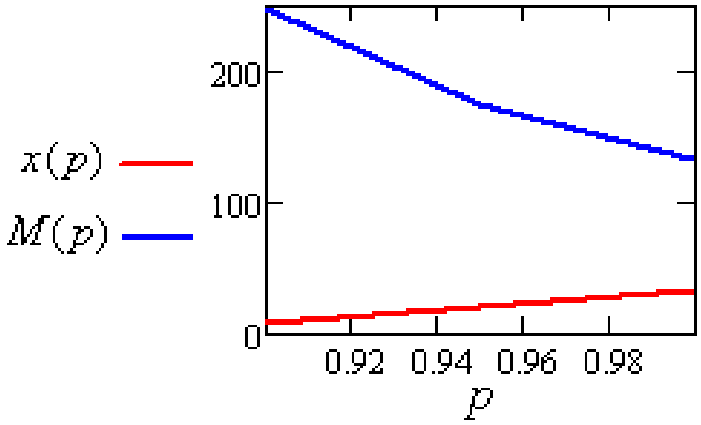

Figure 3. Graphs of variations for $M(x, p)$ and x^* of the facility p

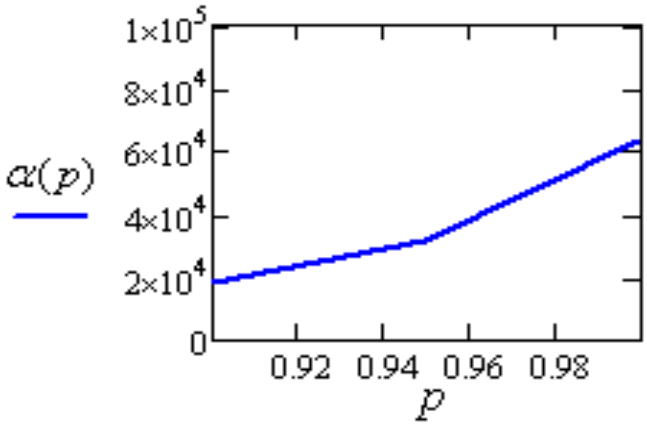

Figure 4. Dependence of the second initial moment of check period for operational condition of the facility p

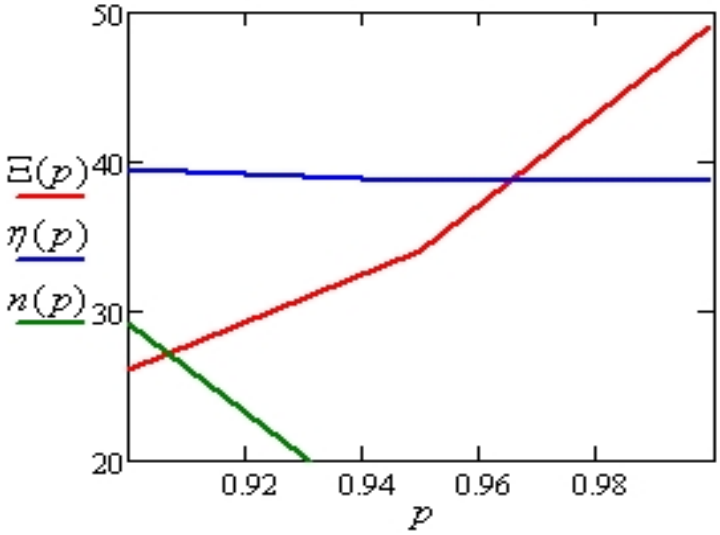

Figure 5. Graphs of standard deviation, variability index, and optimal value of checks

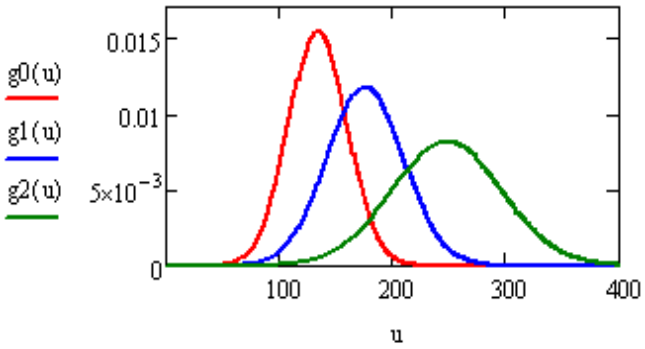

Figure 6. Probability density for random values of operational period of a utility system

Theoretical example 2 for mathematical model 2.

Given data:

Minimal value of $M(x, p, p_{s2})$ can be found at x_0. The duration c of checking the operational condition of the utility system equals 5 time units. The duration c_B of the maintenance equals 100 time units. Random interval T of the estimated time of facility operation is determined by the normal probability law with the mathematical expectancy m = 100 time units and the average squared displacement σ =20 time units. The probability p of the faultless performance of the facility in a time unit equals 0.75.

Required:

Find the value of check period duration x^*, which achieves the minimal value of average overall losses $M(x, p, p_{s2})$ at the check of the utility system in operational period T for the following values of probability p_k of finding a failure at the facility in a time unit: 0.999; 0.75 and 0.50.

Solution:

To solve the problem let us use equation (5). Thus for each value of p_k probability it is necessary to calculate $M(x, p, p_{s2})$ for an allowed area of x.

The results of calculations, carried out by means of MathCad package, are shown in the graphs in figure 7. In this case the graphs of $MT_0(x)$, $MT_1(x)$, $MT_2(x)$ functions are corresponding to the calculated dependence of $M(x, p, p_{s2})$ at p = 0.75 and p_k = 0.999; 0.75; 0.5 accordingly.

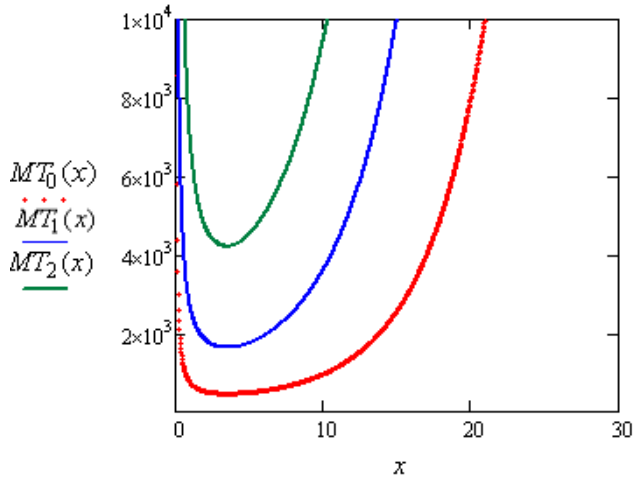

Figure 7. Graphs of $MT_0(x)$, $MT_1(x)$, $MT_2(x)$ functions

Soldatenko V.S., Smagin V.A., Gusenitsa Y.N., Gera V.I., Soldatenko T.N. The method of calculation for the period of checking utility systems. *Magazine of Civil Engineering*. 2017. No. 2. Pp. 72–83. doi: 10.18720/MCE.70.7

Table 1 shows the calculations of $M(x_0)$ – minimal value of average costs for checks and maintenance of the facility in operational period T and x_0 - optimal value of check period for the facility.

Table 1. Results of calculations

Number of model	Parameters	
	$M(x_0)$	x_0
$MT_0(x)$	513	2
$MT_1(x)$	3 803	3
$MT_2(x)$	6 163	4

Theoretical example 3 for mathematical model 3.

Given data:

The data is the same as in example 2. However, three check systems are used.

Required:

Find the value of check period duration x^*, which achieves the minimal value of average overall losses $M(x, p, p_{s3})$ at the check of the utility system in operational period T for the following values of probability p_k of finding a failure at the facility: 0.999; 0.75 and 0.50.

Solution:

To solve the problem let us use the equation (7). Thus for each value of probability p_k it is necessary to calculate $M(x, p, p_{s3})$ for an allowed area of x.

The results of calculations, carried out by means of MathCad package, are shown in the graphs in figure 8. The graphs of $MT_0(x)$, $MT_1(x)$, $MT_2(x)$ functions are corresponding to the calculated dependence of $M(x, p, p_{s3})$ at p = 0.75 and p_k = 0.999; 0.75; 0.5 accordingly.

Figure 8 shows the graphs of $MT_0(x)$, $MT_1(x)$, $MT_2(x)$ functions at p = 0.75 and p_k =0.999; 0.75; 0.5.

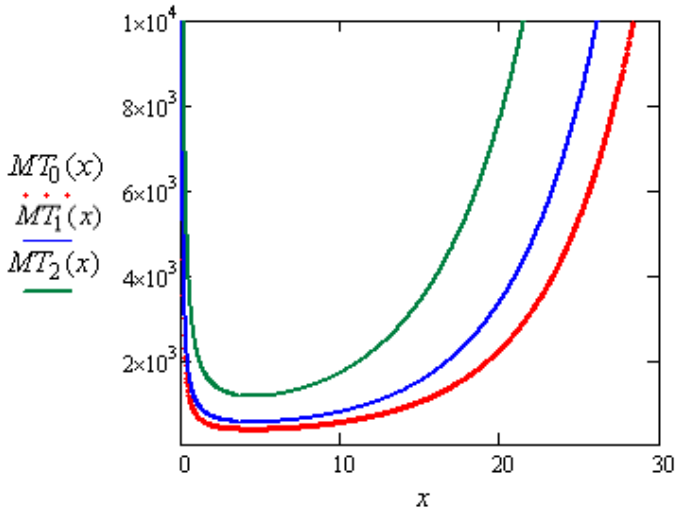

Figure 8. Graphs of $MT_0(x)$, $MT_1(x)$, $MT_2(x)$ functions

Table 2, similar to table 1, presents the results of calculations.

Table 2. Results of calculations

Number of model	Parameters	
	$M(x_0)$	x_0
$MT_0(x)$	498	2
$MT_1(x)$	1 678	3
$MT_2(x)$	4 275	4

Examination of the calculations shows that the majoritary approach is quite efficient for improving the reliability of checking the operational condition of utility systems.

Conclusion

The present work is solving the problem of developing an approach to reasoning an optimal period of checking utility systems. Conducted studies of the results, offered in article allow to receive following conclusions.

1. Optimization of the periods of control on a set of discrete numbers is more adequate to real practice of planning of prevention of utility systems in comparison with the known models.

2. The offered models are based on an assumption about accident of size of an interval of operation of utility systems. It allows to take influence of various factors on work of systems of operation of buildings and constructions into account, which lead to change of the planning between-repairs periods (fig. 2, 7, 8), and also to estimate the accuracy of the received results (Figs. 3–6).

3. In the offered models indicators of non-failure operation of objects of utility systems are entered into consideration (Figs. 2, 7, 8). In the known information models these indicators aren't considered.

4. The offered models consider veracity of operation of control systems of various configuration (Figs. 7, 8, Tables 1, 2). It allows to prove the choice of the corresponding control system and to correct prevention intervals.

The obtained results may be used in the reasoning of advanced utility systems of buildings and constructions, as well as in rationalization of the present utility systems.

References

1. Polovnikov V.YU., Glazyrin E.S. CHislennyj analiz vliyaniya inzhenernyh sooruzhenij na teplovye poteri beskanal'nyh teploprovodov [Numerical analysis of the impact of engineering structures on the channel-free heat loss heat conductors]. *Magazine of Civil Engineering.* 2014. No. 2(46). Pp. 5–13. (rus).
2. Ibrahim O., Fardoun F., Younes R., Louahlia-Gualous H. Review of water-heating systems: general selection approach based on energy and environmental aspects. *Building and Environment.* 2014. Vol. 72. Pp. 259–286.
3. Bovteev S.V., Kanyukova S.V. Development of methodology for time management of construction projects. *Magazine of Civil Engineering*. 2016. No. 2(62). Pp. 102–112.
4. Basok B.I., Bozhko I.K., Nedbajlo A.N., Lysenko O.N. Polivalentnaya sistema teploobespecheniya passivnogo doma na osnove vozobnovlyaemyh istochnikov ehnergii [Polyvalent passive house heating system based on renewable energy sources]. *Magazine of Civil Engineering*. 2015. No. 6(58). Pp. 32–43. (rus).
5. Velichkin V.Z. Upravlenie i nadezhnost realizacii stroitel'nyh programm [Management and reliability of implementation of construction programs]. *Magazine of Civil Engineering*. 2014. No. 7(51). Pp. 74–79. (rus).
6. Soldatenko T.N. Model upravleniya rabotami ehkspluatiruyushchej organizacii po soderzhaniyu

Литература

1. Половников В.Ю., Глазырин Е.С. Численный анализ влияния инженерных сооружений на тепловые потери бесканальных теплопроводов // Инженерно-строительный журнал. 2014. № 2(46). С. 5–13.
2. Ibrahim O., Fardoun F., Younes R., Louahlia-Gualous H. Review of water-heating systems: general selection approach based on energy and environmental aspects. // Building and Environment. 2014. Vol. 72. Pp. 259–286.
3. Bovteev S.V., Kanyukova S.V. Development of methodology for time management of construction projects // Инженерно-строительный журнал. 2016. № 2(62). С. 102–112. (англ.)
4. Басок Б.И., Божко И.К., Недбайло А.Н., Лысенко О.Н. Поливалентная система теплообеспечения пассивного дома на основе возобновляемых источников энергии // Инженерно-строительный журнал. 2015. № 6(58). С. 32–43.
5. Величкин В.З. Управление и надежность реализации строительных программ // Инженерно-строительный журнал. 2014. № 7(51). С. 74–79.
6. Солдатенко Т.Н. Модель управления работами эксплуатирующей организации по содержанию инженерных систем комплекса недвижимости // Инженерно-строительный журнал. 2013. № 2(37). С. 89–103.

Soldatenko V.S., Smagin V.A., Gusenitsa Y.N., Gera V.I., Soldatenko T.N. The method of calculation for the period of checking utility systems. *Magazine of Civil Engineering*. 2017. No. 2. Pp. 72–83. doi: 10.18720/MCE.70.7

inzhenernyh sistem kompleksa nedvizhimosti [Management model of the operating organization for the maintenance of engineering systems of the real estate complex]. *Magazine of Civil Engineering*. 2013. No. 2(37). Pp. 89–103. (rus).

7. Marjyasin O.YU., Kolodkina A.S., Ogarkov A.A. Komp'yuternoe modelirovanie «intellektual'nogo zdaniya» [Computer modeling of «intelligent building»]. *Modeling and Analysis of Information Systems.* 2016. Vol. 23. No. 4(64). Pp. 427–439. (rus).
8. Samarin O.D., Grishneva E.A. Opredelenie optimal'nyh zatrat na upravlenie klimaticheskimi sistemami intellektual'nogo zdaniya [Determination of the optimal management costs climatic systems of intelligent building]. *Magazine of Civil Engineering*. 2012. No. 6 (32). Pp. 60-63. (rus).
9. Campisano A., Modica C., Creaco E. Application of real-time control techniques to reduce water volume discharges from quality-oriented CSO devices. *Journal of Environmental Engineering, ASCE*. 2016. Vol. 42. No. 1. Pp. 12–18.
10. Absalyamov D.R. Povyshenie nadezhnosti inzhenernyh sistem metodom formalizacii poiska otkazov [Improving the reliability of engineering systems by formalizing bounce search]. *Magazine of Civil Engineering*. 2012. No. 2(28). Pp. 39-47. (rus)
11. 11. Soldatenko T.N. Model ostatochnogo resursa inzhenernyh sistem s vysokim urovnem iznosa [Model of a residual resource of engineering systems with the high level of wear]. *Magazine of Civil Engineering*. 2012. No. 6. Pp. 64–72. (rus)
12. Bilalov A.B., Shilyaev D.V., Petrochenkov A.B., Bilous O.A., Habibrahmanova F.R. Vnedrenie avtomatizirovannoj sistemy upravleniya teplovym punktom [Implementation of an automated thermal point control system]. *Fundamental Research.* 2015. No. 8(1). Pp. 87–92. (rus).
13. Liu K.F.R. A possibilistic Petri net model for diagnosing cracks in RC structures. *Computer-Aided Civil and Infrastructure Engineering.* 2003. Vol. 18. Pp. 426–439.
14. Matushkin N.N., YUzhakov A.A. Opredelenie emkostno-vremennyh harakteristik avtomatizirovannoj sistemy kontrolya i dispetcherskogo upravleniya inzhenernym oborudovaniem zdaniya [Definition capacitive-time characteristics of the automated control system and supervisory control BMS]. *Journal of the Kazan State Technical University after named A.N. Tupolev.* 2010. No. 4. Pp. 151–154. (rus)
15. Shprekher D.M., Babokin G.I., Kolesnikov E.B. Sistema nejrosetevogo kontrolya i prognozirovaniya tekhnicheskih sostoyanij ehlektromekhanicheskih sistem [Neural network system monitoring and forecasting technical states of electromechanical systems]. *Proceedings of the II International Scientific and Technical Conference South Ural State University (National Research University).* 2016. Pp. 328–332. (rus)
16. Baranovsky A.M., Privalov A.E. Sistema kontrolja i diagnostirovanija bortovogo oborudovanija malogo kosmicheskogo apparata [Monitoring and diagnosis system on-board equipment of small spacecraft]. *Journal of Instrument Engineering.* 2009. Vol. 52. No. 4. Pp. 51–56. (rus)
17. Berketov G.A., Mikryukov A.A., Fedoseev S.V. Optimizaciya parametrov kontrolya i vosstanovleniya tekhnicheskih sistem [Optimization of control parameters and restore technical systems]. *Innovacii na osnove informacionnyh i kommunikacionnyh tehnologij*. 2011. No. 1. Pp. 202–204. (rus)
18. Tyurin M.V. Matematicheskie modeli sostoyaniya sistem monitoringa i kontrolya tekhnicheski slozhnyh objektov nazemnoj infrastruktury [Mathematical models of condition monitoring and control systems are technically complex objects of ground infrastructure]. *Sovremennye*
7. Марьясин О.Ю., Колодкина А.С., Огарков А.А. Компьютерное моделирование «интеллектуального здания» // Моделирование и анализ информационных систем. 2016. Т. 23. № 4(64). С. 427–439.
8. Самарин О.Д., Гришнева Е.А. Определение оптимальных затрат на управление климатическими системами интеллектуального здания // Инженерно-строительный журнал. 2012. № 6(32). С. 60–63.
9. Campisano A., Modica C., Creaco E. Application of real-time control techniques to reduce water volume discharges from quality-oriented CSO devices/ // Journal of Environmental Engineering, ASCE. 2016. Vol. 42. № 1. Pp. 12–18.
10. Абсалямов Д.Р. Повышение надежности инженерных систем методом формализации поиска отказов // Инженерно-строительный журнал. 2012. № 2(28). С. 39–47.
11. Солдатенко Т.Н. Модель остаточного ресурса инженерных систем с высоким уровнем износа // Инженерно-строительный журнал. 2012. № 6. С. 64–72.
12. Билалов А.Б., Шиляев Д.В., Петроченков А.Б., Билоус О.А., Хабибрахманова Ф.Р. Внедрение автоматизированной системы управления тепловым пунктом // Фундаментальные исследования. 2015. № 8(1). С. 87–92.
13. Liu K.F.R. A possibilistic Petri net model for diagnosing cracks in RC structures // Computer-Aided Civil and infrastructure Engineering. 2003. Vol. 18. Pp. 426–439.
14. Матушкин Н.Н., Южаков А.А. Определение емкостно-временных характеристик автоматизированной системы контроля и диспетчерского управления инженерным оборудованием здания // Вестник казанского государственного технического университета им. А.Н. Туполева. 2010. № 4. С. 151–154.
15. Шпрехер Д.М., Бабокин Г.И., Колесников Е.Б. Система нейросетевого контроля и прогнозирования технических состояний электромеханических систем // ПРОМ-ИНЖИНИРИНГ. Труды II международной научно-технической конференции. ФГБОУ ВПО «Южно-Уральский государственный университет» (национальный исследовательский университет). Челябинск: Издательский центр ЮУрГУ, 2016. С. 328–332.
16. Барановский А.М., Привалов А.Е. Система контроля и диагностирования бортового оборудования малого космического аппарата // Известия высших учебных заведений. Приборостроение. 2009. Т. 52. № 4. С. 51–56.
17. Беркетов Г.А., Микрюков А.А., Федосеев С.В. Оптимизация параметров контроля и восстановления технических систем // Инновации на основе информационных и коммуникационных технологий. 2011. № 1. С. 202–204.
18. Тюрин М.В. Математические модели состояния систем мониторинга и контроля технически сложных объектов наземной инфраструктуры // Современные информационные технологии. 2012. № 15. С. 11–15.
19. Еременко В.Т., Тютякин А.В., Кондрашин А.А. Выбор профилей обработки данных в системах контроля и диагностики технических объектов на основе их качественного анализа // Информационные системы и технологии. 2014. № 5(85). С. 88–97.
20. Кузнецов А.Б., Осипов Н.А., Дорожко И.В. Методика диагностирования автоматизированных систем управления сложными объектами с использованием априорной информации // Известия высших учебных заведений. Приборостроение. 2013. Т. 56. № 1. С. 18.
21. Мануйлов Ю.С., Мышко В.В., Кравцов А.Н., Ткаченко В.В. Основные принципы решения задач анализа технического состояния бортовых систем

Солдатенко В.С., Смагин В.А., Гусеница Я.Н., Гера В.И., Солдатенко Т.Н. Метод расчета периода контроля оборудования инженерно-технических систем // Инженерно-строительный журнал. 2017. № 2(70). С. 72–83.

informacionnye tehnologii. 2012. No. 15. Pp. 11–15. (rus)

19. Eremenko V.T., Tyutyakin A.V., Kondrashin A.A. Vybor profilej obrabotki dannyh v sistemah kontrolya i diagnostiki tekhnicheskih objektov na osnove ih kachestvennogo analiza [Selecting data profiles in the systems of control and diagnostics of technical objects on the basis of qualitative analysis]. *Information Systems and Technologies.* 2014. No. 5(85). Pp. 88–97. (rus)
20. Kuznetsov A.B., Osipov, N.A., Dorozhko I.V. Metodika diagnostirovaniya avtomatizirovannyh system upravleniya slozhnymiobektami s ispolzovaniem apriornoj informacii [Methods of diagnosing of the automated control systems of complex objects using a priori information]. *Journal of Instrument Engineering.* 2013. Vol. 56. No. 1. Pp. 18–26. (rus)
21. Manuilov Y.S., Myshko V.V., Kravtsov A.N., Tkachenko V.V. Osnovnye principy resheniya zadach analiza tekhnicheskogo sostoyaniya bortovyh system kosmicheskogo apparata [Basic principles for solving the technical problems of analysis status onboard spacecraft systems]. *Proceedings of the Military Space Academy named after A.F.Mozhaiskogo.* 2011. No. 631. Pp. 63–70. (rus)
22. Prorok V.Y., Gusenitsa Y.N., Petric D.O. Postroenie sistemy kontrolya i diagnostirovaniya avtomatizirovannyh system upravleniya specialnogo naznacheniya na osnove nechetkih iskusstvennyh nejronnyh setej [Building control systems and automated diagnostics Special purpose control systems based on fuzzy artificial neural networks]. *T-Comm: Telecommunications and Transport.* 2013. Vol. 7. No. 6. Pp. 67–70. (rus)
23. Senchenkov V.I., Absalyamov D.R. Vybor minimalnogo mnozhestva kontroliruemyh priznakov dlya opredeleniya tekhnicheskogo sostoyaniya sistemy [Selection of the minimal set of controlled factors to determine system technical state]. *Journal of Instrument Engineering.* 2011. Vol. 54. No. 3. Pp. 5–10. (rus)
24. Hopfe C.J., Augenbroe G.L.M., Hensen J.L.M. Multi-criteria decision making under uncertainty in building performance assessment. Building and Environment. 2013. Vol. 69. Pp. 81–90.
25. Sotnikov A.G. Analiticheskaya metodika opredeleniya naruzhnyh raschetnyh parametrov v sistemah mikroklimata zdanij [Analytical method of determining the exterior design parameters in buildings Climate systems]. *Magazine of Civil Engineering*. 2013. No. 2(37). Pp. 3–12. (rus)
26. Dmitriev A.K., Kopkin E.V. Optimization of network structures for diagnostics of technical objects on the basis of the Pontryagin maximum principle. *Automatic Control and Computer Sciences.* 2005. Vol. 38. No. 5. Pp. 1–15.
27. Kim Y.W., Kim S.C. Cost analysis of information technology-assisted quality inspection using activity-based costing. *Construction Management & Economics.* 2011. Vol. 29. No. 2. Pp. 163–172.
28. Krack M., Panning-von Scheidt L., Wallaschek J. On the computation of the slow dynamics of nonlinear modes of mechanical systems. *Mechanical Systems and Signal Processing.* 2014. Vol. 42. No. 1–2. Pp. 71–87.
29. Rohani M., Afshar M.H. GA–GHCA model for the optimal design of pumped sewer networks. *Canadian Journal of Civil Engineering.* 2016. Vol. 42. No. 1. Pp. 1–12.
30. Schmidt M., Steinbach M.C., Willert B.M. High detail stationary optimization models for gas networks. *Optimization and Engineering.* 2015. Vol. 16. No. 1. Pp. 131–164.
31. Shprekher D.M., Matveev Yu.N., Bogatikov V.N. Model of recognition of technical condition of electromechanical systems based on parallel classification schemes with excessive number of computing elements. *International Journal of Engineering Research*. 2015. Vol. 9. No. 24.

космического аппарата // Труды Военно-космической академии имени А.Ф. Можайского. 2011. № 631. С. 63–70.

22. Пророк В.Я., Гусеница Я.Н., Петрич Д.О. Построение системы контроля и диагностирования автоматизированных систем управления специального назначения на основе нечетких искусственных нейронных систем // T-Comm: Телекоммуникации и транспорт. 2013. Т. 7. № 6. С. 67–70.
23. Сеньченков В.И., Абсалямов Д.Р. Выбор минимального множества контролируемых признаков для определения технического состояния системы // Известия высших учебных заведений. Приборостроение. 2011. Т. 54. № 3. С. 5–10.
24. Hopfe C.J., Augenbroe G.L.M., Hensen J.L.M. Multi-criteria decision making under uncertainty in building performance assessment. // Building and Environment. 2013. Vol. 69. Pp. 81–90.
25. Сотников А.Г. Аналитическая методика определения наружных расчетных параметров в системах микроклимата зданий // Инженерно-строительный журнал. 2013. № 2(37). С. 3–12.
26. Dmitriev A.K., Kopkin E.V. Optimization of network structures for diagnostics of technical objects on the basis of the Pontryagin maximum principle // Automatic Control and Computer Sciences. 2005. Vol. 38. № 5. Pp. 1–15.
27. Kim Y.W., Kim S.C. Cost analysis of information technology-assisted quality inspection using activity-based costing // Construction Management & Economics. 2011. Vol. 29. № 2. Pp. 163–172.
28. Krack M., Panning-von Scheidt L., Wallaschek J. On the computation of the slow dynamics of nonlinear modes of mechanical systems // Mechanical Systems and Signal Processing. 2014. Vol. 42. № 1–2. Pp. 71–87.
29. Rohani M., Afshar M.H. GA–GHCA model for the optimal design of pumped sewer networks // Canadian Journal of Civil Engineering. 2016. Vol. 42. № 1. Pp. 1–12.
30. Schmidt M., Steinbach M.C., Willert B.M. High detail stationary optimization models for gas networks // Optimization and Engineering. 2015. Vol. 16. № 1. Pp. 131–164.
31. Shprekher D.M., Matveev Yu.N., Bogatikov V.N. Model of recognition of technical condition of electromechanical systems based on parallel classification schemes with excessive number of computing elements // International Journal of Engineering Research. 2015. Vol. 9. № 24. Pp. 45703–45716.
32. Simão M., Ramos H.M., Mora-Rodriguez J. Computational dynamic models and experiments in the fluid–structure interaction of pipe systems. // Canadian Journal of Civil Engineering. 2016. Vol. 43. № 1. Pp. 60–72.
33. Арутюнян А.Р., Арутюнян Р.А. Коррозионный рост трещин и усталостная прочность сложных технических систем // Инженерно-строительный журнал. 2013. № 9(44). С. 42–48.
34. Марков А.С., Рауткин Ю.В. К вопросу об анализе стратегий периодического контроля технических систем // Труды Научно-исследовательского института радио. 2012. № 1. С. 85–90.
35. Шибанов Г.П. Оптимизация процесса контроля бортовых комплексов оборудования летательных аппаратов // Мехатроника, автоматизация, управление. 2014. № 6. С. 56–61.
36. Smagin V.A. Optimum likelihood quantization of the information in space with restriction of zones of influence of quanta // Forum B.V. Gnedenko. RT&A. 2014. Vol.9. № 01(31). Pp. 92–97.
37. Smagin V.A., Novikov A.N., Smagin S.Yu. A probabilistic model of the control of technical systems // Automatic Control and Computer Sciences. 2010. Vol. 44. № 6.

Soldatenko V.S., Smagin V.A., Gusenitsa Y.N., Gera V.I., Soldatenko T.N. The method of calculation for the period of checking utility systems. *Magazine of Civil Engineering*. 2017. No. 2. Pp. 72–83. doi: 10.18720/MCE.70.7

Pp. 45703–45716.

32. Simão M., Ramos H.M., Mora-Rodriguez J. Computational dynamic models and experiments in the fluid–structure interaction of pipe systems. *Canadian Journal of Civil Engineering.* 2016. Vol. 43. No. 1. Pp. 60–72.
33. Arutyunyan A.R., Arutyunyan R.A. Korrozionnyj rost treshchin i ustalostnaya prochnost' slozhnyh tekhnicheskih sistem [The corrosion crack growth and fatigue strength of complex technical systems]. *Magazine of Civil Engineering*. 2013. No. 9(44). Pp. 42–48. (rus)
34. Markov A.S., Rautkin YU.V. K voprosu ob analize strategij periodicheskogo kontrolya tekhnicheskih sistem [On the question of analyzing the strategies for periodic monitoring of technical systems]. *Proceedings of the Scientific-Research Institute of Radio.* 2012. No. 1. Pp. 85–90. (rus)
35. Shibanov G.P. Optimizatsiya protsessa kontrolya bortovyih kompleksov oborudovaniya letatelnyih apparatov [Optimization of process of control of onboard complexes of the equipment of aircraft]. *Mechatronics, Automation, Control.* 2014. No. 6. Pp. 56–61. (rus)
36. Smagin V.A. Optimum likelihood quantization of the information in space with restriction of zones of influence of quanta. *Forum B.V. Gnedenko, RTSA*. 2014. No. 01(31). Pp. 92–97.
37. Smagin V.A., Novikov A.N., Smagin S.Yu. A probabilistic model of the control of technical systems. *Automatic Control and Computer Sciences.* 2010. Vol. 44. No. 6. Pp. 324–329.

Pp. 324–329.

Vladimir Soldatenko,
+7(911)9256841; soldatenko_vs@mail.ru

Vladimir Smagin,
+7(812)2352778; va_smagin@mail.ru

Yaroslav Gusenitsa,
+7(981)8315029; Yaromir226@mail.ru

Vasiliy Gera,
+7(911)8334113; geratv33@mail.ru

Tamara Soldatenko,
+7(911)9545688; soldatenko-tn@bk.ru

Владимир Стальевич Солдатенко,
+7(911)9256841;
эл. почта: soldatenko_vs@mail.ru

Владимир Александрович Смагин,
+7(812)2352778; эл. почта: va_smagin@mail.ru

Ярослав Николаевич Гусеница,
+7(981)8315029; эл. почта: Yaromir226@mail.ru

Василий Иосифович Гера,
+7(911)8334113; эл. почта: geratv33@mail.ru

Тамара Николаевна Солдатенко,
+7(911)9545688; эл. почта: soldatenko-tn@bk.ru

Солдатенко В.С., Смагин В.А., Гусеница Я.Н., Гера В.И., Солдатенко Т.Н. Метод расчета периода контроля оборудования инженерно-технических систем // Инженерно-строительный журнал. 2017. № 2(70). С. 72–83.

doi: 10.18720/MCE.70.8

Hysteretic water-retention capacity of sandy soil

Гистерезис водоудерживающей способности почвы на примере песчаных почв

V.V. Terleev,
A.O. Nikonorov,
I. Togo,
Yu.V. Volkova,
R.S. Ginevsky,
V.A. Lazarev,
E.R. Khamzin,
Peter the Great St. Petersburg Polytechnic University, St. Petersburg, Russia
V.V. Garmanov,
St.Petersburg State Agrarian University, St. Petersburg, Russia
W. Mirschel,
Leibniz-Centre for Agricultural Landscape Research, Müncheberg, Germany
L.I. Akimov,
Peter the Great St. Petersburg Polytechnic University, St. Petersburg, Russia

Д-р с.-хоз. наук, профессор В.В. Терлеев,
аспирант А.О. Никоноров,
канд. техн. наук, заведующий кафедрой И. Того,
канд. техн. наук, доцент Ю.В. Волкова,
студент Р.С. Гиневский,
студент В.А. Лазарев,
студент Э.Р. Хамзин,
Санкт-Петербургский политехнический университет Петра Великого, г. Санкт-Петербург, Россия
канд. экон. наук, доцент В.В. Гарманов,
Санкт-Петербургский государственный аграрный университет, г. Санкт-Петербург, г. Пушкин, Россия
д-р с.-хоз. наук, профессор В. Миршель,
Leibniz-Centre for Agricultural Landscape Research, Müncheberg, Germany
студент Л.И. Акимов,
Санкт-Петербургский политехнический университет Петра Великого, г. Санкт-Петербург, Россия

Key words: soil; water-retention capacity; hysteresis; reversal points; scanning curves; approximation accuracy; “pump effect”, parameters identifying; model verification

Ключевые слова: почва; водоудерживающая способность почвы; гистерезис; поворотные точки; сканирующие кривые; точность аппроксимации; эффект «помпы»; идентификация параметров; верификация модели

Abstract. Before the construction project, it is necessary to investigate the hydrological conditions of territory. For this purpose some hydrophysical indicators of the soil should be measured. Among the most important indicators is the water-retention capacity. It is convenient to use a physically justified model to research sorption-desorption properties of soil with respect to moisture. The authors have investigated the mathematical model, which was developed to describe the hysteresis of water-retention capacity. The computer program “HYSTERESIS” was been used to implement this research. Three computational experiments were carried out with the use of this program. The results allow improving the accuracy of calculating the dynamics of soil moisture. The results of the research could be applied to the agricultural research, hydrological conditions investigations and other area of knowledge.

Аннотация. Перед началом проектирования строительства необходимо исследовать гидрологические условия территории. Для этого необходимо измерить некоторые гидрофизические показатели почвы. Среди наиболее важных показателей – водоудерживающая способность. Целесообразно использовать физически-обоснованную модель для исследования сорбционно-десорбционных свойств почвы по отношению к влаге. Авторы исследовали математическую модель, которая была разработана для описания гистерезиса водоудерживающей способности. Для реализации этого исследования была использована компьютерная программа «HYSTERESIS». С помощью этой программы было проведено три вычислительных эксперимента. Полученные результаты позволяют повысить точность расчета

Terleev V.V., Nikonorov A.O., Togo I., Volkova Yu.V., Ginevsky R.S., Lazarev V.A., Khamzin E.R., Garmanov V.V., Mirschel W., Akimov L.I. Hysteretic water-retention capacity of sandy soil. *Magazine of Civil Engineering*. 2017. No. 2. Pp. 84–92. doi: 10.18720/MCE.70.8

динамики влажности почвы. Результаты исследования могут быть применены к сельскохозяйственным исследованиям, исследованиям гидрологических условий.

Introduction

There is a need for different soil properties modelling, such as water-retention capacity, for various engineering purposes, especially in urban environmental engineering. Water-retention capacity (WRC) of soil is described by a functional dependence of volumetric water content θ ($cm^3 \cdot cm^{-3}$) on capillary pressure (capillary-sorption potential) of moisture ψ (cm H_2O). There are number of problems for the WRC models, such as:

- accounting the hysteresis phenomena during the physical justification and mathematical formulation of the WRC function;
- difficulties during the construction of scanning curves of hysteretic WRC loop, starting from reversal points.

Taking into account the hysteresis phenomena, some extension of the approach proposed by Kosugi [1–4] is developed [5–8]. There the WRC function and its approximation are suggested. This function describes a main drying curve (MDC), a main wetting curve (MWC) and also scanning curves of the hysteretic WRC [5–8].

The purposes of the work are: 1) evaluation of accuracy approximation to WRC function on examples of MDC and MWC; 2) proof on the absence of "pump effect" for hysteretic WRC model; 3) verification of this model using the measured data on sandy soil.

Method

Considering the soil as a capillary-porous media, the physical and statistical description for the hysteresis of water-retention capacity is offered. It is represented in the form of relations:

$$\begin{cases} \theta = \begin{cases} \theta_r + ((\theta_s - \theta_r)/2)\operatorname{erfc}\left(\left(n_d\sqrt{\pi}/4\right)\ln\left(-\alpha_d(\psi-\psi_{ae})\right)\right), \psi < \psi_{ae}; \\ \theta_s, \psi \geq \psi_{ae}; \end{cases} & (1a) \\ \theta \approx \begin{cases} \theta_r + (\theta_s - \theta_r)/\left(1+\left(-\alpha_d(\psi-\psi_{ae})\right)^{n_d}\right), \psi < \psi_{ae}; \\ \theta_s, \psi \geq \psi_{ae}; \end{cases} & (1b) \end{cases}$$

$$\begin{cases} \theta = \begin{cases} \theta_r + ((\theta_s - \theta_r)/2)\operatorname{erfc}\left(\left(n_w\sqrt{\pi}/4\right)\ln\left(-\alpha_w(\psi-\psi_{we})\right)\right), \psi < \psi_{we}; \\ \theta_s, \psi \geq \psi_{we}; \end{cases} & (2a) \\ \theta \approx \begin{cases} \theta_r + (\theta_s - \theta_r)/\left(1+\left(-\alpha_w(\psi-\psi_{we})\right)^{n_w}\right), \psi < \psi_{we}; \\ \theta_s, \psi \geq \psi_{we}, \end{cases} & (2b) \end{cases}$$

where ψ_{ae} – capillary pressure of moisture, is interpreted as a "pressure of air entrance" on drainage isotherm (cm H_2O), $\psi_{ae} \leq 0$;

ψ_{we} – capillary pressure of moisture, is interpreted as a "pressure of water entrance" on the moistening isotherm (cm H_2O), $\psi_{we} \geq \psi_{ae}$;

θ_s – saturated volumetric water content ($cm^3 \cdot cm^{-3}$);

θ_r – minimum specific volume of liquid water in the soil ($cm^3 \cdot cm^{-3}$);

α_d (cm H_2O^{-1}), n_d, α_w (cm H_2O^{-1}), n_w - appropriate to drainage and moistening physically interpreted parameters.

These parameters can be estimated by the formulae:

$$\alpha_d = r_{0,d}/\beta,\ n_d = 4/\left(\sigma_d\sqrt{2\pi}\right),\ \alpha_w = r_{0,w}/\beta \text{ and } n_w = 4/\left(\sigma_w\sqrt{2\pi}\right),$$

Терлеев В.В., Никоноров А.О., Того И., Волкова Ю.В., Гиневский Р.С., Лазарев В.А., Хамзин Э.Р., Гарманов В.В., Миршель В., Акимов Л.И. Гистерезис водоудерживающей способности почвы на примере песчаных почв. 2017. № 2(70). С. 84–92.

where $r_{0,d}$ and $r_{0,w}$ - appropriate to drainage and moistening values of the effective soil pore radii, which correspond to the most probable values of the normally distributed random variable - the natural logarithm of effective soil pore radii;

σ_d and σ_w - appropriate to drainage and moistening values of random variable standard deviation - the natural logarithm of effective soil pore radii;

$\beta = 2\gamma \cos\varphi/(g\rho_w)$ (where: γ - surface tension of water at the interface with air; ρ_w - water density; φ - contact angle of the surface of soil particles with water; g - gravity acceleration); it is estimated as follows: β = 0.149·10-4 m^2 [3, 4, 9, 10].

The relations (1a) и (2a) respectively describe MDC and MWC of the hysteretic WRC loop. The relations (1b) и (2b) respectively describe approximations to MDC and MWC in the class of elementary functions. Further, these approximations are recognized to describe the scanning curves of hysteretic WRC.

The drying scanning curves, starting from the reversal point (which is characterized by ψ_i and θ_i the values), are described by the system of relations:

$$\begin{cases} \left[\begin{array}{l} \theta = \theta_r + \left(\theta_s^* - \theta_r\right) \Big/ \left(1 + \left(-\alpha_d\left(\psi - \psi_{ae}\right)\right)^{n_d}\right), \\ \theta_s^* = \theta_s,\ \psi_{ae} < \psi_{we} \le \psi_i,\ \psi < \psi_{ae}; \\ \theta_s^* = \theta_i,\ \psi_{ae} \le \psi_i \le \psi_{we},\ \psi < \psi_{ae}; \\ \theta_s^* = \theta_i + \left(\theta_i - \theta_r\right)\left(-\alpha_d\left(\psi_i - \psi_{ae}\right)\right)^{n_d},\ \psi_i < \psi_{ae} \le \psi_{we},\ \psi \le \psi_i; \end{array}\right. \\ \left[\begin{array}{l} \theta = \theta_s,\ \psi_{ae} < \psi_{we} \le \psi_i,\ \psi_{ae} \le \psi \le \psi_i; \\ \theta = \theta_i,\ \psi_{ae} \le \psi_i \le \psi_{we},\ \psi_{ae} \le \psi \le \psi_i. \end{array}\right. \end{cases} \quad (3a)$$

The wetting scanning curves, starting from the reversal point (which is characterized by ψ_j and θ_j values), are described by the system of relations:

$$\begin{cases} \left[\begin{array}{l} \theta = \theta_r^* + \left(\theta_s - \theta_r^*\right) \Big/ \left(1 + \left(-\alpha_w\left(\psi - \psi_{we}\right)\right)^{n_w}\right), \\ \theta_r^* = \theta_j = \theta_r,\ \psi_j << \psi_{ae}, \psi_j \le \psi < \psi_{we}; \\ \theta_r^* = \theta_j - \left(\theta_s - \theta_j\right)\left(-\alpha_w\left(\psi_j - \psi_{we}\right)\right)^{-n_w},\ \psi_j < \psi_{ae}, \psi_j \le \psi < \psi_{we}; \end{array}\right. \\ \left[\begin{array}{l} \theta = \theta_s,\ \psi_j < \psi_{ae}, \psi_{we} \le \psi; \\ \theta = \theta_j = \theta_s,\ \psi_{ae} \le \psi_j, \psi_j \le \psi. \end{array}\right. \end{cases} \quad (3b)$$

Results and Discussion

Approximation. On the base of hysteretic WRC model, which was described by relations (3a) and (3b), a computer program “HYSTERESIS” is developed [5]. This program was used to carry out some computational experiments with the hysteretic WRC model. The scenario for variation of the capillary pressure of soil moisture was formed before the start of the experiment in a specific text file with the data source (*.exd). By means of the program “HYSTERESIS” and applying the Levenberg-Marquardt algorithm [11, 12], the hydrophysical parameters for MDC and MWC have been identified. For this purpose it were used the measured WRC data on sandy soil [13].

Then computer program “HYSTERESIS” was used to calculate the θ values for every measured ψ value on MDC and MWC (Fig. 1).

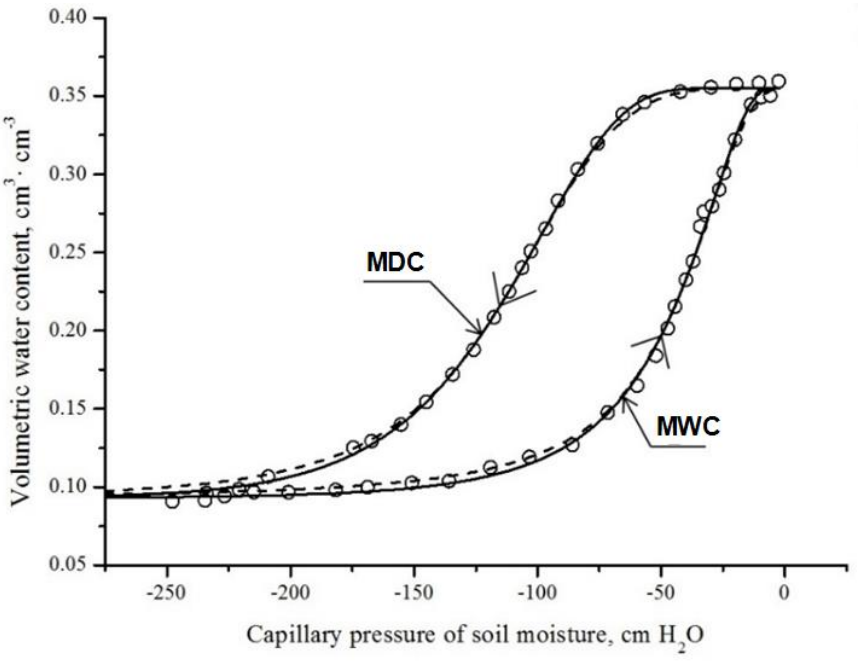

Figure 1. The main hysteretic WRC loop

On the Figure 1 solid lines correspond to the WRC function, describing be relations (1a) and (2a) respectively; dashed lines correspond to approximation for WRC function; circles – measured data. The correlation coefficient between calculated θ values and measured data on MDC and MWC is $R = 0.999$.

Absence of “pump effect”.The internal WRC loops do not go beyond the main drying and wetting curves and approach the previous loops in the process of capillary moisture pressure oscillation (Fig. 2). Therefore, “pump effect” is not manifested in this model.

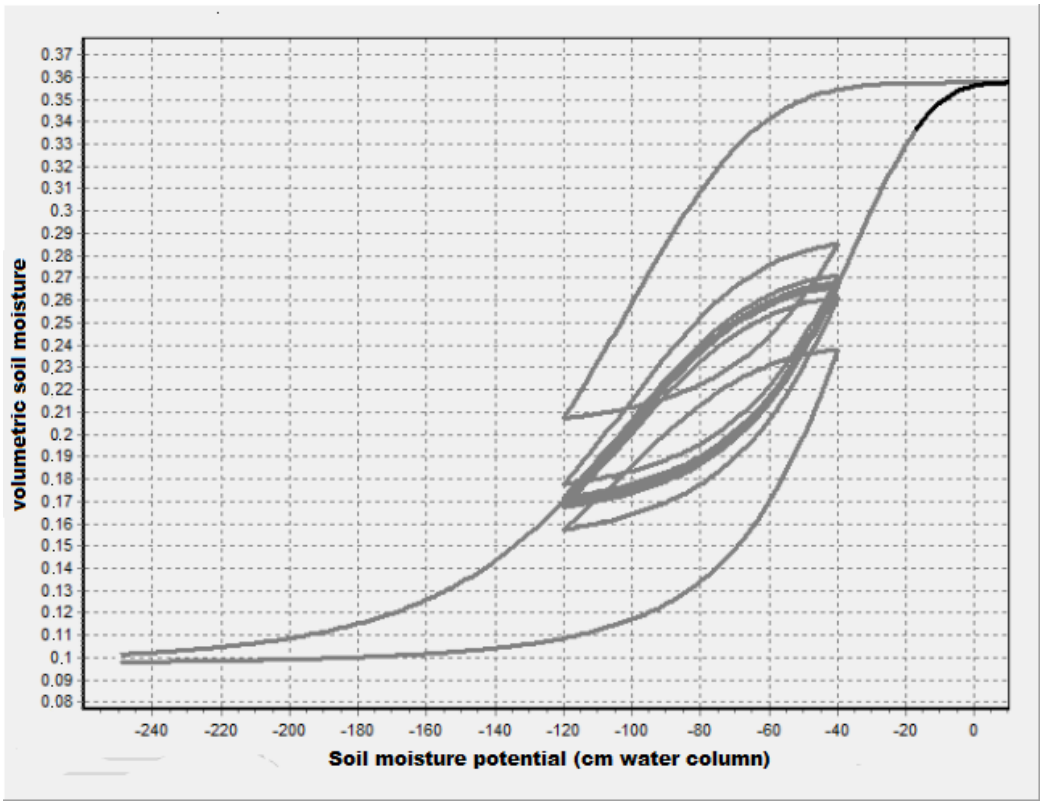

Figure 2. The sequence of the WRC hysteresis loop under the oscillation of the capillary pressure of soil moisture

Терлеев В.В., Никоноров А.О., Того И., Волкова Ю.В., Гиневский Р.С., Лазарев В.А., Хамзин Э.Р., Гарманов В.В., Миршель В., Акимов Л.И. Гистерезис водоудерживающей способности почвы на примере песчаных почв. 2017. № 2(70). С. 84–92.

Verification of WRC model.Using the parameters (identified according to the measured data on MDC and MWC), the θ values for primary drying curve (PDC) and secondary wetting curve (SWC) of the hysteretic WRC have been predicted. Among the parameters of the program the value bubbling pressure ψ_{ae} on MDC had been previously zeroed, because this value (based on the physical representations) cannot be positive, and the corresponding experimental data are not available. The predicted θ values are compared with the measured WRC data. On Figure 3 black dots connected by a continuous curve shows MDC, MWC, PDC and SWC of the hysteresis loop: ψ values plotted on the horizontal axis, θ values - on the vertical axis; red dots shows the measured WRC data. According to the theoretical (predicted) and experimental (measured) ordinates (θ values) for PDC and SWC of WRC hysteresis loop the correlation coefficient $R = 0.995$ was calculated. This coefficient suggests about the high predictive (extrapolating) accuracy of investigated hysteretic WRC model for sandy soils.

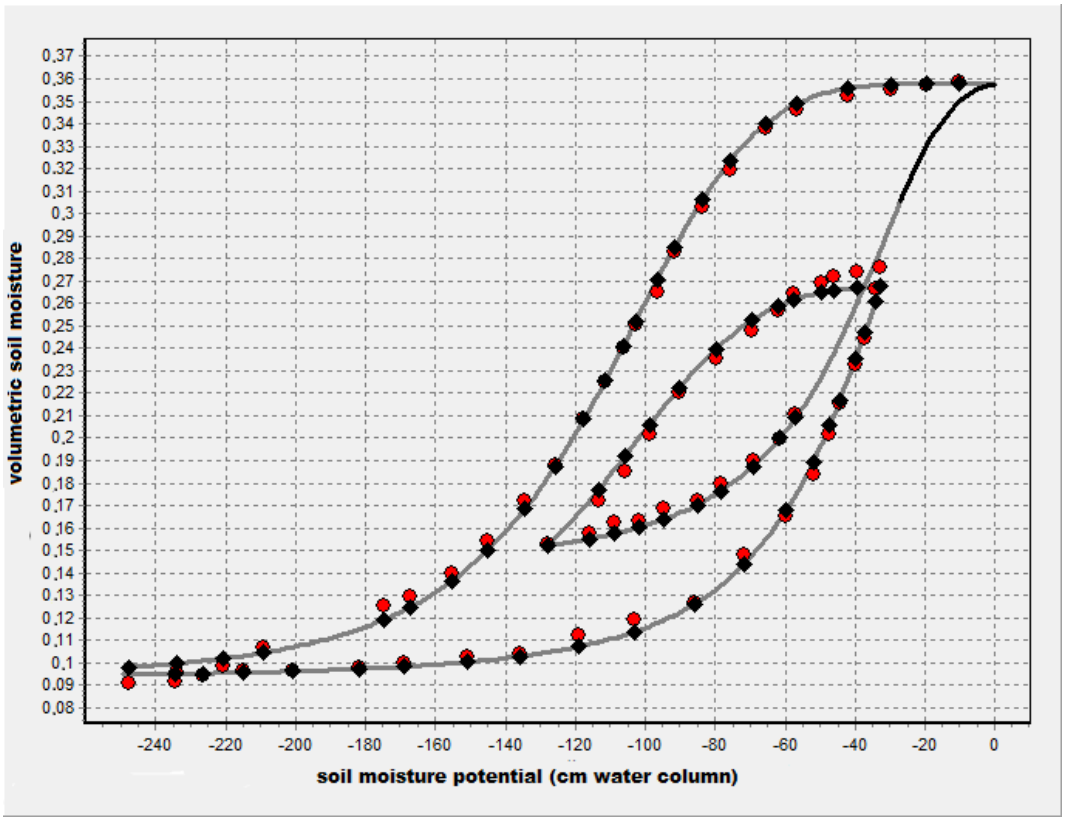

Figure 3. Predicting the internal WRC hysteretic loop formed by the primary drying and secondary wetting curves

On Figure 4 the comparison of the predicted values of volumetric water content with the measured data is represented: here black dots on 1:1 line shows the high convergence of the simulation results and data of the direct measurements (the measured data [13–17] are on the horizontal axis; the computational results are on the vertical axis).

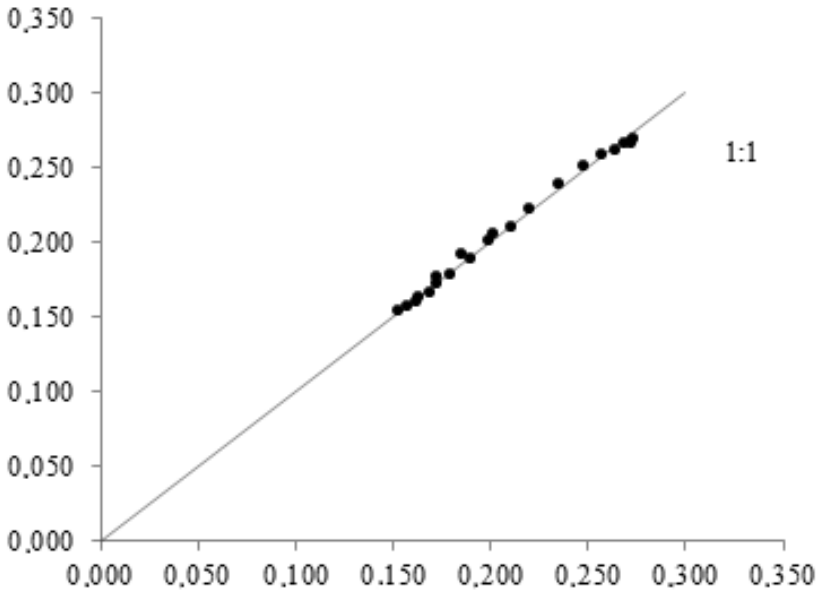

Figure 4. Comparison of the predicted values of volumetric water content with the measured data

Estimates of the scanning curves of the hysteresis loop are important to improve the accuracy of calculating the dynamics of soil moisture [18, 19]. The results of these calculations are used to forecasting the crop yield [20–24], to study the hydrological conditions of the area in the design of irrigation and drainage systems, underground constructions and artificial foundation based on weak soils. In addition, evaluation of the scanning curves are of great importance in the calculating the precision irrigation rates [5] to reduce the wastage of irrigation water, to prevent the removal of agricultural chemicals beyond the root layer of soil and subsequent eutrophication of water bodies, as well as to provide rational use of water resources in general. Soil-hydrophysical investigations and hydrological calculations are also significant for the bank protection tasks [25–27], drainage problems [28, 29], marine works [30, 31], hydropower protection [32], urban ecological, environmental and economical challenges [33, 34]; it helps to find the effective engineering solution based on knowledge of the hydrophysical properties of soils. All these factors indicate the encouraging prospects for the practical use of the proposed WRC model.

Conclusion

Thus, 1) two systems of relations (1a,b) and (2a,b) are received for calculating the main drying and wetting curves of hysteretic WRC; 2) two systems of relations (3a) and (3b) are offered for predicting the scanning drying and wetting curves as well as for calculating the reversal points of hysteretic loop of water-retention capacity. The approximations (1b) and (2b) have quite high accuracy to describe the main drying and wetting curves of hysteretic WRC.

Computer program “HYSTERESIS” was developed on the basis of the proposed model, which is formulated ratios (1b), (2b) and (3a, b). The program allows identifying the model parameters according to direct measurements of the water-retention capacity of soil. Three computational experiments were carried out with the use of this program. The measured data on the water-retention capacity of sandy soil were used in the previous experiments.

The first experiment consisted of comparing the interpolation accuracy using relations (1a) and (2a), on the one hand, and the ratios (1b) and (2b), on the other hand. The result of this experiment shows the high accuracy of the proposed approximations for the function of the water-retention capacity of soil. The second experiment with oscillating values of capillary pressure showed no negative "pump effect". The third experiment was to identify the parameters of the WRC model using data on the main drying and wetting curves and then - in the subsequent prediction of the primary drying curve and secondary wetting curve of hysteresis loop. The result of the third experiment showed high accuracy for extrapolation (prediction) of volumetric water content values for the scanning curves of the hysteresis loop in the absence of data on these curves. This result is explained by the fact that adequate physical representation about the nature of the phenomenon of hysteretic water-retention capacity is the basis for

Терлеев В.В., Никоноров А.О., Того И., Волкова Ю.В., Гиневский Р.С., Лазарев В.А., Хамзин Э.Р., Гарманов В.В., Миршель В., Акимов Л.И. Гистерезис водоудерживающей способности почвы на примере песчаных почв. 2017. № 2(70). С. 84–92.

the offered model. The practical significance of the proposed model is the availability of the option in the program “HYSTERESIS” for predicting the scanning curves using the data about the main drying and wetting curves of the hysteresis loop. The particular importance of this option is that the measurement of the totality of the scanning curves practically impossible, while the data on the main drying and wetting curves are relatively accessible.

Estimation of the scanning curves of the hysteresis loop allows improving the accuracy of calculating the dynamics of soil moisture. The results of the research could be applied to the agricultural investigations, hydrological conditions measurements and other measures. All these factors indicate the encouraging prospects for the practical use of the proposed WRC model.

Acknowledgement

The research was supported by DAAD (A/10/01103), DFG (MI 526/3-1) and Russian Foundation for Basic Research (#16-04-01473-a).

References

1. Kosugi K. Three-parameter lognormal distribution model for soil water retention. *Water Resour. Res.* 1994. Vol. 30. Pp. 891–901.
2. Kosugi K. Lognormal distribution model for unsaturated soil hydraulic properties. *Water Resour. Res.* 1996. Vol. 32. Pp. 2697–2703.
3. Kosugi K., Hopmans J.W. Scaling water retention curves for soils with lognormal pore-size distribution. *Soil Sci. Soc. Amer. J.* 1998. Vol. 62. Pp. 1496–1505.
4. Kosugi K. General model for unsaturated hydraulic conductivity for soil with lognormal pore-size distribution // Soil Sci. Soc. Amer. J. 1999. Vol. 63. Pp. 270–277.
5. Terleev V.V., Topaj A.G., Mirschel W. The improved estimation for the effective supply of productive moisture considering the hysteresis of soil water-retention capacity. *Russian Meteorology and Hydrology.* 2015. Vol. 40. Pp. 278–285.
6. Terleev V., Petrovskaia E., Sokolova N., Dashkina A., Guseva I., Badenko V.,. Volkova Yu., Skvortsova O., Nikonova O., Pavlov S., Nikonorov A., Garmanov V., Mirschel W. Mathematical modeling of hydrophysical properties of soils in engineering and reclamation surveys. *MATEC Web of Conferences.* 2016. Vol. 53. Article ID 01013.
7. Terleev V., Nikonorov A., Badenko V., Guseva I., Volkova Yu., Skvortsova O., Pavlov S., Mirschel W. Modeling of hydrophysical properties of the soil as capillary-porous media and improvement of Mualem-Van Genuchten method as a part of foundation arrangement research. *Advances in Civil Engineering.* 2016. Vol. 2016. Article ID 8176728.
8. Terleev V., Petrovskaia E., Nikonorov A., Badenko V., Volkova Y., Pavlov S., Semenova N., Moiseev K., Topaj A., Mirschel W. Mathematical modeling the hydrological properties of soil for practical use in the land ecological management. *MATEC Web of Conferences.* 2016. Vol. 73. Article ID 03001.
9. Brutsaert W. Probability laws for pore-size distribution. *Soil Sci.* 1966. Vol. 101. Pp. 85–92.
10. Brutsaert W. A concise parameterization of the hydraulic conductivity of unsaturated soils. *Adv. in Water Res.* 2000. Vol. 23. Pp. 811–815.
11. Levenberg K. A Method for the solution of certain non-linear problems in least squares. *Quarterly Appl. Math.* 1944. Vol. 2. Pp. 164–168.
12. Marquardt D.W. An algorithm for least-square estimation on non-linear parameters. *J. Soc. Ind. Appl. Math.* 1963. Vol. 11. Pp. 431–441.
13. Huang H.C., Tan Y.C., Liu C.W., Chen C.H. A novel hysteresis model in unsaturated soil. *Hydrol. Process.* 2005.

Литература

1. Kosugi K. Three-parameter lognormal distribution model for soil water retention // Water Resour. Res. 1994. Vol. 30. Pp. 891–901.
2. Kosugi K. Lognormal distribution model for unsaturated soil hydraulic properties // Water Resour. Res. 1996. Vol. 32. Pp. 2697–2703.
3. Kosugi K., Hopmans J.W. Scaling water retention curves for soils with lognormal pore-size distribution // Soil Sci. Soc. Amer. J. 1998. Vol. 62. Pp. 1496–1505.
4. Kosugi K. General model for unsaturated hydraulic conductivity for soil with lognormal pore-size distribution // Soil Sci. Soc. Amer. J. 1999. Vol. 63. Pp. 270–277.
5. Terleev V.V., Topaj A.G., Mirschel W. The improved estimation for the effective supply of productive moisture considering the hysteresis of soil water-retention capacity // Russian Meteorology and Hydrology. 2015. Vol. 40. Pp. 278–285.
6. Terleev V., Petrovskaia E., Sokolova N., Dashkina A., Guseva I., Badenko V.,. Volkova Yu., Skvortsova O., Nikonova O., Pavlov S., Nikonorov A., Garmanov V., Mirschel W. Mathematical modeling of hydrophysical properties of soils in engineering and reclamation surveys // MATEC Web of Conferences. 2016. Vol. 53. Article ID 01013.
7. Terleev V., Nikonorov A., Badenko V., Guseva I., Volkova Yu., Skvortsova O., Pavlov S., Mirschel W. Modeling of hydrophysical properties of the soil as capillary-porous media and improvement of Mualem-Van Genuchten method as a part of foundation arrangement research // Advances in Civil Engineering. 2016. Vol. 2016. Article ID 8176728.
8. Terleev V., Petrovskaia E., Nikonorov A., Badenko V., Volkova Y., Pavlov S., Semenova N., Moiseev K., Topaj A., Mirschel W. Mathematical modeling the hydrological properties of soil for practical use in the land ecological management // MATEC Web of Conferences. 2016. Vol. 73. Article ID 03001.
9. Brutsaert W. Probability laws for pore-size distribution // Soil Sci. 1966. Vol. 101. Pp. 85–92.
10. Brutsaert W. A concise parameterization of the hydraulic conductivity of unsaturated soils // Adv. in Water Res. 2000. Vol. 23. Pp. 811–815.
11. Levenberg K. A Method for the solution of certain non-linear problems in least squares // Quarterly Appl. Math. 1944. Vol. 2. Pp. 164–168.
12. Marquardt D.W. An algorithm for least-square estimation on non-linear parameters // J. Soc. Ind. Appl. Math. 1963. Vol. 11. Pp. 431–441.
13. Huang H.C., Tan Y.C., Liu C.W., Chen C.H. A novel hysteresis model in unsaturated soil // Hydrol. Process.

Terleev V.V., Nikonorov A.O., Togo I., Volkova Yu.V., Ginevsky R.S., Lazarev V.A., Khamzin E.R., Garmanov V.V., Mirschel W., Akimov L.I. Hysteretic water-retention capacity of sandy soil. *Magazine of Civil Engineering*. 2017. No. 2. Pp. 84–92. doi: 10.18720/MCE.70.8

Vol. 19. Pp. 1653–1665.

14. Poluektov R.A., Terleev V.V. Modeling of the water retention capacity and differential moisture capacity of soil. *Russian Meteorology and Hydrology.* 2002. Vol. 11. Pp. 70–75.
15. Poluektov R.A., Terleev V.V. Modeling the moisture retention capacity of soil with agricultural and hydrological characteristics. *Russian Meteorology and Hydrology.* 2005. Vol. 12. Pp. 73–77.
16. Terleev V.V., Mirschel V., Schindler U., Wenkel K.-O. Estimation of soil water retention curve using some agrophysical characteristics and Voronin's empirical dependence. *International Agrophysics.* 2010. Vol. 24. Pp. 381–387.
17. Terleev V.V., Mirschel W., Badenko V.L., Guseva I.Yu. An Improved Mualem-Van Genuchten Method and Its Verification Using Data on Beit Netofa Clay. *Eurasian Soil Science.* 2017. Vol. 50. Pp. 445–455.
18. Poluektov R.A., Oparina I.V., Terleev V.V. Three methods for calculating soil water dynamics. *Russian Meteorology and Hydrology.* 2003. Vol. 11. Pp. 61–67.
19. Semenova N.N., Terleev V.V., Suhoruchenko G.I., Orlova E.E., Orlova N.E. On one method for the numerical solution of a system of parabolic equations. *Vestnik St. Petersburg University: Mathematics.* 2016. Vol. 49. Pp. 138-146.
20. Poluektov R.A, Fintushal S.M., Oparina I.V., Shatskikh D.V., Terleev V.V., Zakharova E.T. Agrotool – a system for crop simulation. *Archives of Agronomy and Soil Science.* 2002. Vol. 48. Pp. 609–635.
21. Poluektov R.A., Terleev V.V. Crop simulation model of the second and the third productivity levels. *Modelling Water and Nutrient Dynamics in Soil-crop Systems.* Springer, Dordrecht, The Netherlands. 2007. Pp. 75–89.
22. Badenko V., Terleev V., Topaj A. AGROTOOL software as an intellectual core of decision support systems in computer aided agriculture. *Applied Mechanics and Materials.* 2014. Vols. 635–637. Pp. 1688–1691.
23. Medvedev S., Topaj A., Badenko V., Terleev V. Medium-term analysis of agroecosystem sustainability under different land use practices by means of dynamic crop simulation. *IFIP Advances in Information and Communication Technology.* 2015. Vol. 448. Pp. 252–261.
24. Badenko V., Terleev V., Arefiev N., Volkova J., Nikonova O. Agroecosystem model AGROTOOL coupled with GIS for simulation of the spatial variability of the soil hydrophysical properties. *Proceedings of the AASRI International Conference on Industrial Electronics and Applications (IEA 2015).* Book Series: AER-Advances in Engineering Research. 2015. Vol. 2. Pp. 452–455.
25. Makarov A., Mihailova A., Arefiev N., Pavlov S., Chashchina T., Terleev V., Badenko V. Country area territory protection from flooding; Construction conditions, problem definition and solution. *Procedia Engineering.* Vol. 117. Pp. 225–231.
26. Arefiev N. Badenko V., Nikonorov A., Terleev V., Volkova Y. Bank protection on storage reservoirs for municipal coastal areas. *Procedia Engineering.* 2015. Vol. 117. Pp. 20–25.
27. Nikonorov A., Pavlov S., Terleev V., Arefiev N., Badenko V., Volkova Y. Use of enclosing and temporary special structures under the reconstruction of hydraulic facilities in Saint-Petersburg. *Procedia Engineering.* 2015. Vol. 117. Pp. 258–263.
28. Chechevichkin V., Vatin N. Megacities land drainage and land runoff features and treatment. *Applied Mechanics and Materials.* 2014. Vols. 641–642. Pp. 409–415.
29. Vatin N., Lavrov N., Loginov G. Processes at water intake from mountain rivers into hydropower and irrigation systems. *MATEC Web of Conferences*. 2016. Vol. 73. Article ID 01006.
30. Arefiev N., Mikhalev M., Zotov D., Zotov K., Vatin N., 2005. Vol. 19. Pp. 1653–1665.
14. Poluektov R.A., Terleev V.V. Modeling of the water retention capacity and differential moisture capacity of soil // Russian Meteorology and Hydrology. 2002. Vol. 11. Pp. 70–75.
15. Poluektov R.A., Terleev V.V. Modeling the moisture retention capacity of soil with agricultural and hydrological characteristics // Russian Meteorology and Hydrology. 2005. Vol. 12. Pp. 73–77.
16. Terleev V.V., Mirschel V., Schindler U., Wenkel K.-O. Estimation of soil water retention curve using some agrophysical characteristics and Voronin's empirical dependence // International Agrophysics. 2010. Vol. 24. Pp. 381–387.
17. Terleev V.V., Mirschel W., Badenko V.L., Guseva I.Yu. An Improved Mualem-Van Genuchten Method and Its Verification Using Data on Beit Netofa Clay // Eurasian Soil Science. 2017. Vol. 50. Pp. 445–455.
18. Poluektov R.A., Oparina I.V., Terleev V.V. Three methods for calculating soil water dynamics // Russian Meteorology and Hydrology. 2003. Vol. 11. Pp. 61–67.
19. Semenova N.N., Terleev V.V., Suhoruchenko G.I., Orlova E.E., Orlova N.E. On one method for the numerical solution of a system of parabolic equations // Vestnik St. Petersburg University: Mathematics. 2016. Vol. 49. Pp. 138-146.
20. Poluektov R.A, Fintushal S.M., Oparina I.V., Shatskikh D.V., Terleev V.V., Zakharova E.T. Agrotool – a system for crop simulation // Archives of Agronomy and Soil Science. 2002. Vol. 48. Pp. 609–635.
21. Poluektov R.A., Terleev V.V. Crop simulation model of the second and the third productivity levels // Modelling Water and Nutrient Dynamics in Soil-crop Systems. Springer, Dordrecht, The Netherlands. 2007. Pp. 75–89.
22. Badenko V., Terleev V., Topaj A. AGROTOOL software as an intellectual core of decision support systems in computer aided agriculture // Applied Mechanics and Materials. 2014. Vols. 635–637. Pp. 1688–1691.
23. Medvedev S., Topaj A., Badenko V., Terleev V. Medium-term analysis of agroecosystem sustainability under different land use practices by means of dynamic crop simulation // IFIP Advances in Information and Communication Technology. 2015. Vol. 448. Pp. 252–261.
24. Badenko V., Terleev V., Arefiev N., Volkova J., Nikonova O. Agroecosystem model AGROTOOL coupled with GIS for simulation of the spatial variability of the soil hydrophysical properties // Proceedings of the AASRI International Conference on Industrial Electronics and Applications (IEA 2015). Book Series: AER-Advances in Engineering Research. 2015. Vol. 2. Pp. 452–455.
25. Makarov A., Mihailova A., Arefiev N., Pavlov S., Chashchina T., Terleev V., Badenko V. Country area territory protection from flooding; Construction conditions, problem definition and solution // Procedia Engineering. Vol. 117. Pp. 225–231.
26. Arefiev N. Badenko V., Nikonorov A., Terleev V., Volkova Y. Bank protection on storage reservoirs for municipal coastal areas // Procedia Engineering. 2015. Vol. 117. Pp. 20–25.
27. Nikonorov A., Pavlov S., Terleev V., Arefiev N., Badenko V., Volkova Y. Use of enclosing and temporary special structures under the reconstruction of hydraulic facilities in Saint-Petersburg // Procedia Engineering. 2015. Vol. 117. Pp. 258–263.
28. Chechevichkin V., Vatin N. Megacities land drainage and land runoff features and treatment // Applied Mechanics and Materials. 2014. Vols. 641–642. Pp. 409–415.
29. Vatin N., Lavrov N., Loginov G. Processes at water intake from mountain rivers into hydropower and irrigation systems // MATEC Web of Conferences. 2016. Vol. 73. Article ID 01006.

Терлеев В.В., Никоноров А.О., Того И., Волкова Ю.В., Гиневский Р.С., Лазарев В.А., Хамзин Э.Р., Гарманов В.В., Миршель В., Акимов Л.И. Гистерезис водоудерживающей способности почвы на примере песчаных почв. 2017. № 2(70). С. 84–92.

Nikonova O., Skvortsova O., Pavlov S., Chashina T., Kuchurina T., Terleev V., Badenko V., Volkova Y., Salikov V., Strelets K., Petrochenko M., Rechinsky A. Physical modeling of suspended sediment deposition in marine intakes of nuclear power plants. *Procedia Engineering.* 2015. Vol. 117. Pp. 32–38.

31. Badenko V., Badenko N., Nikonorov A., Molodtsov D., Terleev V., Lednova J., Maslikov V. Ecological aspect of dam design for flood regulation and sustainable urban development. *MATEC Web of Conferences*. 2016. Vol. 73. Article ID 03003.
32. Skvortsova O., Dashkina A., Petrovskaia E., Terleev V., Nikonorov A., Badenko V., Volkova Yu., Pavlov S. The classification of accidental situations scenarios on hydropower plants. *MATEC Web of Conferences.* 2016. Vol. 53. Article ID 01014.
33. Arefiev N., Garmanov V., Bogdanov V., Ryabov Yu., Terleev V., Badenko V. A market approach to the evaluation of the ecological-economic damage dealt to the urban lands. *Procedia Engineering.* 2016. Vol. 117. Pp. 26–31.
34. Arefiev N., Terleev V., Badenko V. GIS-based fuzzy method for urban planning. *Procedia Engineering.* 2015. Vol. 117. Pp. 39–44.

30. Arefiev N., Mikhalev M., Zotov D., Zotov K., Vatin N., Nikonova O., Skvortsova O., Pavlov S., Chashina T., Kuchurina T., Terleev V., Badenko V., Volkova Y., Salikov V., Strelets K., Petrochenko M., Rechinsky A. Physical modeling of suspended sediment deposition in marine intakes of nuclear power plants // Procedia Engineering. 2015. Vol. 117. Pp. 32–38.
31. Badenko V., Badenko N., Nikonorov A., Molodtsov D., Terleev V., Lednova J., Maslikov V. Ecological aspect of dam design for flood regulation and sustainable urban development // MATEC Web of Conferences. 2016. Vol. 73. Article ID 03003.
32. Skvortsova O., Dashkina A., Petrovskaia E., Terleev V., Nikonorov A., Badenko V., Volkova Yu., Pavlov S. The classification of accidental situations scenarios on hydropower plants // MATEC Web of Conferences. 2016. Vol. 53. Article ID 01014.
33. Arefiev N., Garmanov V., Bogdanov V., Ryabov Yu., Terleev V., Badenko V. A market approach to the evaluation of the ecological-economic damage dealt to the urban lands // Procedia Engineering. 2016. Vol. 117. Pp. 26–31.
34. Arefiev N., Terleev V., Badenko V. GIS-based fuzzy method for urban planning // Procedia Engineering. 2015. Vol. 117. Pp. 39–44.

Vitaly Terleev,
vitaly_terleev@mail.ru

Aleksandr Nikonorov,
+7(921)3852180; coolhabit@yandex.ru

Issa Togo,
+7(921)3373730; issatogo@mail.ru

Yulia Volkova,
yv1975@mail.ru

Roman Ginevsky,
rginevski@gmail.com

Viktor Lazarev,
lviktor.97@mail.ru

Emil Khamzin,
Ham_mer97@mail.ru

Vitaly Garmanov,
garmanovv@mail.ru

Wilfried Mirschel,
wmirschel@zalf.de

Luka Akimov,
+7(921)4178833; lukas-ak@mail.ru

Виталий Викторович Терлеев,
эл. почта: vitaly_terleev@mail.ru

Александр Олегович Никоноров,
+7(921)3852180; эл. почта: coolhabit@yandex.ru
Исса Того,
+7(921)3373730; эл. почта: issatogo@mail.ru

Юлия Валерьевна Волкова,
эл. почта: yv1975@mail.ru

Роман Сергеевич Гиневский,
эл. почта: rginevski@gmail.com

Виктор Андреевич Лазарев,
эл. почта: lviktor.97@mail.ru

Эмиль Рамилевич Хамзин,
эл. почта: Ham_mer97@mail.ru

Виталий Валентинович Гарманов,
эл. почта: garmanovv@mail.ru

Вильфред Миршель,
эл. почта: wmirschel@zalf.de

Лука Игоревич Акимов,
+7(921)4178833; эл. почта: lukas-ak@mail.ru

Terleev V.V., Nikonorov A.O., Togo I., Volkova Yu.V., Ginevsky R.S., Lazarev V.A., Khamzin E.R., Garmanov V.V., Mirschel W., Akimov L.I. Hysteretic water-retention capacity of sandy soil. *Magazine of Civil Engineering*. 2017. No. 2. Pp. 84–92. doi: 10.18720/MCE.70.8

Федеральное государственное автономное образовательное учреждение высшего образования
Санкт-Петербургский политехнический университет Петра Великого

ПОЛИТЕХ
Санкт-Петербургский политехнический университет Петра Великого

Инженерно-строительный институт
Центр дополнительных профессиональных программ

195251, г. Санкт-Петербург, Политехническая ул., 29,
тел/факс: 552-94-60, www.stroikursi.spbstu.ru,
stroikursi@mail.ru

Приглашает специалистов проектных и строительных организаций,
не имеющих базового профильного высшего образования
на курсы профессиональной переподготовки (от 500 часов)
по направлению «Строительство» по программам:

П-01 «Промышленное и гражданское строительство»

Программа включает учебные разделы:

- ***Основы строительного дела***
- ***Инженерное оборудование зданий и сооружений***
- ***Технология и контроль качества строительства***
- ***Основы проектирования зданий и сооружений***
- ***Автоматизация проектных работ с использованием AutoCAD***
- ***Автоматизация сметного дела в строительстве***
- ***Управление строительной организацией***
- ***Управление инвестиционно-строительными проектами. Выполнение функций технического заказчика***

П-02 «Экономика и управление в строительстве»

Программа включает учебные разделы:

- ***Основы строительного дела***
- ***Инженерное оборудование зданий и сооружений***
- ***Технология и контроль качества строительства***
- ***Управление инвестиционно-строительными проектами. Выполнение функций технического заказчика и генерального подрядчика***
- ***Управление строительной организацией***
- ***Экономика и ценообразование в строительстве***
- ***Управление строительной организацией***
- ***Организация, управление и планирование в строительстве***
- ***Автоматизация сметного дела в строительстве***

П-03 «Инженерные системы зданий и сооружений»

Программа включает учебные разделы:

- ***Основы механики жидкости и газа***
- ***Инженерное оборудование зданий и сооружений***
- ***Проектирование, монтаж и эксплуатация систем вентиляции и кондиционирования***
- ***Проектирование, монтаж и эксплуатация систем отопления и теплоснабжения***
- ***Проектирование, монтаж и эксплуатация систем водоснабжения и водоотведения***
- ***Автоматизация проектных работ с использованием AutoCAD***
- ***Электроснабжение и электрооборудование объектов***

П-04 «Проектирование и конструирование зданий и сооружений»

Программа включает учебные разделы:

- ***Основы сопротивления материалов и механики стержневых систем***
- ***Проектирование и расчет оснований и фундаментов зданий и сооружений***
- ***Проектирование и расчет железобетонных конструкций***
- ***Проектирование и расчет металлических конструкций***
- ***Проектирование зданий и сооружений с использованием AutoCAD***
- ***Расчет строительных конструкций с использованием SCAD Office***

П-05 «Контроль качества строительства»

Программа включает учебные разделы:

- ***Основы строительного дела***
- ***Инженерное оборудование зданий и сооружений***
- ***Технология и контроль качества строительства***
- ***Проектирование и расчет железобетонных конструкций***
- ***Проектирование и расчет металлических конструкций***
- ***Обследование строительных конструкций зданий и сооружений***
- ***Выполнение функций технического заказчика и генерального подрядчика***

По окончании курса слушателю выдается диплом о профессиональной переподготовке установленного образца, дающий право на ведение профессиональной деятельности